

Biotic and Abiotic Alterations of Hydrocarbons in the Southern Gulf of Mexico

Characterization of Polar Hydrocarbons in the Aqueous Phase via GC-MS

Master Thesis M.Sc. Marine Geosciences

Department of Geosciences

University of Bremen

Submitted by: Kingsley Ifeanyi Nwabor

1. Examiner: Dr. Florence Schubotz

2. Examiner: Dr. Christian Hallmann

Bremen, 2020



Contents

Contents	2
List of Figures and Tables.....	4
Abbreviations	6
Abstract.....	7
1. Introduction	8
1.1 Marine hydrocarbon seeps and associated ecosystems.....	9
1.2 Campeche knolls, Southern Gulf of Mexico	10
1.2.1 Chapopote Knoll	11
1.2.2 Mictlan Knoll	13
1.2.3 Tsanyao Yang Knoll	16
1.3 Petroleum Biodegradation.....	18
1.3.1 Persistence of Heavy oil and fate of the oil	18
1.3.2 Aerobic biodegradation.....	19
1.4 Previous asphalt incubation study	20
1.5 Objectives and Motivation	21
1.5.1 Research questions.....	22
2. Materials and methods.....	24
2.1 Environmental samples	24
2.2 Incubation experiments	25
2.3 Liquid –liquid extraction.....	26
2.3.1 Asphalt incubation samples	27
2.3.2 Environmental samples.....	27
2.4 Asphaltenes precipitation.....	28
2.5 Column separation.....	29
2.6 Gas chromatography coupled to flame ionization detection (FID) and mass spectrometry (GC-MS).....	29
3. Results	31
3.1 Asphalt Incubation Experiment.....	31
3.1.1 Contaminants	33
3.1.2 <i>n</i> -Alkanes	33
3.1.3 Cycloalkanes	35
3.1.4 Aromatic alcohol.....	35
3.1.5 Aromatic ketones	36
3.1.6 Aromatic acids	38
3.1.7 Thiols and thiophenic acids	39
3.1.8 Halogenated compounds	40
3.1.9 Fatty acids	41
3.2 Environmental samples	43

3.2.1	Chapopote samples	43
3.2.2	Mictlan samples	44
3.2.3	Tsanyao Yang samples	46
3.3	Aromatic hydrocarbons and NSO compounds.....	47
3.4	Biodegradation and water washing parameters.....	47
4.	Discussion.....	55
4.1	Asphalt incubation experiments	55
4.1.1	<i>n</i> -Alkanes and Cycloalkanes.....	55
4.1.2	Aromatic alcohols	57
4.1.3	Aromatic Ketones	59
4.1.4	Aromatic acids	61
4.1.5	Thiols and Thiophenic acids	62
4.1.6	Halogenated compounds	63
4.1.7	Fatty acids	65
4.2	Environmental samples	66
4.2.1	Branched alkanes with quaternary carbon (BAQCs) and other contaminants	66
4.2.2	Comparison of environmental samples with asphalt incubation samples	67
4.2.3	Grouping of environmental samples into different sample types	67
4.2.4	Biotic and abiotic processes affecting dissolved petroleum hydrocarbons	70
5.	Conclusion.....	73
6.	Outlook	75
	Acknowledgement	76
	References.....	77
	Appendix.....	89
	Supplementary Figures.....	89
	Supplementary Tables	96

List of Figures and Tables

Figure 1. Swath bathymetry of the Campeche Knolls Gulf of Mexico (R/V METEOR Cruise M114) Sahling et al., 2016.....	11
Figure 2. Bathymetry map of Chapopote Knoll (A) AUV-based bathymetry draped over ship-based bathymetry. (B) Enlarged view of ROV QUEST dive tracks. (Sahling et al., 2016).....	12
Figure 3. (A and B) Ropy asphalt colonized by whitish microbial mats and tubeworms. (C) Extensively altered asphalt (D) Bubble fabric gas hydrate outcrop hosting mytilids, gastropods, galatheid crab and mussels. Sahling et al., 2016; Marcon et al.; 2018	13
Figure 4. Bathymetry map of Mictlan Knoll (A) AUV-based bathymetry draped over ship-based bathymetry. (B) Enlarged view of ROV QUEST dive tracks. (Sahling et al., 2016).....	14
Figure 5. (A) White-coated chimneys releasing oil drops (B) Gas Bubble Sampler (GBS) collecting samples from the asphalt tubes , (C&D) microscopic analysis showing the interior of the white asphalt tubes (E) Vestimentiferan tubeworms on an exposed gas hydrate block at the seafloor (Mictlan Knoll, Hydrate Hills). (F) Oily mussel and tube worm site. (Sahling et al., 2016, 2017).....	15
Figure 6. AUV-based high-resolution bathymetry of the main seep field at Tsanyao Yang knoll and seafloor positions of flares (red dots) observed during M114. ROV QUEST dives tracks (black lines). Detailed investigations and gas sampling Sites 1 to 4 are indicated by white arrows. Römer et al., 2019.	16
Figure 7. (A) Pillar-like structure of oily gas hydrates bubbles with a cap of carbonate and tube worms (B) a much closer look (red box in image A) at the features of the structure showing oil bubbles (dark color) and hydrate (white) covered by yellowish brown microbial mat (C) Carbonate rock sample with oil drapes.	17
Figure 8. Aerobic degradation of naphthalene by bacteria (Bamforth and Singleton 2005).....	20
Figure 9. Schematic of the steps employed for the analysis of the water samples from asphalt incubation experiments and the environmental water samples.....	28
Figure 10. Total ion chromatogram (TIC) for all the asphalt incubation experiments	32
Figure 11. Extracted ion chromatogram (EIC m/z 85) for the ‘Asphalt Only’ incubation experiments	33
Figure 12. Bar chart showing hexadecane concentration in the asphalt incubation experiment	34
Figure 13. Bar chart showing concentration of the (C_{17} to C_{24}) <i>n</i> -alkanes in the asphalt incubation experiment	34
Figure 14. Bar chart showing concentration of cycloalkanes in the asphalt incubation experiment.....	35
Figure 15. Bar chart showing concentration of aromatic alcohols in the asphalt incubation experiment	36
Figure 16. Bar chart showing concentration of aromatic ketones in the asphalt incubation experiment	37
Figure 17. Bar chart showing concentration of Coumarin in the asphalt incubation experiment	38
Figure 18. Bar chart showing concentration of aromatic acids detected in the asphalt incubation experiment	39
Figure 19. Bar chart showing concentration of thiol compound and thiophenic acids detected in the asphalt incubation experiment	40
Figure 20. Bar chart showing concentration of halogenated compounds in the asphalt incubation experiment.....	41
Figure 21. Bar chart showing concentration of fatty acids detected in the asphalt incubation experiment. The ‘y’ axis was reduced so as to make room for ‘Asphalt Only’ and ‘Naphthalene’	42
Figure 22. Images of locations and extracted ion chromatograms (EIC) m/z 85 of the water samples collected from Chapopote. (a) Sonne Field (b) oil bubble site (c) Main Asphalt Field. IS: internal standard, black circles: <i>n</i> -alkane homologous series, inverted black triangles: isoprenoids pristane (Pr) and phytane (Ph) red and orange squares: branched alkanes with quaternary carbon atoms (BAQCs) series. Images from the M114 cruise report (Sahling and Bohrmann, 2017).....	43
Figure 23. Images of locations and extracted ion chromatograms (EIC) m/z 85 of the water samples collected from Mictlan. (a) oil slick, (b) mussel bed, (c) white asphalt tubes. IS: internal standard, black circles: <i>n</i> -alkane homologous series, inverted black triangles: isoprenoids pristane (Pr) and phytane (Ph) red and orange squares: branched alkanes with quaternary carbon atoms (BAQCs) series. Images from the M114 cruise report (Sahling and Bohrmann, 2017).....	45
Figure 24. Images of locations and extracted ion chromatograms (EIC) m/z 85 of the water samples collected from Tsanyao Yang (a) oil slicks (b) oil bubble Site 1. IS: internal standard, black circles: <i>n</i> -alkane homologous series, inverted black triangles: isoprenoids pristane (Pr) and phytane (Ph), red and orange squares: branched alkanes with quaternary carbon atoms (BAQCs) series. Images gotten from. Römer et al. (2019).	46
Figure 25. Cross-plot of Pr/C17 versus Ph/C18 ratios for all sample types.....	50
Figure 26. Cross-plot of C1-Phen/C2-Phen versus C1-DBT/C2-DBT ratios for all sample types	50
Figure 27. Cross-plot of C1-Phen/C2-Phen versus C1-Phen/C1-DBT for all sample types	51

Figure 28. Cross-plot of Phen/C1-Phen versus DBT/C1-DBT ratios, for only fresh and weathered samples.....	52
Figure 29. Relative abundance of all compounds identified and quantified in the environmental water samples. Samples classification is based on the level of biodegradation defined by <i>n</i> -alkane patterns and Pr/C17 and Ph/C18 ratios (see Table 4)	53
Figure 30. The figure shows the proposed catabolic pathways of naphthalene degradation by bacteria. Image gotten from Seo et al., (2009)	60
Figure 31. Tentative Structures and mass spectral data of cycloalkanes detected in the asphalt incubation experiments.....	89
Figure 32. Mass spectral data with tentative structures and sum formulae for the detected aromatic alcohols in the asphalt incubation experiments. MW: Molecular weight, R.T: Retention time (in minutes).....	90
Figure 33. Mass spectral data with tentative structures and sum formulae for the detected aromatic ketones in the asphalt incubation experiments. MW: Molecular weight, R.T: Retention time (in minutes)	91
Figure 34. Mass spectral data with tentative structures and sum formulae for the detected aromatic acids in the asphalt incubation experiments. MW: Molecular weight, R.T: Retention time (in minutes)	92
Figure 35. Mass spectral data with tentative structures and sum formulae for the detected thiol and thiophenic acid in the asphalt incubation experiments. MW: Molecular weight, R.T: Retention time (in minutes)	93
Figure 36. Mass spectral data with tentative structures and sum formulae for the 4 detected halogenated compounds in the asphalt incubation experiments. MW: Molecular weight, R.T: Retention time (in minutes)	93
Figure 37. Mass spectral data with tentative structures and sum formulae for the fatty acid compounds in the asphalt incubation experiments. MW: Molecular weight, R.T: Retention time (in minutes)	94
Figure 38. Plots showing the distribution of the concentration of fatty acids detected in the ‘Asphalt Only’, ‘Naphthalene’ and ‘Hexadecane’ incubation experiment.....	95

Table 1. Investigated environmental samples, location, depth (masf) and collection instruments. Cruise: M 114-2 GOM 2015. Sample type: water HC.....	24
Table 2. Biotic and abiotic asphalt incubation experiment (GeoB19339-1)	26
Table 3. Separation protocol for the column chromatography	29
Table 4. Biodegradation ratios of Pr/C17 and Ph/C18 and aromatic compounds	49
Table 5. Absolute concentrations of the 18 analyzed samples. The bold figures represent the sum total for each sample type.....	52
Table 6. Compounds identified in the asphalt incubation experiment and their respective concentration values. Also, the calculated standard deviation for the triplicate is shown.	96
Table 7. List of some suspected contaminants encountered in the asphalt incubation samples.....	97
Table 8. The table shows the solubility of representative <i>n</i> -alkanes in an aqueous medium at 25°C. The table is gotten from F. Rojo 2010. Original data obtained from Eastcott et al., 1988.....	97
Table 9. Absolute abundance [ng/ml] of compounds (GC-MS) in type 1 ‘fresh’ samples; the emboldened figures represent the sum total of all the compounds in each compound class.....	98
Table 10. Absolute abundance [ng/ml] of compounds (GC-MS) in type 2 ‘biodegraded’ samples; the emboldened figures represent the sum total of all the compounds in each compound class.....	100
Table 11. Absolute abundance [ng/ml] of compounds (GC-MS) in type 3 weathered samples; the emboldened figures represent the sum total of all the compounds in each compound class.....	102
Table 12. Absolute abundance [ng/ml] of compounds (GC-MS) in the Oil slicks samples; the emboldened figures represent the sum total of all the compounds in each compound class.....	104
Table 13. Shows the list of identified contaminants encountered in the environmental water sample. The absolute concentrations of these branched alkanes with quaternary carbon atoms (BAQCs) were calculated by integration of the m/z 85 signal during GC-mass spectrometry (GC-MS).....	105

Abbreviations

AB:	Analytical blank
AUV:	Automated under-water vehicle
BAQCs:	Branched alkanes with quaternary carbon atoms
DBT:	Dibenzothiophene
DCM:	Dichloromethane
DOM:	Dissolved organic matter
EEM:	Excitation-emission matrix
EI:	Electron impact
EIC:	Extracted ion chromatogram
FDOM:	Fluorescent dissolved organic matter
FID:	Flame ionization detector
FT-ICR-MS:	Fourier Transform Ion Cyclotron Resonance Mass Spectrometry
GBS:	Gas bubble sampler
GC-MS:	Gas chromatography coupled to mass spectrometer
GCxGC-MS:	Two-dimensional gas chromatography coupled to a time of flight mass spectrometer
GFF:	Glass fiber filter
GoM:	Gulf of Mexico
HC:	Hydrocarbon
MAF:	Main Asphalt Field
MeOH:	Methanol
MSD:	Mass Selective Detector
Naph:	Naphthalene
NSO:	Nitrogen, sulfur, oxygen compounds
PAA:	Phenylacetic acid
PAH:	Polycyclic aromatic hydrocarbon
PASH:	Polycyclic aromatic sulfur heterocycles
Ph:	Phytane
Pr:	Pristanes
ROV:	Remotely operated vehicle
TEA:	Terminal electron acceptors
TIC:	Total ion chromatogram
TLE:	Total lipid extract
UCM:	Unresolved Complex Mixture

Abstract

The release of petroleum hydrocarbons into the environment occurs naturally or via anthropogenic input. Large-scale natural hydrocarbon emissions observed at crude oil seeps at the seafloor of the Campeche Knolls in the Southern Gulf of Mexico result from salt tectonics in the subsurface. They introduce potentially harmful substances into the ocean and serve as energy source for benthic communities through hydrocarbon-degrading microorganisms. These substances include polycyclic aromatic hydrocarbons (PAHs) and can also contain sulfur (PASHs), which are toxic and recalcitrant groups of contaminants, with two or more fused benzene rings. The goal of this research is to shed further light on the types and amount of PAHs that are released into the environment or are recycled through microbial activities. Water samples from asphalt incubation experiments as well as water samples collected from the Southern Gulf of Mexico were analyzed by gas chromatography coupled to mass spectrometry (GC-MS). Saturate and aromatic oil compounds were identified and quantified as well as polar intermediates associated with microbial hydrocarbon degradation. Both the incubation and environmental samples were exposed to alteration processes owing to biotic and abiotic processes. Abiotic processes mainly included dissolution of water soluble compounds, a process which is also called water washing. Laboratory experiments were carried out by incubating asphalt samples under room temperature using artificial sea water amended with nutrients and showed the release of a number of polar hydrocarbons into the water phase as a result of biotic processes. Notably, many of these compounds were not observed in any of the water samples collected from three locations at the Campeche area in the southern Gulf of Mexico. While *n*-alkanes were consumed quickly in the asphalt incubation experiments, they were readily detected in the environmental water samples along with other oil compounds including the isoprenoids pristane and phytane and many PAHs and PASHs. These compounds were used to assess the alteration level of the environmental samples and allowed classification into ‘fresh’, ‘biodegraded’ and ‘weathered’ samples, whereby some samples were affected more by microbial processes while other samples were more affected by water washing processes. Overall, these investigations show that the microbial degradation of petroleum compounds in the water column occurs more slowly in the environment compared to more optimal laboratory conditions.

1. Introduction

Petroleum hydrocarbons are complex substances made up of primarily carbon and hydrogen and in some cases, oxygen, sulfur, as well as nitrogen. The commercial exploitation of petroleum recorded throughout history shows a tremendous increase in the global energy production over the decades. Due to the insatiable increase in global demand, oil has become the most valuable fossil fuel in the world today as there has been an increased consumption on petroleum hydrocarbon as a reliable source of energy. In 2000, the global production of crude oil recorded about 68 million barrels (bbl) per day (Cozzarelli et.al, 2003). 85% of the global energy was derived from fossil fuels, with 40% of the energy emerging from oil production (Edwards, 2001). However, a recent report from the U.S. Energy Information Administration (EIA) has shown that the global petroleum production about 82.86 million barrels (bbl) per day. Increase in global population, modern technology, invention of automobile, as well as industrialization has brought about increased demand of petroleum products.

The release of petroleum into the marine environment occurs naturally through oil seeps (e.g., Campeche Knolls Southern Gulf of Mexico) or as a result of anthropogenic activities such as oil spills (e.g., Deep Water Horizon oil spill) which introduces potentially harmful petroleum substances into the ocean. Evidence of anthropogenic hydrocarbon contamination persists until today in the Northern Gulf of Mexico. The disastrous explosion of the Deep Water Horizon drilling rig in April 2010 led to the release of large amount of crude oil into the marine waters. The well been drilled (Macondo 252) sits in more than 1500 m water depth (>5,000 ft) which appears to be deeper than most underwater wells. About 62,000 barrels (2.6 million gallons) got into the water column on a daily basis, and over the course of 89 days an estimate of 4.9 million barrels (more than 200 million gallons) was released into the Gulf. This incident is known to be the largest and most expensive marine oil spill ever recorded in history (Ruddy et al., 2014, Aeppli et al., 2012). With respect to natural hydrocarbon seepage, the Campeche Knolls (Figure 1) located in the Southern Gulf of Mexico exhibits large-scale occurrence of hydrocarbon emissions at the sea floor. MacDonald et al. (2004) first described this discovery as asphalt volcanism since the structures portrayed by the asphalt beds resembles solidified lava thereby exhibiting unique features compared with other forms of seepage (oil and gas). Asphalt deposits have been reported in various locations worldwide such as the southern and northern Gulf of Mexico (MacDonald et al., 2004; Weiland et al., 2008; Williamson et al., 2008; Sahling et al., 2016; NOAA, 2017). Asphalt volcanoes have also been observed at water depths of around 150 to 180 m at the Santa Barbara Basin off California (Vernon and Slater, 1963), which occurs as a result of compressional tectonic or due to salt diapirism (Marcon et. al., 2018). On the seafloor, petroleum compounds serve as energy and carbon source for benthic communities such as hydrocarbon-degrading microorganisms (Wegener et al., 2020; Hahn et al., 2020; Meckenstock et al., 2004). Nevertheless, petroleum hydrocarbons are one of the most important reoccurring contaminants in the environment as its exploration, transportation, and storage has long lasting effects on the environment (Aeppli et al., 2012; Ruddy et al., 2014).

1.1 Marine hydrocarbon seeps and associated ecosystems

The marine environment is often faced with challenges associated with petroleum spills and hydrocarbon emission which can occur either through natural or anthropogenic means. Toxic substances introduced into the environment as a result of these processes are obviously of worrisome concern. The Gulf of Mexico (GoM) is a good location to study natural and anthropogenic hydrocarbon contamination in the marine environment. The escape of petroleum hydrocarbon from the subsurface reservoirs to the sea floor occurs on both active and passive continental margins along faults and fissures in underlying sediments. This can occur as a result of processes such as but not limited to; tectonic activities e.g. salt diapirism (as seen in the Gulf of Mexico) (MacDonald et al., 2004), mud volcanism which is seen in areas with rapid sedimentation associated with high subsidence (e.g. Nile delta); as well as in subduction zones and in areas with high geothermal gradient (Ceramicola et al., 2018).

Kvenvolden and Cooper (2003) showed that the amount of natural crude oil seepage occurring annually is estimated to be 600,000 metric tons per year with a range of uncertainty of 200,000 metric tons per year. Hydrocarbon seepage is not limited to escape of lighter hydrocarbons, in the form of gas and oil bubbles that migrate to the sea surface to form oil slicks, but also involve seepage of heavy petroleum deposits (asphalt) from the sea floor (MacDonald et al., 2004). Oil seepage is also coupled with elevated gas content observed as gas flares, which is evident within the water column (Sahling et al., 2016). Numerous studies (MacDonald et al., 2004; Sahling et al., 2016; Brüning et al., 2010) have reported deposits of heavy oil in the marine environment and how they act as energy sources for chemosynthetic life. Hydrocarbon seeps, like the asphalt volcanoes in the Gulf of Mexico provides sustenance for chemosynthetic and non-chemosynthetic communities (Cordes et al., 2009), as asphalt flows in most cases creates fields of hard substrata for benthic life on the sea floor (Bruning et al. 2010; Sahling et al., 2016). As the asphalt material settles on the sea floor, the exterior solidifies due to release of light hydrocarbons into the surrounding water column, while the interior core remains ductile. Remotely operated vehicle (ROV) survey revealed that the asphalts deposit undergoes gradual transformation, as freshly discharged asphalts appear to be ductile and are colonized by whitish microbial mats (Figure 3A), whereas shrinkage in volume of the older brittle materials results to hardening and subsequent fragmentation in addition to the formation of a generally rough surface as a result of weathering (Figure 3C) (Sahling et al., 2016). Expulsion of heavy hydrocarbons to the sea floor in the Gulf of Mexico is as a result of salt tectonics as movement of salt diaps creates migration pathways, thereby influencing the subsurface reservoirs (Macgregor, 1993). Asphalt volcanism is characterized by episodic expulsion of heavy hydrocarbons that spread across a substantial area.

Biodegraded asphalt samples illustrate that petroleum hydrocarbons serve as substrates for the diverse chemosynthetic communities (Schubotz et al. 2011), bacterial diester and diether phospholipids found in asphalt samples containing gas hydrate reveals the presence of hydrocarbon-degrading bacteria. Whitish microbial mats that spread across recent asphalt flows

prove that light hydrocarbons such as methane is still present. Evidence of this is seen in a recent study by Wegner et al., 2020 that analyzed the gut content of the mat-grazing sea cucumbers and discovered the presence of methanotrophic biomarkers associated with the microbial mats.

Vestimentiferan tube worms were also seen to flourish on the asphalts by extending the posterior end of their tubes into asphalt fissures or in areas with mixture of asphalt and sea floor sediment. At cold seep sites sulfide is predominantly produced by the activity of sulfate reducing bacteria in the anoxic sediments (Boetius et al., 2000). At the asphalt seeps, these sulfate-reducing bacteria are likely involved in hydrocarbon degradation as has been suggested by isotopic investigations (Schubotz et al., 2011a). Mussels were found residing on some old fragmented asphalt at the bubble site in the Gulf of Mexico, where gas hydrates were detected and methane escaped via vigorous bubbling into the water column (Rubin- Blum et al., 2017; Sahling et al., 2017). In addition, non-chemosynthetic organisms such as galatheid crabs, shrimp, octopods, urchins, and anemones were also discovered to directly or indirectly access the energy provision from the seep system.

1.2 Campeche knolls, Southern Gulf of Mexico

The Campeche Knolls (Figure 1) are home to the deepest active asphalt volcanoes currently known with depths ranging from 2,900 m and 3,150 m (Sahling et al., 2016). This region is a well-known active salt province located in the southern Gulf of Mexico alongside the Sigsbee Knolls (Bryant et al., 1991). Salt tectonics involving the upward migration of salt from deeper strata (Ding et al., 2008) led to formation of knolls and elongated ridges found in the Campeche region. Most of the salt was probably deposited during the opening of the gulf in Late Jurassic (Salvador, 1991b). Sediment thickness of about 5–10 km overlay the salt unit. Movement of the salt influences formation of traps and seals in form of faults and fissures encountered beneath the subsurface which serve as conduit for migration of hydrocarbons to the seafloor. Biomarker analysis from Schubotz et al., 2011b reveals that the oils are derived from Upper Jurassic carbonate source rocks (Tithonian in age) deposited under anoxic and hyper saline conditions.

The deep-seated asphalts deposits serve as natural laboratories for research with regards to the occurrence of oil on deep sea ecosystems. In March 2015, the R/V METEOR Cruise M114 explored the deep sea phenomenon related to deposition of heavy oil in the Campeche area of the southern Gulf of Mexico. The research was carried out to discern the circumstances surrounding the expulsion of heavy oil at the seafloor and its fate over time. During the expedition, samples were recovered at various sites. This thesis will analyze samples from three of these sites, the Chapopote, Mictlan and Tsanyao Yang knolls, which will be introduced in the next chapter.

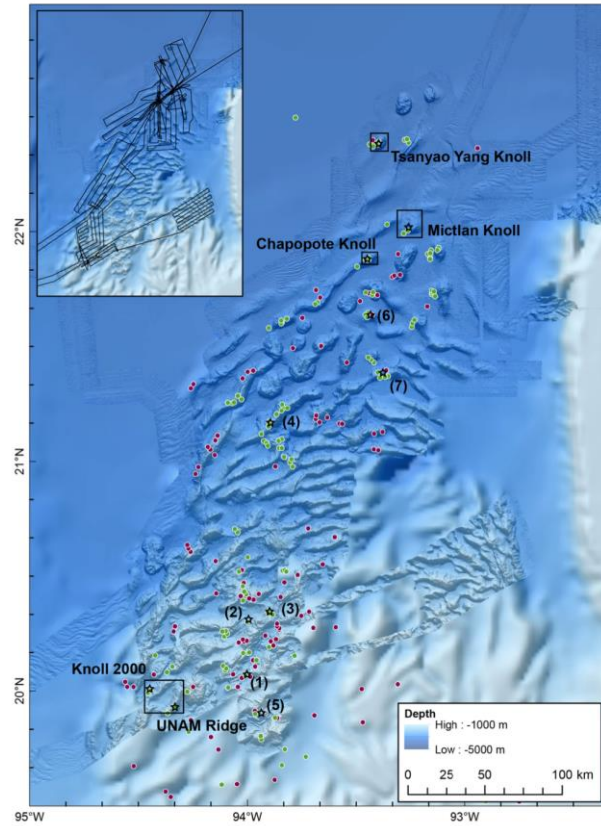


Figure 1. Swath bathymetry of the Campeche Knolls Gulf of Mexico (R/V METEOR Cruise M114) Sahling et al., 2016

1.2.1 Chapopote Knoll

Chapopote Knoll is located in the Northern part of the Campeche Knolls (Figure 1). Chapopote which is the Aztec name for tar is located at the crest of a salt diapir. Highly viscous heavy oil in about 3000 m water depth, is expelled from the subsurface and settles in lava-like flows on the seafloor covering a distance of about 100 to 1000m² (Brüning et al., 2010). The asphalt likely originates from shallow reservoirs located between 100 m and 200 m sediment depth (Ding et al. 2008) and after deposition serves as habitat for benthic biological communities (Sahling et al., 2016). Figure 2 shows the bathymetry map as well as the dive tracks of the Chapopote areas obtained during the R/V METEOR Cruise M114 in 2015 (Sahling et al., 2016). Samples from the three distinct sites (figure 2) obtained during the Cruise M114 in 2015 were further investigated in this study, and these include the old and fragmented Sonne Field (MacDonald et al., 2004), the MAF (main asphalt field) (Brüning et al., 2010) and the bubble site (Rubin-Blum et al., 2017). The study by MacDonald et al., 2004 described asphalt sample recovered from the Sonne Field to be brittle and had no residual stickiness having characteristics of a molten flow subsequently followed by rapid cooling. Further examinations showed that the molecular and isotopic compositions of the gas hydrate as well as sediment headspace was observed to be moderately mature and of thermogenic origin. The ebullition of gas from fragmented asphalts at

the “bubble site” serves as energy source in the form of short-chain *n*-alkanes to invertebrate communities (vestimentiferan tubeworms, bathymodiolin mussels, vesicomyid clams and sponges) that live symbiotically with chemosynthetic bacteria, which provide them with nutrients (methane and hydrogen sulfide) since the invertebrate communities are not capable of directly utilizing them (RubinBlum et al., 2017; Sahling et al., 2017). Samples recovered from the bubble site were incorporated in this study. At the MAF, The sequential overlapping of younger deposits over older ones suggests that three flow units accounts for three distinctive eruptive scenarios (Marcon et al 2018). Unit 3 exhibits a smooth flow structure and appears to be the youngest and least-altered deposits which is overlapping the second oldest flow, Unit 2. The Unit 2 comprises of weathered fragmented asphalt, with visibleropy flow shapes, while the unit 1 which is the oldest deposit however has undergone extensive alteration, and appears to be highly fragmented compared to the overlying units (Marcon et. al.; 2018). The interruption of individual eruption phases allows chemosynthetic fauna to flourish (MacDonald et al., 2004; Sahling et al., 2016). The estimated volume of the main asphalt field (MAF) deposit ranges between $0.8 \times 10^4 \text{ m}^3$ and $1 \times 10^4 \text{ m}^3$ (Marcon et al 2018) and display variable range in viscosity and stickiness which is influenced by loss of lighter or more soluble hydrocarbon compounds (Brüning et al., 2010) as well as effects of microbial biodegradation (Schubotz et al., 2011b). Under water surveys in the Chapopote area have reported gas hydrate occurrences (MacDonald et al., 2004; Schubotz et al., 2011b; Klapp et al., 2010; Sahling and Bohrmann, 2017), gas venting (Brüning et al., 2010), and authigenic carbonates (Naehr et al., 2009), in addition to oil-soaked sediments (MacDonald et al., 2004; Schubotz et al., 2011a, b; Sahling and Bohrmann, 2017).

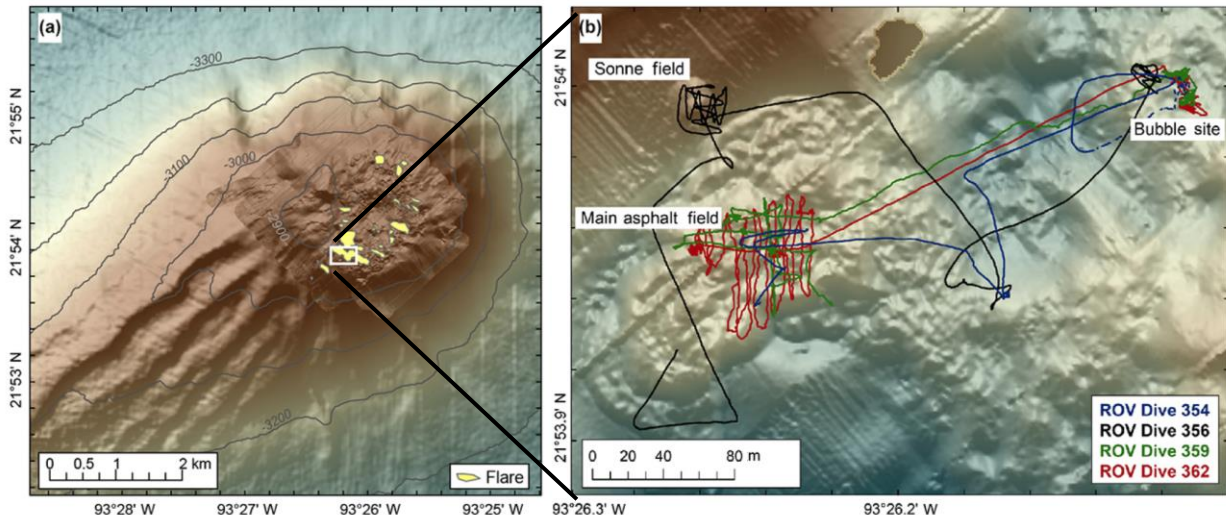


Figure 2. Bathymetry map of Chapopote Knoll (A) AUV-based bathymetry draped over ship-based bathymetry. (B) Enlarged view of ROV QUEST dive tracks. (Sahling et al., 2016)

The expelled heavy oils have a density slightly greater than water (Bruning et, al. 2010) in addition to having a high asphaltene content, and consists of complex high molecular weight NSO-compounds (hydrocarbons that contain nitrogen, sulfur, oxygen) (MacDonald et al., 2004;

Schubotz, 2009; Smit, 2016). Also, the asphalts appear to be oversaturated with methane and higher hydrocarbons; thereby forming gas hydrates (Figure 3D) of thermogenic origin (e.g. Schubotz et. al, 2011, Klapp et al., 2010).

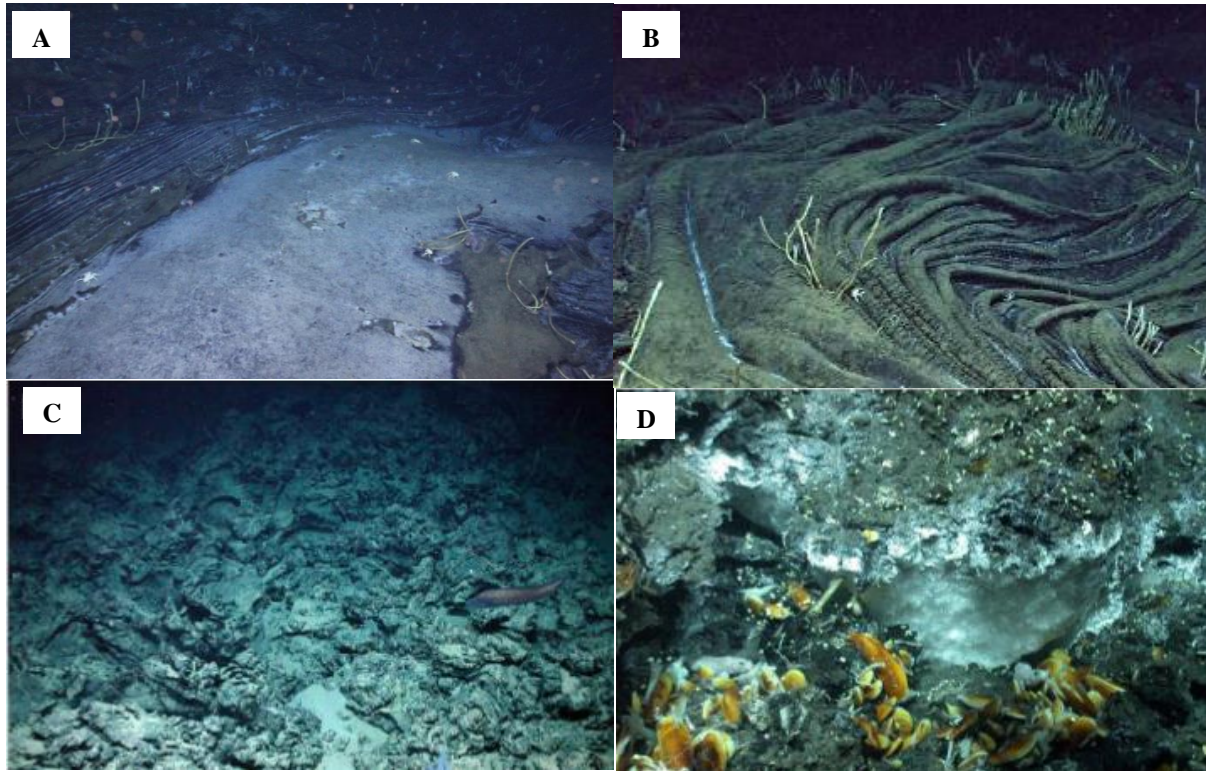


Figure 3. (A and B) Ropy asphalt colonized by whitish microbial mats and tubeworms. (C) Extensively altered asphalt (D) Bubble fabric gas hydrate outcrop hosting mytilids, gastropods, galatheid crab and mussels. Sahling et al., 2016; Marcon et al.; 2018

Chemosynthetic and non-chemosynthetic megafauna (Figure 3) were found to survive off the heavy oil deposit across the MAF, (MacDonald et al., 2004; Brüning et al., 2010; Sahling et al., 2016; Rubin-Blum et al., 2017; Sahling et al., 2017). Intense clustering of white microbial mats were discovered around the most recent deposits in the MAF (Figure 3), and scientific studies have shown that density distribution of the microbial mats relates to how recent the asphalt flow is (Marcon et al 2018).

1.2.2 Mictlan Knoll

Mictlan is the name for underworld in the Aztec language; this knoll exhibits characteristics of an asphalt volcano similar to the Chapopote Knoll (MacDonald et al., 2004, Sahling et. al., 2016). The structural features show evidence of seepage of heavy hydrocarbons as well as gas ebullition along the crater rim located in about 3100 m water depth. Figure 4 shows the AUV-

based bathymetry map as well as the dive tracks of the Mictlan Knoll which was obtained during the R/V METEOR Cruise M114 in 2015 (Sahling et al., 2016). Some characteristic features observed at the Mictlan Knoll include white coated chimney tubes, also called white asphalt tubes (Figure 5A). Gas bubble samplers (Figure 5B) were used to recover samples from the white asphalt tubes. These tubes expel oil droplets at a much slower rate into the water as compared to other sites such as the oily bubble site at Chapopote. It can be speculated that these white asphalt tubes might have formed as a result of hydrocarbon expulsion with similar or just slightly lower density than water, where microbes were able to colonize the outside of these hydrocarbon strings over time. The interior of these white asphalt tubes were analyzed under a microscope and was observed to host ‘fleshy’ microbial mat, oil droplets as well as white precipitate (Figure 5C & D). Escape of hydrocarbon gas from the sea floor as well as gas hydrates exposures were observed around Hydrate Hill (Figure 5E). This area hosts a dense community of vestimentiferan tubeworm. Study by (Sahling et. al., 2016) speculated that hydrates observed at Mictlan Knoll occupy voids between fragmented asphalt.

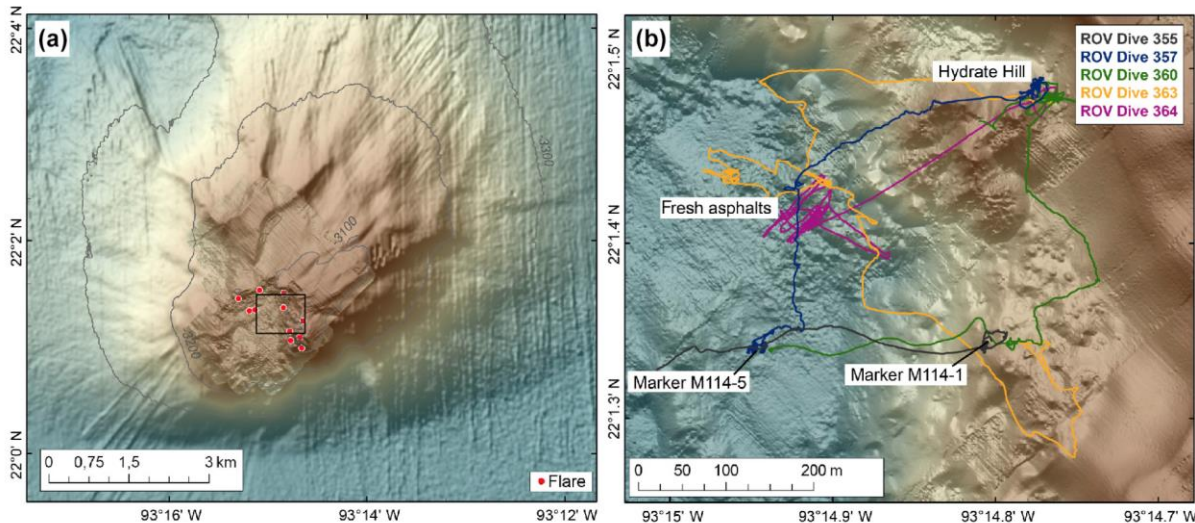


Figure 4. Bathymetry map of Mictlan Knoll (A) AUV-based bathymetry draped over ship-based bathymetry. (B) Enlarged view of ROV QUEST dive tracks. (Sahling et al., 2016)

The study also suggested that the Hydrate Hill is accumulated asphalt that is overlain on top by vestimentifera tube worms and authigenic carbonates. In some other areas within this region, host communities of white bacterial mats, mytilid bivalves (*Bathymodulus brooksi*) and diverse groups of suspension feeders such as anemones, and sponges were detected. Tube worms and mussels were also discovered to be draped with oil (as seen in Figure 5F). Fresh asphalts were observed to display structures that are related to deposition of heavy oil at the seafloor. Flow structures illustrate two types of heavy-oil emission characteristics which include; the extrusion of sheets of heavy oil floating in the water due to positive buoyancy while still attached to the sea surface due to cohesion. The emissions of viscous oil in some cases produce whip-like structures that stay connected to the sea floor. However, as time goes on, the strands and sheets loose buoyancy and accumulate at the sea floor. The other is the seepage of heavy oils with density

higher than that of sea water, which eventually spreads across the sea floor and solidifies with time. Oil bubbles were observed escaping from the sea floor. Sediment samples as well as organisms recovered with the ROV were saturated with oil (Meteor cruise M144).

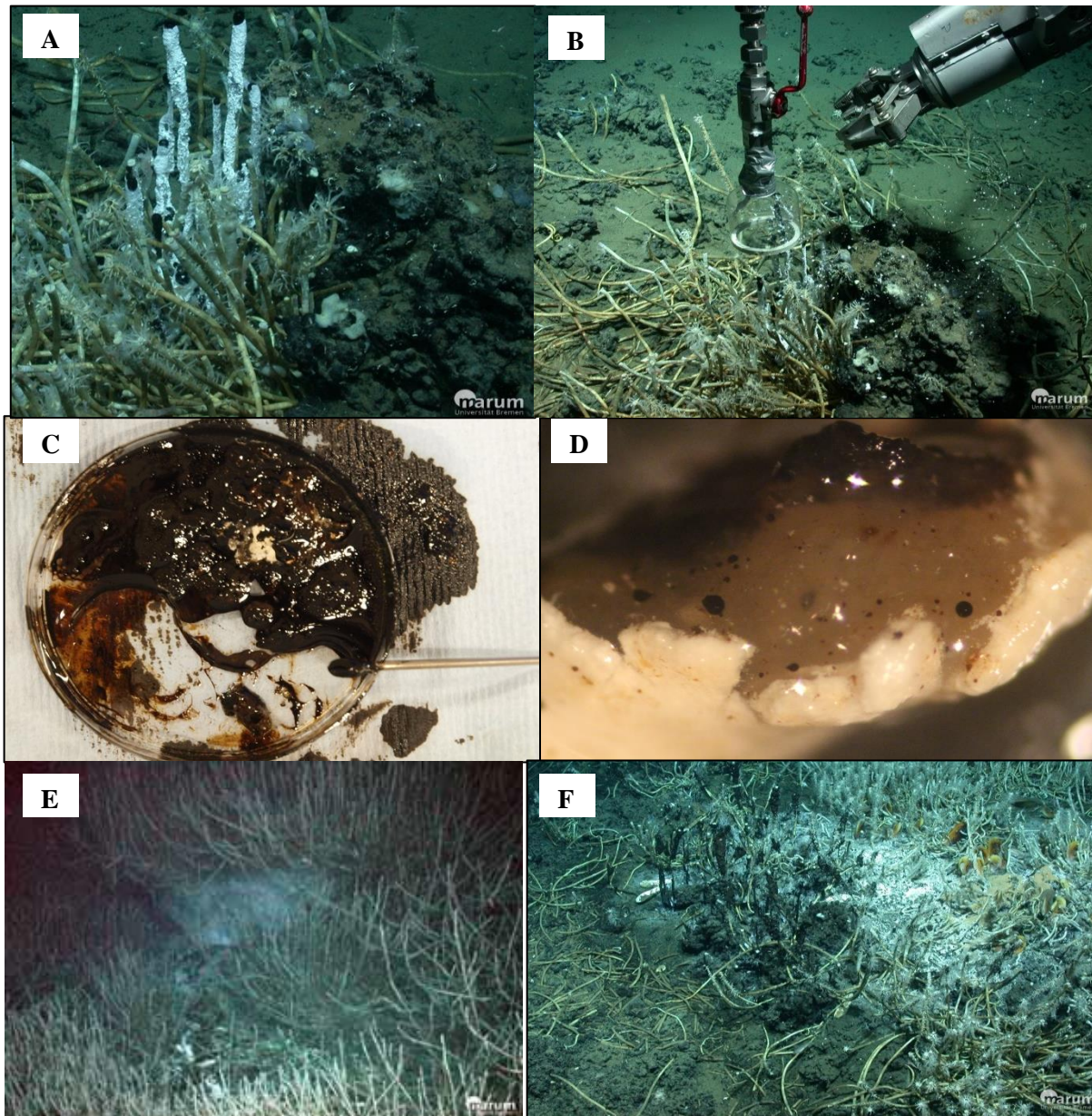


Figure 5. (A) White-coated chimneys releasing oil drops (B) Gas Bubble Sampler (GBS) collecting samples from the asphalt tubes , (C&D) microscopic analysis showing the interior of the white asphalt tubes (E) Vestimentiferan tubeworms on an exposed gas hydrate block at the seafloor (Mictlan Knoll, Hydrate Hills). (F) Oily mussel and tube worm site. (Sahling et al., 2016, 2017)

1.2.3 Tsanyao Yang Knoll

Tsanyao Yang Knoll is one of the most active seepage structures found in a deep marine setting at approximately 3366 m water depth. The knoll is a 400 m high sub-circular structure which stretches about 6 km wide in SW-NE direction, characterized by crater-like central depressions (Sahling et al., 2016). Upon discovery, the knoll was named after Prof. Tsanyao Yang from the Department of Geosciences, National University of Taiwan who passed away during the course of the research cruise M114. Investigation was carried out with the aid of ship-based and AUV-based hydroacoustic mapping (Figure 6) together with seafloor TV-sled and a remotely operated vehicle (ROV). Compared to the Chapopote and Mictlan knolls, there was no evidence of extensive asphalt deposits at the Tsanyao Yang knoll. However, a number of oil and gas emission sites, gas hydrate outcrops in addition to oil slicks at the sea surface were identified (Figure 6). Tsanyao Yang oils also had lower asphaltene and resin constituent compared to Chapopote and Mictlan asphalts, which suggests the oils must have originated from more matured carbonate source rocks (Smit 2016), which was supported by a comparison of the biomarker distributions in oils of the three knolls. Oil slicks observed at the sea surface in this region shows that oil-coated bubbles migrate through water column even from such great depth. Gas bubble emission sites, in form of ‘flares,’ were seen escaping from crater-like structures on top of the knoll. Estimate of about 550–4650 L of hydrocarbons per hour (or 8300–70,600 mol CH₄ per hour) are released in the form of gas bubbles (Römer et al 2019). Pressure-tight gas bubble sampler (GBS) was used to collect samples of gas bubbles escaping the seafloor during ROV dives (Römer et al 2019; Pape et al., 2010). These bubbles comprise of transparent white gas hydrates bubbles as well as oil-coated dark colored hydrates. The gas hydrates were observed to have substantial thickness in the sediments that was observed within mound structures (Sahling et al., 2016) extending about 1-2 m in height and 3-10 m wide.

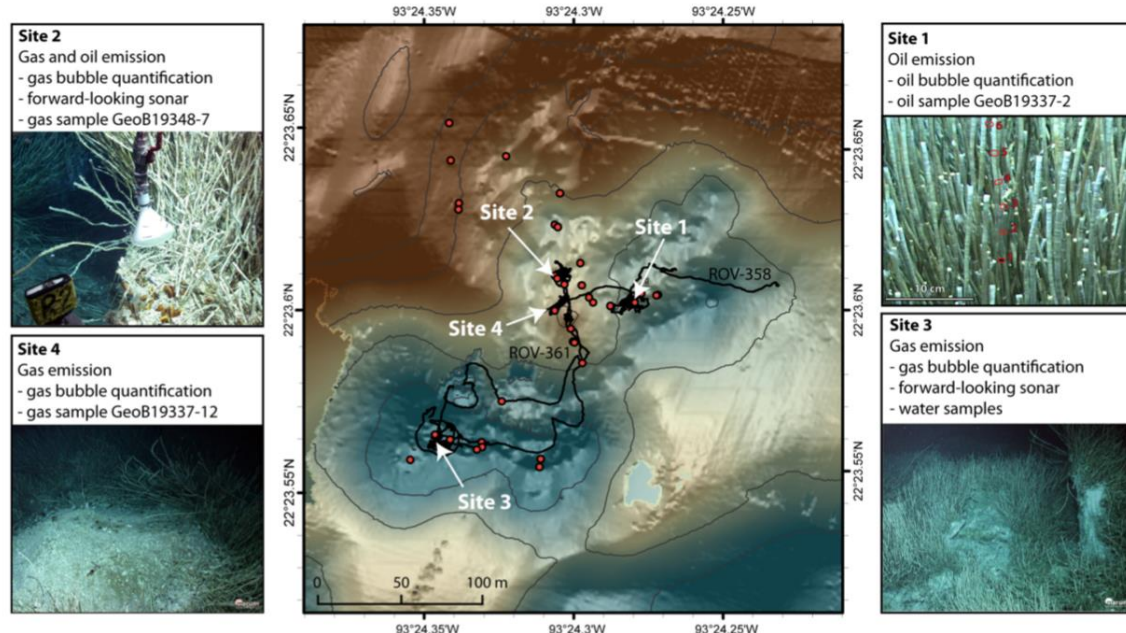


Figure 6. AUV-based high-resolution bathymetry of the main seep field at Tsanyao Yang knoll and seafloor positions of flares (red dots) observed during M114. ROV QUEST dives tracks (black lines). Detailed investigations and gas sampling Sites 1 to 4 are indicated by white arrows. Römer et al., 2019.

These mound structures were immensely covered by tubeworms mussels, clams and other microbial communities. The hydrates function as methane reservoir (Sahling et al., 2002) which influences the diffusion of methane as well as other short-chained hydrocarbons into the surrounding seawater. A vast colony of vestimentiferan tubeworms was observed to be associated with the gas hydrate outcrops in this knoll. Ice worms (cf. *Hesiocaeaca methanicola*) were also discovered residing in the bubble-fabric hydrate.

A pillar like structure (Figure 7) that constitutes of oil bubbles and oily gas hydrate with a cap of carbonate was observed to host chemosynthetic life such as vestimentiferan tubeworms and mussels. These bubbles of gas hydrate were formed from rising bubbles that accumulate on a vertical structure due to adhesion (Sahling and Bohrmann, 2017; Sahling et al., 2016). The vestimentiferan tubes were dominated by colonies of epifaunal suspension feeders the such as hydrozoans and anemones. The carbonate was believed to have formed under anoxic conditions as a result of the interior of the rhizosphere of the tube worms.

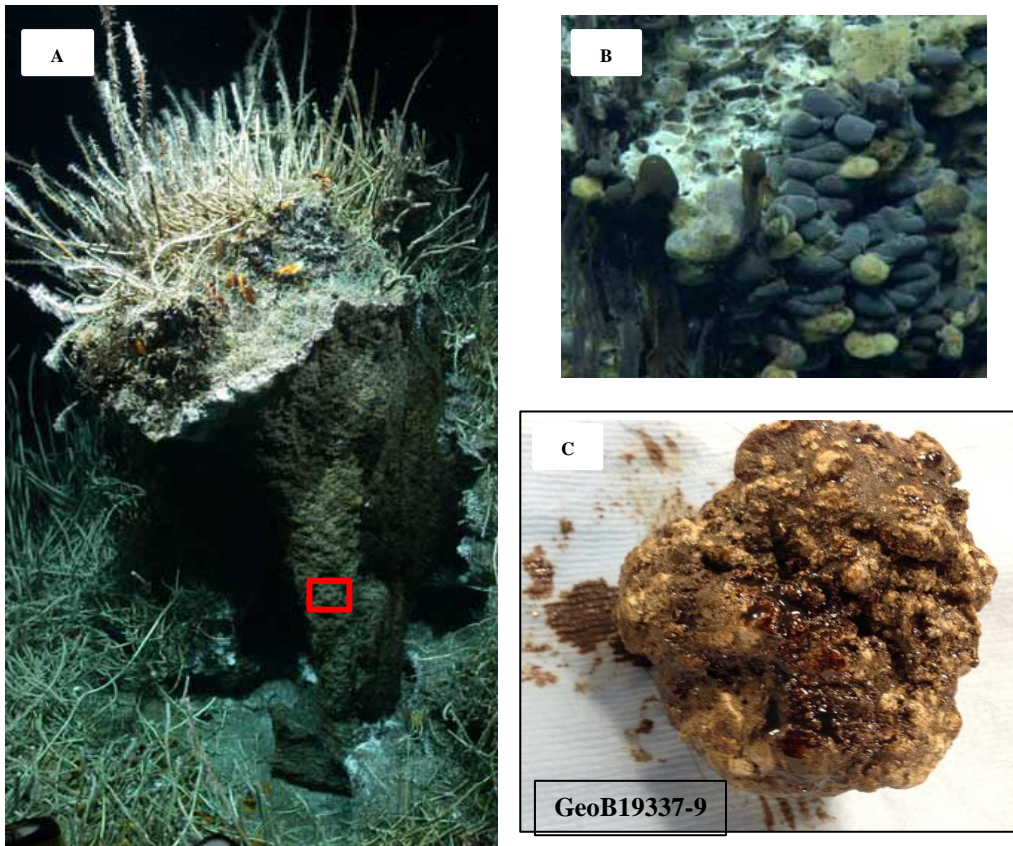


Figure 7. (A) Pillar-like structure of oily gas hydrates bubbles with a cap of carbonate and tube worms (B) a much closer look (red box in image A) at the features of the structure showing oil bubbles (dark color) and hydrate (white) covered by yellowish brown microbial mat (C) Carbonate rock sample with oil drapes.

1.3 Petroleum Biodegradation

1.3.1 Persistence of Heavy oil and fate of the oil

Oil is comprised of thousands of different compounds having unique chemical structures and distinct properties. Studies (e.g. Ruddy et al., 2014, Aeppli et al., 2012) investigated the long-term effects of the deep water horizon oil spill with the aid of Two-dimensional gas chromatography coupled to a time of flight mass spectrometer (GCxGC-MS) and Fourier Transform Ion Cyclotron Resonance Mass Spectrometry (FT-ICR-MS). They observed that oxygen-containing hydrocarbons increased with time and are likely to get into the water phase. Escape of hydrocarbon and its constituents into the environment is alarming as some of the organic pollutants such as polycyclic aromatic hydrocarbon (PAHs) have carcinogens and neurotoxic effects and are also known to have high environmental persistence, low volatility and resistance to microbial degradation (Bamforth et. al, 2005). This unfortunately poses great danger to the environment as well as the marine ecosystem. PAHs are toxic recalcitrant group of contaminants, with two or more fused benzene rings, which come about as a result of incomplete combustion of petroleum fuels (Tsai et. al, 2009). Low molecular weight PAHs having two or three rings (e.g. naphthalene and phenanthrene) are soluble in water and can easily come in contact with ground or surface water thereby posing a significant threat to the environment (Meckenstock et al., 2004). Numerous studies described how the polarity of a compound affects their solubility as hydrocarbon molecules tend to be more soluble in water as they get more polar. The effects of exposure of these contaminants to the environment are quite tremendous. In contrast, high molecular weight PAHs which comprises of four or more benzene rings, (e.g. pyrene, benzo [b] fluoranthene and benzo [g,h,i] perylene) can combine with sediment particles, thereby minimizing their contamination in the environment (Meckenstock et al., 2004). However, numerous studies have proven that some microbial communities thrive in such environment and are able to degrade and remineralize some unique types of PAHs. Petroleum hydrocarbons undergo a series of weathering processes as soon as it is exposed to the marine waters and the duration for these processes range from hours to years up to as much as decades (Sadek et al. 2017), lighter hydrocarbon compounds evaporate as soon as a spill or seepage occurs. Microbial activity as well as other natural weathering processes, in the form of evaporation, dispersion, and water washing influences the composition of the petroleum hydrocarbon after its release as these activities results in the formation of polar hydrocarbon compounds and other related intermediates. These polar compounds are more readily soluble in water and tend to have longer residual time (Meckenstock et al. 2004).

Petroleum is a complex mixture of various hydrocarbon components which is comprised of aliphatic, cycloalkanes, aromatics, asphaltenes and resins of which a number of these compounds have been proven to be toxic and carcinogenic (Philip et. al. 2005, Yemashova et. al. 2007).

Saturates have been proven to show the highest biodegradation rates, which is superseded by the light aromatic compounds. High molecular weight PAHs such as asphaltenes and resins display exceptionally low to no degradation (Atlas and Bragg 2009). Hydrocarbons in the environment are primarily biodegraded by bacteria, yeast, and fungi (Leahy & Colwell 1990), with bacteria being the dominant degrader in marine ecosystems and fungi becoming influential with respect to freshwater as well as terrestrial environments (Olajire and Essien 2014). The activities of

microorganisms on the oil compounds involve the natural breakdown of complex oil components into simpler substances. Studies have described a systematic breakdown of hydrocarbon with respect to their degree of susceptibility to microbial biodegradation. Firstly the short chain *n*-alkanes are removed, followed by branched and isoprenoid aliphatic compounds and then low molecular weight aromatics, cyclic alkanes which is the followed by the aromatic hydrocarbons and finally biomarkers such as steranes and terpanes (Wenger and Isaksen, 2002) of which are the most resistant. The systematic breakdown of organic substances into smaller components by the enzymes which are produced by microorganisms (Haddock 2010), subsequently transforms these substances to end products such as carbon dioxide or methane and water. This can occur either by aerobic or anaerobic processes (Head et al., 2014; Prince et al., 2007). Aerobic processes has to do with the microbial incorporation of oxygen to degrade hydrocarbon compounds while anaerobic processes occurs in the absence of oxygen and requires other electron acceptors such as ferric iron (Fe^{3+}), sulfate (SO_4^{2-}) and nitrate (NO_3^-) (Foght 2008). A study by Borgne and Ayala (2010) investigated the microorganisms which degrade and utilize sulfur containing PAHs via the 4S pathway, owing to the fact that sulfur is the most abundant heteroatom in petroleum hydrocarbon and also one of the most recalcitrant in nature. Sulfur containing components are mainly found in thiophenes and other NSO compounds. However, the focus in this study is primarily centered on the aerobic processes associated with microbial degradation.

1.3.2 Aerobic biodegradation

The complete breakdown of most organic pollutants occurs under aerobic conditions (Bamforth et al., 2005) see figure 8. The fundamental intracellular interaction with organic pollutants is an oxidative process that involves incorporation of oxygen. Oxygen serves as a high-energy-yielding terminal electron acceptors (TEA). The enzymatic key reaction is catalyzed by oxygenases and peroxidases which activates the hydrocarbons (Widdel and Musat, 2010; Fritzsche and Hofrichter 2000). A Paper by Lemkau et al., 2014 has demonstrated that aerobic hydrocarbon degradation is primarily controlled by microbial activity, in which the transformation results to the release of oxygenated dissolved organic matter (DOM). Figure 8 shows the main principle of aerobic degradation of hydrocarbons. Haddock 2010 summarized the aerobic degradation pathways for aromatic hydrocarbons and also described the mechanisms involved. Petroleum hydrocarbons are an abundant source of carbon and energy for microbial growth (Haddock 2010) and the systematic break down involved in degradation pathways (Fritzsche and Hofrichter 2000) sequentially convert organic pollutants into intermediates such as alcohols, aldehyde / ketones and carboxylic (fatty) acids. For example, alkanes undergo oxidation by monooxygenase to yield secondary alcohols, and subsequent intermediates like ketones, and then to fatty acids (Whyte et. al., 1998, McDonald et. al., 2006). Cycloalkanes are to some extent resistant to microbial attack (Fritzsche and Hofrichter 2000) due to lack of a defined methyl component.

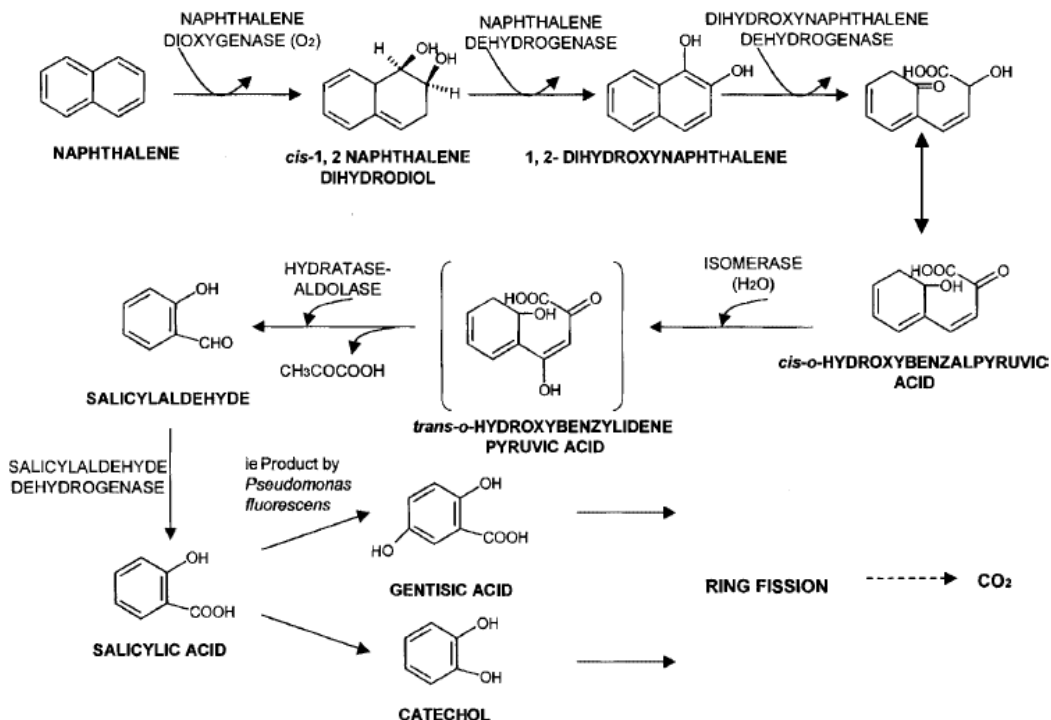


Figure 8. Aerobic degradation of naphthalene by bacteria (Bamforth and Singleton 2005)

A study by (Hazen et al. 2016) summarized the microbial response following the deep water horizon oil spill which showed that the effectiveness of hydrocarbon degradation by microbial communities depends on a number of factors including environmental conditions (such as nutrient availability, dissolved oxygen, water temperature), physical conditions of the system (e.g., currents, eddies, waves) which influences the dispersion and diffusion of oil in the water column. In addition, the diversity and adaptability of the microbial communities in an oil contaminated site enhances the biodegradability of the oil components.

1.4 Previous asphalt incubation study

A previous study by Jonas Brünjes (Master Thesis 2018) used asphalt samples collected during expedition M114 to investigate the release of oil-derived dissolved organic matter (DOM) into the water column. With the aid of ultra-high-resolution mass spectrometry (FT-ICR-MS) and excitation-emission matrix (EEM) spectroscopy changes in the molecular composition in the DOM could be monitored. In this study, hydrocarbon degradation was investigated through a laboratory simulation using artificial seawater and a non-biodegraded asphalt sample (GeoB19339-1), collected with a gravity corer (at 2905 m water depth) from the main asphalt field at Chapopote during the M114 cruise in march 2015 (Sahling et al., 2017). The artificial seawater used during the experiments was prepared according to Widdel and Bak (1992), and consisted of salts, trace metals, inorganic nutrients and a carbonate buffer, to mimic natural seawater. Biotic and abiotic weathering processes were distinguished by conducting triplicate live incubations as well as dead control which was pasteurized at 60°C for 2 hrs. The

experiments were conducted over 28 days period without light at room temperature. ^{13}C labelled substrates (aliphatic hexadecane and aromatic naphthalene) were added to some of the incubations in order to stimulate microbial activity and also enable tracing of intermediates of aliphatic and aromatic degradation pathways, while one experiment (asphalt only) was prepared with no additional substrate to mimic most closely natural conditions. For the biotic experiments, Jonas Brünjes observed humic-acid like fluorescent compounds as well as an increasing proportion of polyphenols in addition to the large quantities of dissolved organic carbon released into the water which comprises of oxygenated DOM with small molecular masses. The abiotic weathering on the other hand released slightly more saturated DOM with higher molecular masses. The experiment recorded a decrease in oxygen concentrations in all samples, including the dead controls. On the other hand, an increase in CO_2 concentrations was observed in the biotic experiment but remained unchanged in the dead controls, indicating that the live incubations were indeed active while the dead controls remained inactive.

For this thesis, I will be investigating the same water samples of the incubation experiments from Jonas Brünjes 2018, but will be focusing on characterizing the hydrocarbon composition by GC-MS, which will provide complementary information to the existing DOM and FDOM (fluorescent DOM) data sets. In addition a number of environmental samples from the above described sites from the Campeche Knolls, including oil slick samples recovered during the Meteor Cruise M114 in 2015, will be investigated to compare the laboratory incubation results with.

1.5 Objectives and Motivation

The working hypothesis of this thesis is that during petroleum biotic and abiotic weathering processes different types of hydrocarbon compounds get released into the water column. It is currently not clear whether these hydrocarbons are potentially toxic or harmful for the environment or whether they are detoxified and the pollutants are efficiently removed from the environment. Most investigation of oil spills up to date have primarily focused on changes occurring with the solid phase, but the knowledge of the compounds released into the water phase in the environment is still limited. The southern Gulf of Mexico provides an excellent opportunity to investigate the fate of oil in a natural petroleum seepage environment and the involvement of microorganism. A lot of studies have emphasized the influence of microorganism with respect to hydrocarbon degradation which results in the formation of oxygenated compounds (e.g. Lemkau et al., 2014, Aepli et al., 2012, Smit 2016, Brünjes 2018), which have a greater affinity to go into the water phase. With this opportunity, I envision that the results of my thesis will add to the knowledge about petroleum transformations in the environment and will provide important insights for future bioremediation approaches.

The aim of this thesis is to investigate the dissolved organic matter of asphalt incubations and environmental samples using gas chromatography coupled to mass spectrometry (GC-MS) in order to obtain structural information of the petroleum compounds and their intermediates which are released into the water phase. These investigations will enable to determine the fate of the oil

following exposure to the environment where it is subjected to both aerobic and anaerobic processes. Since the asphalt incubation studies are designed to enable deciphering between biotic or abiotic processes this will also allow to assess the relative significance of biotic and abiotic processes occurring in the environment. Environmental water samples investigated in this study were collected at different depths of the three knolls Chapopote, Mictlan and Tsanyao Yang.

1.5.1 Research questions

Environmental oil spill studies were so far mainly centered on the analyses of the solid phase, however for this study, the main interest is to look at the changes of the dissolved organic matter pool using GC-MS. My primary goals pertaining to this research would be to determine the fate of the oil following exposure into the environment by providing answers to these research questions:

- (1) Which of the hydrocarbon compounds (apolar and polar) are released into the water phase during hydrocarbon degradation in the asphalt incubation experiments?

Hereby, I envision encountering aromatic compounds such as naphthalene and phenanthrene and their alkylated derivatives as well as heteroatomic (oxygen, sulfur, nitrogen) containing PAHs (e.g., dibenzothiophene) as these are abundantly found in the asphalts (Smit, 2016) and at the same time are compounds that are comparably soluble. Furthermore, Brünjes (2018) reported a relative increase over time for PAH compounds in his live asphalt incubations. I also expect to find compounds proposed to be intermediates of aromatic hydrocarbon biodegradation (especially in the naphthalene incubation experiment) as well as other oxygenated intermediates formed during microbial transformation (Lemkau et al., 2014; Aeppli et al., 2012).

- (2) Do the identified compounds represent intermediates of microbial hydrocarbon degradation?

To answer this question, the results obtained from the analysis in this thesis will be compared with what is known from the literature pertaining to biotic (microbially influenced) and abiotic (dissolution) processes.

A primary indicator of hydrocarbon biodegradation is the loss of *n*-alkanes, while dissolution of petroleum hydrocarbons is most likely to occur for PAHs and PASHs compared to saturate compound with the same number of carbon atoms (McAuliffe, 1980), due to their differences in solubility. For instance, PASH such as dibenzothiophene is more soluble than phenanthrene. In addition, alcohols are known to be more soluble in water due to the polar hydroxyl group than hydrocarbons and are also known biodegradation intermediates. It is likely that alcohols would be detected in the biotic experiments and to a lesser degree in the abiotic incubation experiment.

- (3) Comparing experimental results with field-based data: Are the short-term observations made during the asphalt incubation experiments also observed in the environment?

Considering that biodegradation of petroleum hydrocarbons is influenced by a number of factors such as dissolved oxygen concentration, water temperature, nutrient availability and salinity (Hazen et al. 2016; Wang et al., 1998; Palmer 1984), particularly temperature and nutrients could play a major role for any observed differences between the incubation experiment and the environmental samples. Since the asphalt incubation experiment was carried out under room temperature and with the addition of substantial nutrients in the millimolar range, this could eventually speed up biodegradation processes that would take longer at the seafloor where temperatures are only 4°C and nutrients are in the micromolar range. It is also to be expected that the microbial community present as well as the time scales of biodegradation influences the types of compounds that are released into the environment. Therefore, I would expect to see some similarities in metabolites in both the asphalt incubation and the environmental experiments since the microbial community involved is expected to be the same although the influencing factors might vary in both experiments.

2. Materials and methods

This study investigates the transfer of petroleum hydrocarbons into the water column by analyzing water samples from asphalt incubations as well as environmental oily water samples retrieved from three hydrocarbon seeps sites (Chapopote, Mictlan and Tsanyao Yang) in the southern Gulf of Mexico (Sahling et al., 2016). The samples analyzed in this thesis were collected during Meteor expedition M114 cruise in March 2015, the individual sample sites are detailed in the introduction.

2.1 Environmental samples

Water samples were collected either in Niskin bottles mounted onto the remotely operated vehicle (ROV) QUEST 4000 or by a gas bubble sampler also operated by the ROV (Pape et al., 2010; Römer et al., 2020). Oil slick samples were collected either with a rubber boat using combusted glass bottles sealed with a solvent-cleaned aluminum cap or with a bucket from the side of the research vessel. Table 1 shows list of analyzed samples with their exact location and sampling devices.

Table 1. Investigated environmental samples, location, depth (masf) and collection instruments. Cruise: M 114-2 GoM 2015. Sample type: water HC

Location	Station (GeoB)	Dive	Gear	Latitude N	Longitude W	Depth (masf)	Water vol. (ml)	Comments
Chapopote Sonne Field	19333-4	D356	ROV	21°53.990	93°26.255	0.5	210	'Niskin 1
Chapopote Sonne Field	19333-7	D356	ROV	21°54.005	93°26.127	bottom	240	'Niskin 2
Chapopote Main asphalt Field (MAF)	19340-2	D359	ROV	21°53.954	93°26.238	bottom	235	Niskin 1, top of fresh asphalt covered by bacterial mat
Chapopote Oil bubble site	19340-4	D359	ROV	21°53.995	93°26.113	3	495	'Niskin 2
Chapopote Oil bubble site	19351-14	D362	ROV	21°53.994	93°26.111	bottom	200	PC16, bottom water moderately oily
Mictlan Mussel bed	19327-3	D355	ROV	22°01.352	93°14.906	0.5	575	'Niskin 1 0.5m above seafloor
Mictlan Mussel bed	19327-4	D355	ROV	22°01.349	93°14.802	1	680	'Niskin 2 1m above mussels
Mictlan Asphalt tubes	19336-6 oily	D357	ROV	22°01.341	93°14.948	bottom	225	Bio-box Oil from asphalt tube, solid phase
Mictlan Asphalt tubes	19336-6	D357	ROV	22°01.341	93°14.948	bottom	545	Bio-box Surrounding water (asphalt tube)
Mictlan Asphalt tubes	19336-5	D357	ROV	22°01.341	93°14.951	bottom	270	GBS black oily
Mictlan Oily mussel bed	19346-4	D360	ROV	22°01.485	93°14.769	bottom	370	GBS blue
Mictlan	19346-	D360	ROV	22°01.343	93°14.792	bottom	125	GBS black moderately

Oily mussel bed	15							oily
Mictlan	Oil slick					Surface	2000	collected with bucket
Tsanyao Yang Oil bubble site 1	19337-2	D358	ROV	22°23.604	93°24.279	bottom	395	GBS black (oily)
Tsanyao Yang Oil bubble site 1	19337-3	D358	ROV	22°23.604	93°24.280	1.5	505	Niskin 1
Tsanyao Yang Oil bubble site 1	19337-9	D358	ROV	22°23.603	93°24.279	bottom	60	(very oily) droplets in yellow net
Tsanyao Yang	Oil slick	Site 1				Surface	3180	moderately oily
Tsanyao Yang	Oil slick	Site 2				Surface	2000	moderately oily

2.2 Incubation experiments

The asphalt incubation experiments was carried out by Jonas Brünjes (Master Thesis 2018) using asphalt samples (GeoB19339-1) retrieved with the aid of a gravity corer during the M114 cruise from the main asphalt field at Chapopote at a water depth of 2905 m at the geographical location (Lat N 21°53.951) (Long W 93°26.210). The sample material is attributed to be a soft asphalt (Marcon et al. 2018), from the most recent asphalt flow unit 3, having no distinctive microbial coverage. Investigations by Sahling et al. (2017) showed elevated methane concentrations in this sample. For the asphalt incubation, different ¹³C-labeled substrates were added to stimulate microbial activities associated to different compounds classes of petroleum hydrocarbons and to allow tracing the flow of carbon in the system: ¹³C-labeled hexadecane was added to stimulate aliphatic hydrocarbons degraders (from here on termed “Hexadecane”) while ¹³C labeled naphthalene was added to stimulate aromatic hydrocarbon degraders (from here on termed “Naphthalene”). In addition, an incubation experiment was prepared with no added substrates (from here on termed “Asphalt only”) to mimic most closely natural conditions. All experiments were conducted in triplicates in artificial seawater over a period of 28 days at room temperature in the absence of light. Table 2 shows an overview of the samples available for this study. To monitor abiotic asphalt weathering processes such as water washing (dissolution) and their respective products and intermediates, microbial activity was inhibited by pasteurization (2 hrs. at 60 °C) of the samples. It is suspected that this process might not have completely eliminated the microbial influence in oil degradation, but has greatly reduced them (for details see Brünjes, 2018). The biotic and abiotic experiments allow distinguishing intermediates in the transformation of the oil components related to these two processes that can help to tell them apart in the environment.

After 10 days and 28 days water samples were collected for each of the asphalt incubation experiments for hydrocarbon analyses. For this, ca. 20 ml of the water used during the incubation was filtered through a combusted glass fiber filter (0.3 µM GFF, Sartorius, USA) and stored at -20 °C in 40 mL glass vials sealed with Teflon caps.

Table 2. Biotic and abiotic asphalt incubation experiment

Incubations	Time point	Replicate samples	water ml	TLE aliquot %	BAME Std ng
Sample ID	Days	Biotic			
Asphalt only	10	1	20	29.8%	100
		2	20	29.8%	100
		3	20	29.8%	100
	28	1	20	29.8%	100
		2	20	29.8%	100
		3	20	29.8%	100
Naphthalene	10	1	20	29.8%	100
		2	20	29.8%	100
		3	20	29.8%	100
	28	1	20	29.8%	100
		2	20	29.8%	100
		3	20	29.8%	100
Hexadecane	10	1	20	29.8%	100
		3	20	29.8%	100
		1	20	29.8%	100
	28	2	20	29.8%	100
		3	20	29.8%	100
		Abiotic			
Asphalt only	10	Analytical blank	20 water+solvent	29.8%	100
			20	29.8%	100
			20	29.8%	100
Asphalt only	28		20	29.8%	100
			20	29.8%	100
			20	29.8%	100

2.3 Liquid –liquid extraction

All of the glass ware used in this thesis were combusted before use or solvent-cleaned with methanol (MeOH) and then dichloromethane (DCM). The materials used for the liquid-liquid extraction consists of the incubated samples, DCM, MeOH, hexane, 6 M HCl, separatory funnels and caps, flat bottom flasks, turbovap vials and concentration workstation (for drying), statives and rings, stoppers, Pasteur pipette, tweezers, racks, litmus paper and nitrile gloves.

2.3.1 Asphalt incubation samples

Regarding the asphalt incubations samples, one of the samples (asphalt only dead control, 10 days) was empty and one (hexadecane replicate 2, 10 days) was missing. We continued to use the empty vial by rinsing it with Milli Q water and DCM and treating it the same way as the other samples and consequently used it as an analytical blank for the extraction and sample work-up. The water samples from the incubations (ca. 20 ml) were transferred into separatory funnels using Pasteur pipettes. Subsequently, 20 ml of DCM and ethyl acetate (1:1, v/v) was added to the content in the separatory funnel, with caps closed and vigorously shaken. Gas build up was release by gently opening the stoppers at intervals while holding the separating funnel in an inverted position with caps tightly closed. The content was allowed to settle for few minutes after which separation of the organics from the aqueous phase was achieved. The organic phase was collected into a flat bottom flask and the procedure was repeated two more times to ensure a higher extraction efficiency. The remaining aqueous phase in the separatory funnel was then acidified with 6 M HCl to a pH of 2 in order to yield organic acids and then the extraction process using DCM and ethyl acetate was repeated two to three more times and the organic phase collected in the flat bottom flask. The residue aqueous phase was disposed and the organic phase was further washed with milli Q water for three times to remove any aqueous residue in the organic phase. After the third wash, the organic phase are collected in turbovap vials and placed in the concentration work station to dry in a water bath (37 °C) under a stream of nitrogen. The dried samples were transferred into 4ml vials using DCM and a Pasteur pipette and placed under a stream of nitrogen gas (N_2) in a protected fume hood to dry after which they were stored at -20 °C for further analysis.

2.3.2 Environmental samples

Different volumes of the collected water from the environment (60 to 3180 mL; (Table 1) were already extracted with DCM on board the research vessel Meteor in the cold room using 5 to 100 ml DCM and subsequently frozen at -20 °C in combusted glass vials and sealed with solvent-cleaned Teflon caps. In the laboratory onshore, the DCM extracts were transferred to a separatory funnel and extracted again with 20 ml of DCM and ethyl acetate (1:1, v/v) and water following the same protocol as described above for the asphalt incubation samples.

After the liquid-liquid extraction, these samples had undergone further separation procedures just before they are passed on for GC-MS analysis. The (Figure 9) shows a stepwise illustration of the various procedures employed in this study.

2.4 Asphaltene precipitation

Due to the very oily nature of some of the environmental samples, complete evaporation became difficult to achieve. Furthermore, prolonged evaporation would facilitate the loss of the light end of the petroleum mixture. Very oily samples were further cleaned up by asphalt precipitation and subsequent column chromatography. For this, the TLE was dissolved in a mixture of DCM and MeOH (9:1) and either 2% (for samples GeoB19336-5, GeoB19337-2, GeoB19337-9) or 10% of the TLE (for samples GeoB19336-6 oily, GeoB19346-15, GeoB19351-14, and the oil slick from Tsanyao Yang site 1 and 2) were subjected to asphaltene precipitation by using *n*-hexane to separate the asphaltenes from the maltenes (Bowden et al., 2006). Asphaltenes are highly polar macromolecules which are not soluble in apolar solvents (e.g. *n*-hexane) while maltenes consists of low molecular weight compounds that are readily dissolved in *n*-hexane. After the addition of *n*-hexane to each sample, they were sonicated for 10- 15 minute in an ultra-sonic bath and then stored in the fridge for 2 hours or more (in some cases overnight). The samples were thereafter centrifuged for 10 minutes at a rate of 1500 rpm (ramps per minute), after which the samples were effectively separated with the asphaltene precipitates settling at the bottom. Using a pipette, the maltene mixtures were transferred to newly prepared 4ml vials. Additional *n*-hexane was introduced into the asphaltene precipitate and the above described procedure was repeated two more times. The collected maltene fractions were then dried in the fume hood over night to allow the *n*-hexane to evaporate. These were the fractions used for further analyses described below.

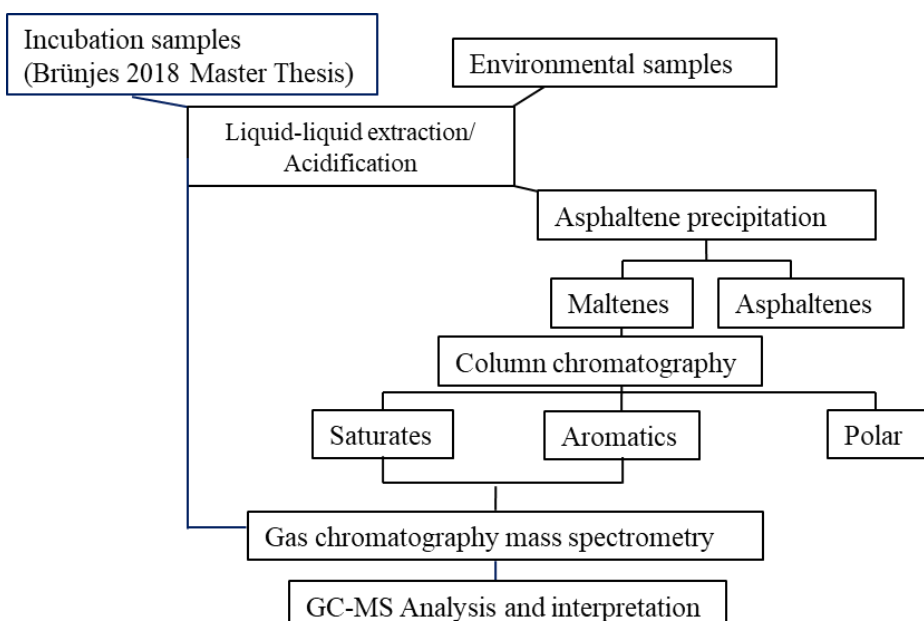


Figure 9. Schematic of the steps employed for the analysis of the water samples from asphalt incubation experiments and the environmental water samples.

2.5 Column separation

The dried maltene fractions of the asphaltene precipitated samples were further separated into three fractions by silica gel column chromatography (Wang et al., 1994). This technique involves the use of different solvents with different polarities to elute chemical components into fractions of saturates (F1), aromatics (F2) and a polar fraction (F3) (Table 3). The column was packed with combusted glass wool and filled with about 5 g of silica gel and systematically compacted by slightly hitting the column to allow settling of the glass wool and silica gel in order to avoid gaps in the column. The maltene fractions were dissolved in a small volume of DCM (ca. 40 to 100 µL) and then transferred to the top of the silica gel in the column and allowed to dry. The dead volume (dV) was determined by progressively adding a known volume of *n*-hexane into the column until the first drop comes out. The dead volume is the volume of solvent needed to wet the packed silica gel column. The saturates fraction (F1) were eluted with 1.5 times the dV of *n*-hexane, the aromatics fraction (F2) were eluted with a mixture of *n*-hexane: DCM with a ratio (7:3) 3 times the dV, polar hydrocarbon containing fraction (F3) were eluted with DCM: methanol (1:1) 4 times the dV (Table 3). In this study, the main focus is directed to the F1 and F2 fractions while the F3 are excluded from further analysis.

Table 3. Separation protocol for the column chromatography

Fractions	Solvent(s)	Dead volume (dV)	Compound class
F1	<i>n</i> -Hexane	1.5	Saturates
F2	<i>n</i> -Hexane:DCM (7:3)	3	Aromatics
F3	DCM:MeOH (1:1)	4	Polar hydrocarbons

2.6 Gas chromatography coupled to flame ionization detection (FID) and mass spectrometry (GC-MS)

Gas Chromatography is used to analyze small and volatile molecules and by combination with mass spectrometry allows identifying various components within a given sample. Most of the samples were analyzed as TLEs by gas chromatography (GC) coupled to flame ionization detection (FID) and mass spectrometry (GC), but a select set of samples where the oil mixture was very complex, only the saturates (F1) and aromatics (F2) fractions were analyzed. These include samples GeoB19336-5, GeoB19337-2, GeoB19337-9 and GeoB19351-14. First, the samples were analyzed on a ThermoFinnigan Trace GC coupled to a FID without the addition of a standard to check the overall abundance of hydrocarbons in the extracts. For these analyses and aliquot of 10% of the samples were used. The GC was equipped with a Restek Rxi-5ms column (30 m length, 0.25 mm internal diameter, 0.25 µm film thickness), Restek GmbH, Bad Homburg, Germany). Helium was the carrier gas at a flow rate of 1.0 ml min⁻¹. Sample injection was performed in splitless injection mode and separation of compounds was achieved with the following temperature program: initial oven temperature 60 °C (held for 5 min), then ramped to

175 °C at a rate of 6 °C min⁻¹ and ramped to a final temperature of 300 °C at a rate of 3 °C min⁻¹ (held for 10 min). Identification and quantification of petroleum hydrocarbons was accomplished using an Agilent 6890N GC instrument coupled to an Agilent 5973 inert Mass Selective Detector (MSD) with an electron impact (EI) source. The GC was equipped with the same column as described above for the GC-FID analyses and separation of compounds followed the same temperature program. For GC-MS analyses 10 to 40% of a sample aliquot was amended with 100 ng of an injection standard (behenic-acid-methylester, Sigma Aldrich) with a final injection of volume of 0.3 to 2% of the sample (depending on hydrocarbon abundance in the sample).

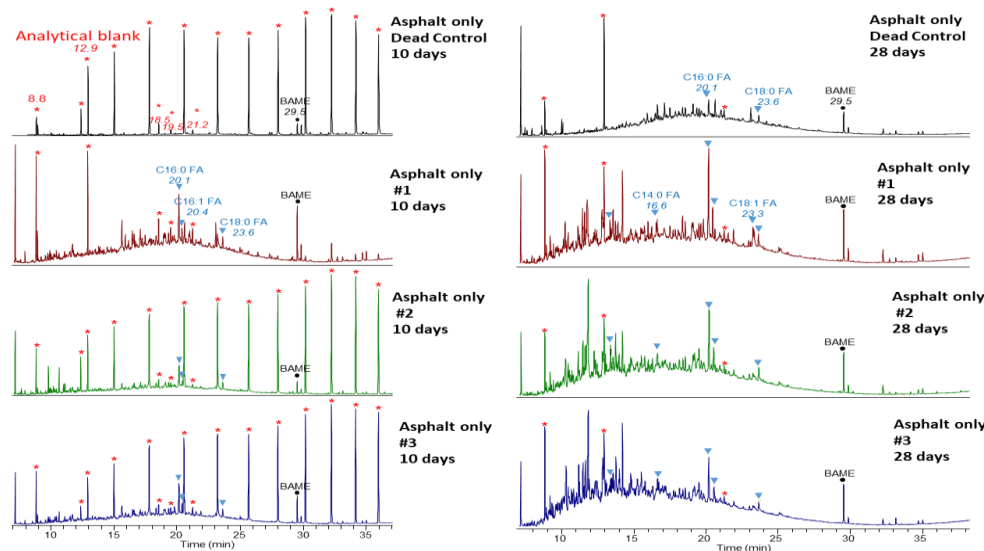
3. Results

3.1 Asphalt Incubation Experiment

Analytical Blank: As already mentioned in the Methods section, the vial labeled “asphalt only dead control, time point 10 days” was empty. The vial was rinsed with MilliQ water and a mixture of DCM and methanol and was subsequently treated as an analytical blank (AB) sample. It is to be expected that little or no oil components would be present in this sample, therefore, whichever compounds are detected in this sample is most likely derived from contamination during sample work-up.

Figure 10 shows the total ion chromatograms (TIC) of the extracted water samples from the different asphalt incubation experiments. There are some notable differences among the three different incubation types ‘Asphalt Only’, ‘Hexadecane’ and ‘Naphthalene’ as well as all the live incubations compared to the dead controls. While all of the samples exhibit a notable increase in an unresolved complex mixture (UCM) between 7 and 27 minutes, the UCM is most pronounced in the ‘Asphalt Only’ and the ‘Naphthalene’ samples. Both of these samples types also show an increase of compounds eluting between 10 and 15 minutes when comparing the 10 days samples with the 28 days samples. The ‘Naphthalene’ samples are particularly dominated by two peaks eluting at around 11 minutes, while these peaks seem to be absent in both the ‘Asphalt Only’ and ‘Hexadecane’ incubations. Instead, the ‘Hexadecane’ incubations are dominated by a cluster of peaks eluting at around 20 minutes.

In the following the identification and quantification of these and other compounds by GC-MS will be detailed and compared among the samples. All values can be found in Supplementary Table 6.



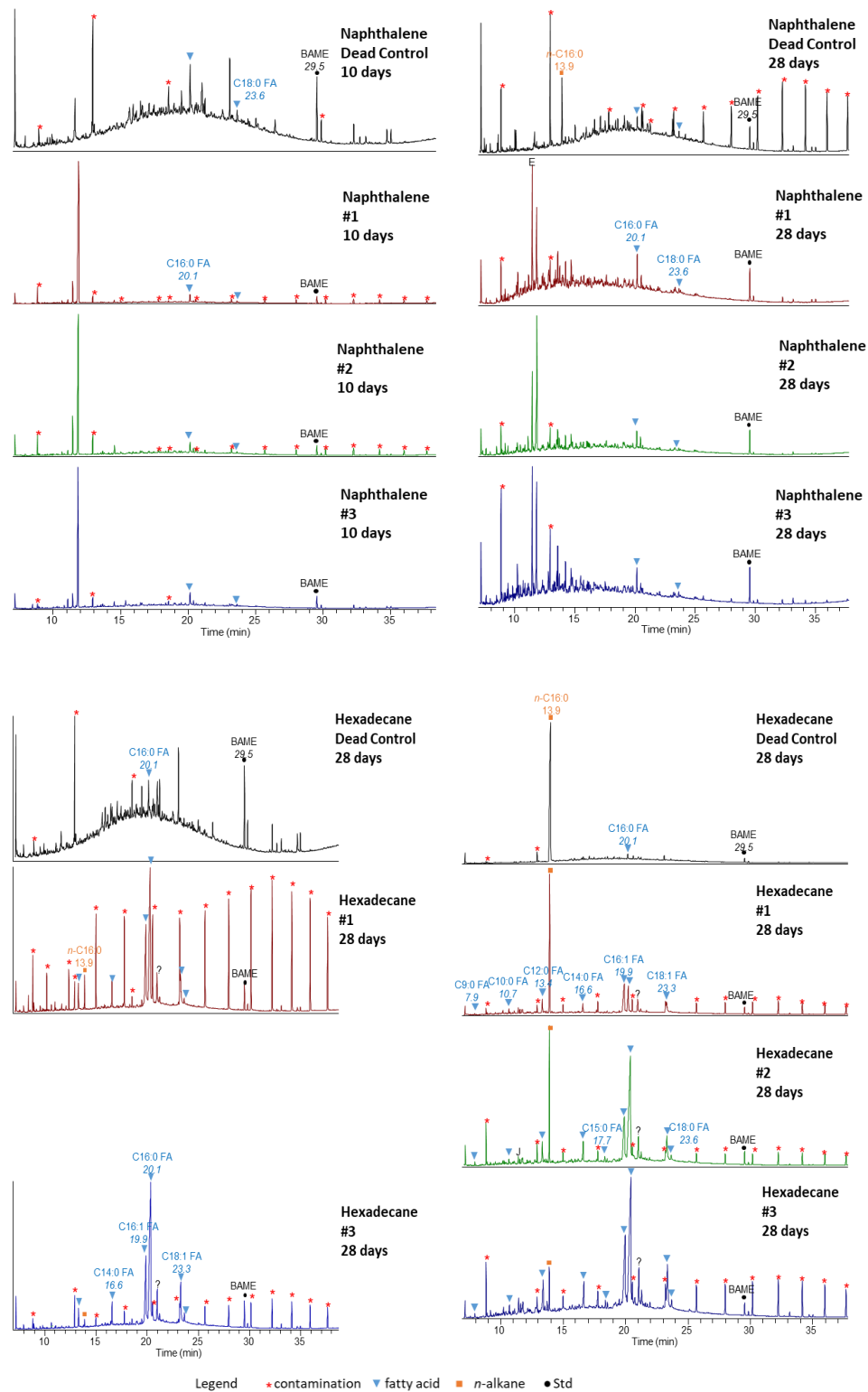


Figure 10. Total ion chromatogram (TIC) for all the asphalt incubation experiments

3.1.1 Contaminants

Some of the samples showed influence of siloxanes, which are plastic contaminants that could have been derived from handling the samples during and after the incubations, even though precautions have been met to avoid the use of plastic where possible. The siloxanes are not present in every sample with no obvious pattern; therefore, it is hard to pin down the exact source of contamination. In addition to the siloxanes, the analytical blank shows several peaks that are present in all of the samples and were thus also identified as contaminants. Supplementary Table 7 gives an overview over the tentative identification of the compounds identified as contaminants.

3.1.2 *n*-Alkanes

n-Alkanes were identified and quantified by extracting the ion trace m/z 85. Figure 11 shows the representative EIC m/z 85 chromatograms of the ‘Asphalt Only’ biotic and abiotic incubations. Although low in abundance, all samples contained varying amounts of *n*-alkanes, mostly in the carbon range from C₁₆ to C₂₄. Since hexadecane was added as a substrate to the ‘Hexadecane’ experiments, its abundance is very high in these samples (Figure 12) and thus this compound is plotted separately from the remaining *n*-alkanes.

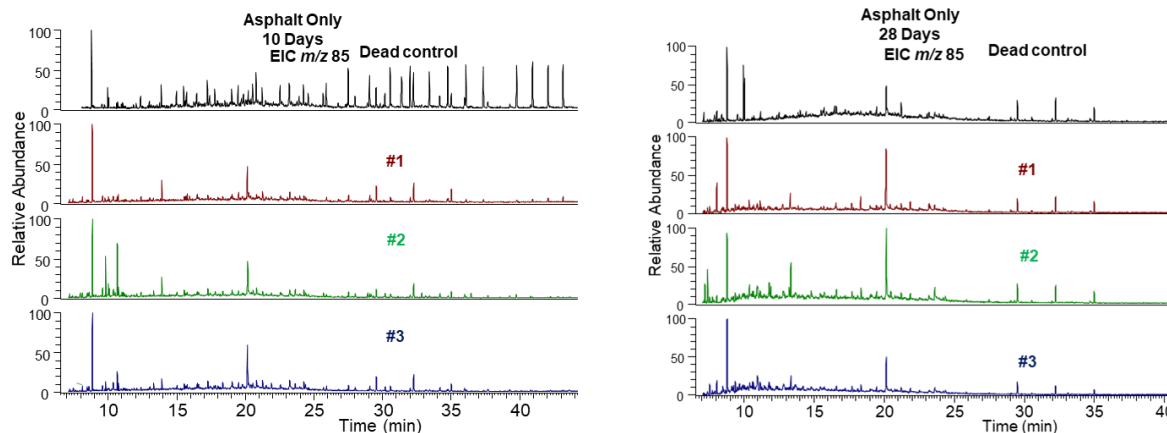


Figure 11. Extracted ion chromatogram (EIC m/z 85) for the ‘Asphalt Only’ incubation experiments

3.1.2.1 Hexadecane

Hexadecane was either low in concentration or absent in most samples after 10 and 28 days, with the exception of the ‘Naphthalene’ and ‘Hexadecane abiotic experiments after 28 days where it increased up to mean values of 117.1 ng/ml and 3366 ng/ml in the ‘Naphthalene’ abiotic control.

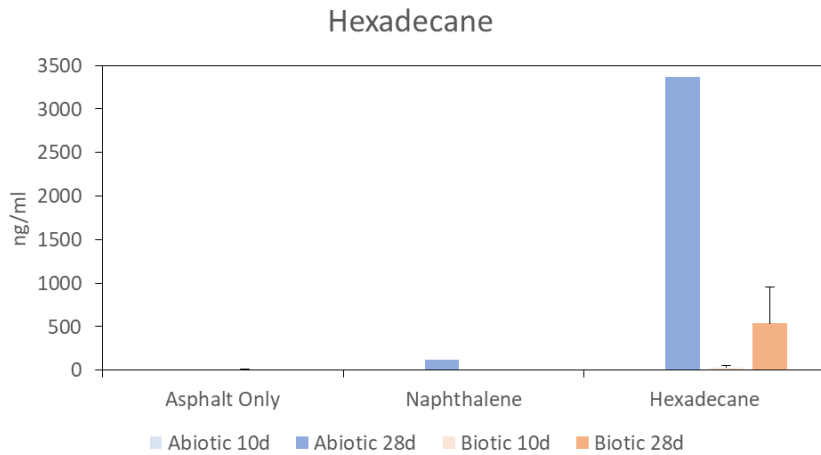


Figure 12. Bar chart showing hexadecane concentration in the asphalt incubation experiment

3.1.2.2 C₁₇ to C₂₄ n-alkane

C₁₇ to C₂₄ *n*-alkanes were present in almost all of the samples in varying abundances (Figure 13, see also Supplementary Table 6). In the ‘Hexadecane’ dead control only C₂₄ was detected, while the ‘Naphthalene’ dead control only contained C₂₂ and C₂₄ after 10 days. After 28 days no *n*-alkanes were detected in the ‘Asphalt Only’ abiotic control, while *n*-alkane concentrations remained the same in the ‘Naphthalene’ and increased notably in the ‘Hexadecane’ dead control. In the abiotic controls values were highest in the ‘Naphthalene’ experiment (6.6 ng/ml), followed by ‘Hexadecane’ experiment (1.8 ng/ml). After 28 days *n*-alkanes were absent in the ‘Asphalt Only’ abiotic control, but slightly to moderately increased in the ‘Naphthalene’ and ‘Hexadecane’ samples with values of 7.3 ng/ml and 17.5 ng/ml, respectively (see Supplementary Table 6). The average abundance of *n*-alkanes in the ‘Asphalt Only’ and ‘Hexadecane’ biotic experiment after 10 days is similarly high around 5.3 ng/ml and 7.8 ng/ml, while it is slightly lower in the ‘Naphthalene’ experiments with 1.06 ng/ml. No *n*-alkanes were detected after 28 days in the ‘Asphalt Only’ and ‘Naphthalene’ biotic experiments and decreased to 3.8 ng/ml in the ‘Hexadecane’ experiment.

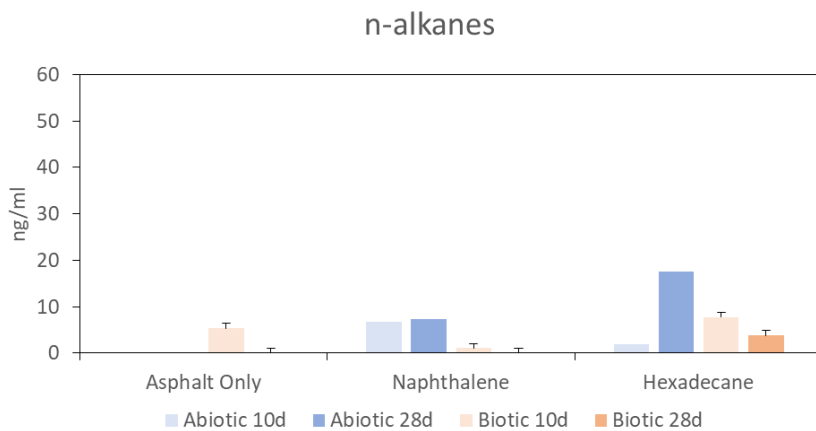


Figure 13. Bar chart showing concentration of the (C₁₇ to C₂₄) *n*-alkanes in the asphalt incubation experiment

3.1.3 Cycloalkanes

Select cycloalkanes were identified and quantified using the extracted ion chromatogram m/z 95 (Supplementary Table 4). These cycloalkanes include C2-and C3-alkylated decahydro-naphthalene and C2-alkylated indane (see supplementary Figure 31 tentative structures) which were detected in varying quantities in the samples. After 19 days in the ‘Naphthalene’ and ‘Hexadecane’ dead control samples cycloalkanes were detected in similar abundance with 82 ng/ml and 74.9 ng/ml, respectively (Figure 14). After 28 days cycloalkane abundance increased to around 200 ng/ml in both the ‘Asphalt Only’ and ‘Naphthalene’ abiotic samples and 157.7 ng/ml for ‘Hexadecane’. In contrast to this strong increase by over 100% between the two time points, the cycloalkane abundance in the biotic experiments either decreased (for the ‘Asphalt Only’ and ‘Naphthalene’ experiments) or remained the same (in the ‘Hexadecane’ experiment).

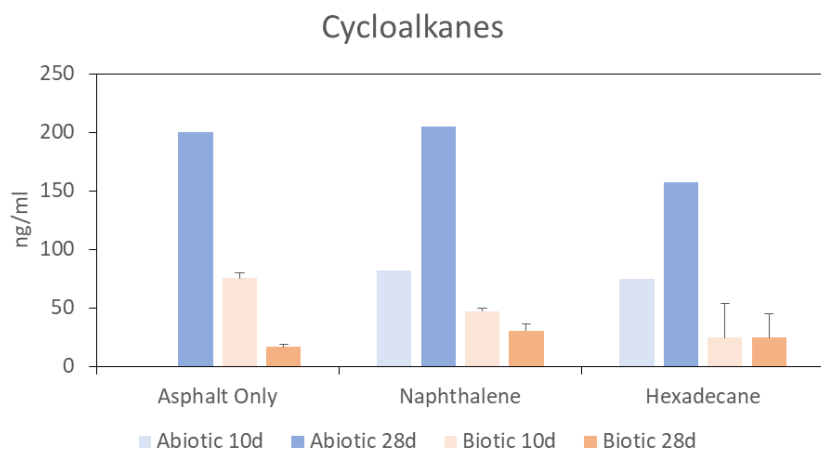


Figure 14. Bar chart showing concentration of cycloalkanes in the asphalt incubation experiment

3.1.4 Aromatic alcohol

Compounds that were assigned to the group aromatic alcohols were identified and quantified using the extracted ion traces m/z 91 and m/z 95, these compounds include benzyl alcohol, C3-benzyl alcohol, C3-phenol, butyl-phenol, C2-benzenethanol and a coellusion of methyl phenol and benzenedimethanol (see supplementary Figure 32 for tentative structures). Aromatic alcohols were on a similar level in the ‘Naphthalene’ and ‘Hexadecane’ dead controls with 31.9 and 27.7ng/ml after 10 days (see Figure 15 and supplementary Table 6). Abundances increased in the Naphthalene dead controls after 28 days to from ca. 32 to 59 ng/ml, whereas values remained the same in the Hexadecane experiment after 10 and 28 days. The live experiments contained very comparable amounts of aromatic alcohols, although the abundance of individual compounds varied. All three experiments showed more than 100 % increase after 28 days for aromatic alcohols from ca. 25 ng/ml to 107 ng/ml. Taking a closer look at some of these compounds, benzyl alcohol and phenol-p-tert butyl- was detected in the three asphalt incubation (Asphalt only, Naphthalene and Hexadecane), for both abiotic and biotic experiments after 10

and 28 days (with an exception in for asphalt only abiotic experiment after 10). C3-phenol was detected in the Asphalt only and Hexadecane biotic experiments after 10 and 28 days, while C3-benzyl alcohol appeared only in the biotic experiments after 10 and 28 days.

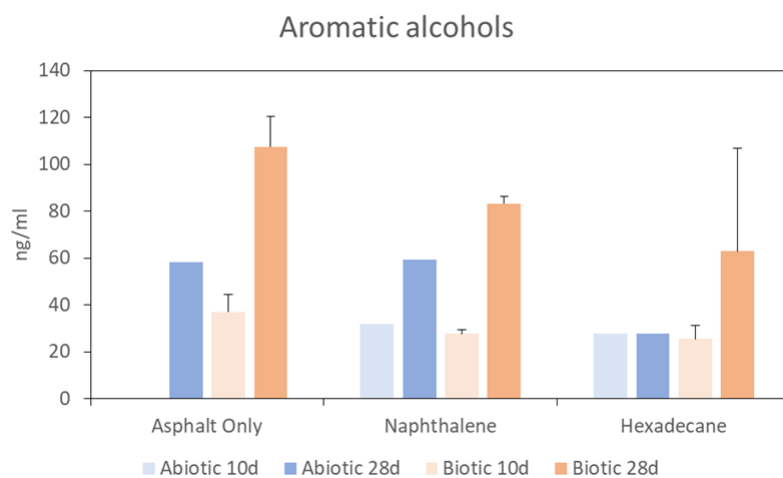


Figure 15. Bar chart showing concentration of aromatic alcohols in the asphalt incubation experiment

C2-benzenethanol was also observed to be predominant in the biotic incubation experiment after 28 days (for Asphalt only, Naphthalene and Hexadecane) with minimal appearance in the Hexadecane incubation experiment. Benzenedimethanol and methyl phenol were observed to elute at the same retention time (7.6 minutes) but in different incubation experiments, with benzenedimethanol showing only in the Hexadecane incubations while methyl phenol was observed in the Asphalt only and Naphthalene incubations

3.1.5 Aromatic ketones

Compounds that were assigned to the compound class ‘aromatic ketones’ include C1- to C3-benzaldehyde, hydrocoumarin, naphthalenedione and isomers of C2-isobenzofuran (see Supplementary Figure 33 for tentative structures of identified aromatic ketones). These seven compounds were identified and quantified using ion mass traces m/z 89, 91, 104 and 105. They were mainly absent in all dead controls except for the ‘Naphthalene’ experiment (9.87 ng/ml) where only hydrocoumarin, and naphthalenedione were detected after 28 days. Aromatic ketones increased in abundance in all experiments between 10 days and 28 days, from 2 ng/ml to 26 ng/ml in the ‘Asphalt Only’ experiments and from 5 ng/ml to 46 ng/ml in the ‘Hexadecane’ experiments, but were particularly abundant in the ‘Naphthalene’ experiment (Figure 16 and supplementary Table 6). C2-benzaldehyde, is also present in all the replicates of the living samples after 10 and 28 days in the ‘Asphalt Only’ incubation, while C3-benzaldehyde and C2-isobenzofuran were also detected in the ‘Asphalt Only’ and ‘Hexadecane’ incubation after 28 days. Alkylated benzaldehyde compounds were mostly present after 28 days in the ‘Hexadecane’

biotic experiment whereas only C1 and C2 benzaldehyde was detected in the replicates after 10 days.

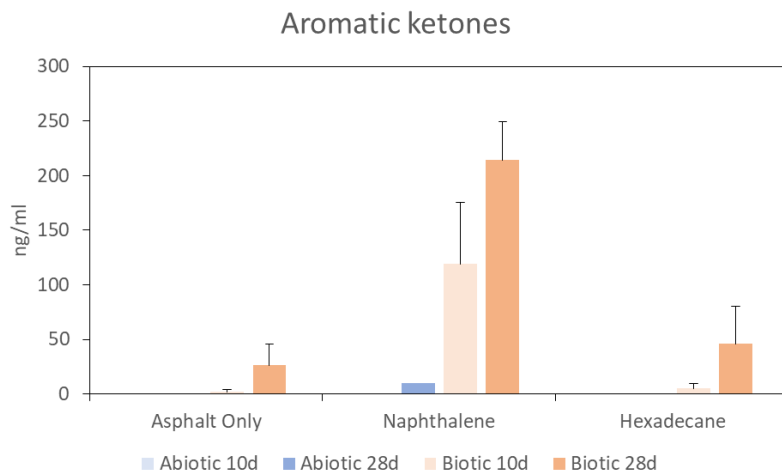


Figure 16. Bar chart showing concentration of aromatic ketones in the asphalt incubation experiment

A distinctive trend of increase over time was observed for all biotic experiments with the ‘Naphthalene’ incubation having the highest concentration values of 117 to 214ng/ml while ‘Asphalt Only’ and ‘Hexadecane’ increased from 2 to 26 ng/ml and 5 to 46 ng/ml after 28 days (Figure 16).

3.1.5.1 Coumarin

The ‘Naphthalene’ live incubations were dominated by one peak at 11.8 minutes, which was identified as coumarin (*EIC m/z* 89), which also belongs to the compound class aromatic ketones, but will be discussed separately due to its high abundance in the ‘Naphthalene’ samples. It is found in both the 10 and 28 days biotic and abiotic ‘Naphthalene’ incubations (Figure 17) where it increases from 1.4 ng/ml to 8.4 ng/ml. In the biotic ‘Naphthalene’ samples coumarin exhibited a drastic decrease from 832 ng/ml after 10 days to 79.7 ng/ml after 28 days. It is absent in the abiotic ‘Asphalt Only’ experiments after 28 days, but is present in the triplicates of the live ‘Asphalt Only’ samples with an average of 3 ng/ml after 10 days and again absent after 28 days. Coumarin is also present in the abiotic incubations with a negligible decrease from 1.72 ng/ml to 1.12ng/ml after 10 and 28 days in the ‘Hexadecane’ experiment as well as in two replicates of the live incubations with comparably low average values of 1.67 ng/ml.

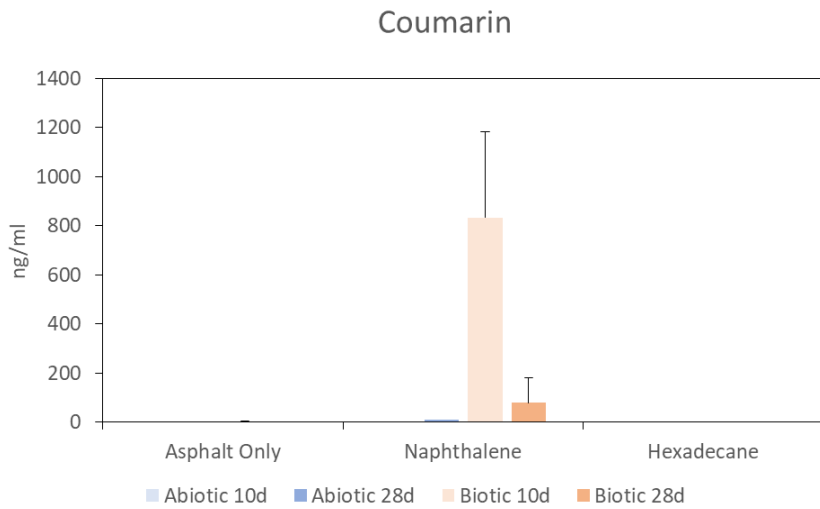


Figure 17. Bar chart showing concentration of Coumarin in the asphalt incubation experiment

3.1.6 Aromatic acids

This compound class includes isomers of alkylated C2-, C3- and C4- benzoic acids, C2-phenylacetic acid and mesitylactic acid. These compounds were identified and quantified in the samples using the ion trace m/z 91 (Supplementary. Figure 34). While these compounds were absent in the dead control of the ‘Asphalt Only’ experiment, only C2-phenylacetic acid was present in the ‘Naphthalene’ abiotic control, where it exhibited a slight decrease between 10 and 28 days. In the ‘Hexadecane’ abiotic experiments only C2-phenylacetic acid and C2-benzoic acid were detected with fairly stable concentrations between the two time points. In the live incubations for all samples these compounds increased over time. The ‘Asphalt Only’ biotic samples rose from the 10 days value of 19.9 to 211.7 ng/ml after 28 days, and in a similar manner from 2.4 to 73.2 ng/ml in the ‘Naphthalene’ experiments and from 7.9 ng/ml to 118.5 ng/ml in the ‘Hexadecane’ experiments (Figure 18 and Supplementary Table 6). Mesitzlactic acid is only present after 28 days in the biotic samples of both the ‘Asphalt Only’ and ‘Naphthalene’ incubations, while tetramethyl benzoic acid was detected after 28 days in the biotic samples of all three experiments.

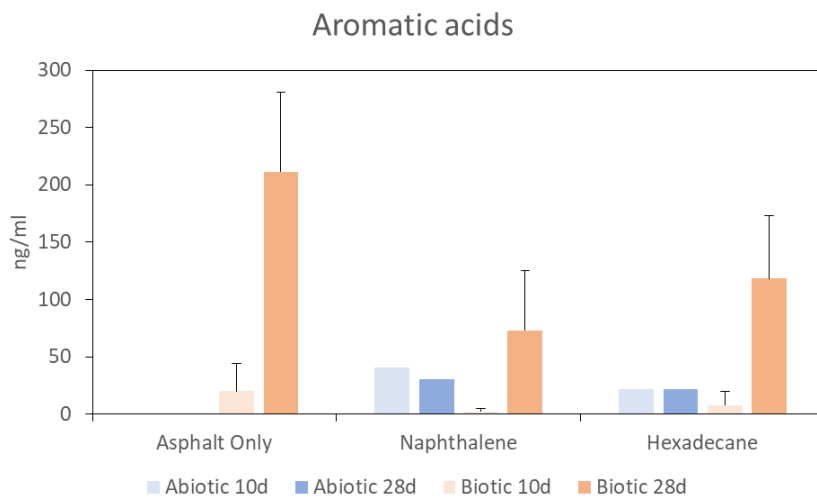


Figure 18. Bar chart showing concentration of aromatic acids detected in the asphalt incubation experiment

3.1.7 Thiols and thiophenic acids

The three compounds dimethylthiophene-2-thiol, methyl-benzothiazolethione, dimethylbenzo(b)thiophene-carboxylic acid were tentatively identified and grouped together as thiols and thiophenic acids in the investigated samples and quantified using ion traces m/z 91, 101 and 115 (Supplementary Figure 35). This group of compounds was seen to be absent in all the abiotic incubations (Figure 19). All of these compounds increased significantly between the 10 day and 28 day time point in all live experiments (see Supplementary Table 6) except for the ‘Hexadecane’ incubation, which only contained dimethylthiophene-2-thiol, but also with highest abundances after 28 days. Concentrations after 28 days ranged between 52.1 ng/ml, 23. ng/ml and 5.13 ng/ml for the respective ‘Asphalt Only’, ‘Naphthalene’ and ‘Hexadecane’ incubations.

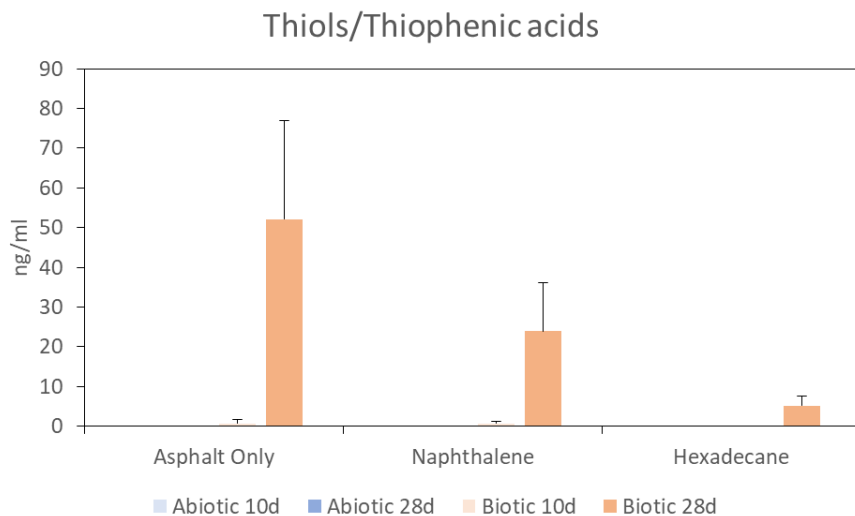


Figure 19. Bar chart showing concentration of thiol compound and thiophenic acids detected in the asphalt incubation experiment

3.1.8 Halogenated compounds

A total of four compounds were identified as halogenated compounds, they were quantified using ion traces m/z 212, 213, 222, and 227 (Supplementary Figure. 36). These compounds were mainly phenol related compounds and include phenol, 2,6-dibromo-4-(1,1-dimethylethyl)-, phenol, 2-bromo-4-(1,1-dimethylethyl)-, 2-Naphthalenol, 1-bromo-, and 2,2-Dichloro-1,1-bis(4-methoxyphenyl)ethane. These compounds were most abundant in the dead controls, where they exhibited similar concentrations of ca. 120 ng/ml in the ‘Naphthalene’ and ‘Hexadecane’ samples after 10 days and decreased to values between 90 to 113 ng/ml in all dead controls after 28 days (Figure 20 and Supplementary Table 6). Notably, 2,2-Dichloro-1,1-bis(4-methoxyphenyl)ethane is only compound which was detected in the abiotic controls, while the biotic experiments contain generally all four compounds, but in lower concentrations. In all live experiments the detected halogenated compounds decrease in concentration between the two time points (Figure 20).

‘Asphalt Only’ samples showed a reduction from 50.3 to 18.6 ng/ml between the two time points while the naphthalene samples show an ca. 80% decrease from 74.1 ng/ml to 14.6 ng/ml albeit with a large standard deviation among the triplicates. In the ‘Hexadecane’ incubation halogenated compounds comprise 32.8 ng/ml after 10 days while all of them have been removed after 28 days.

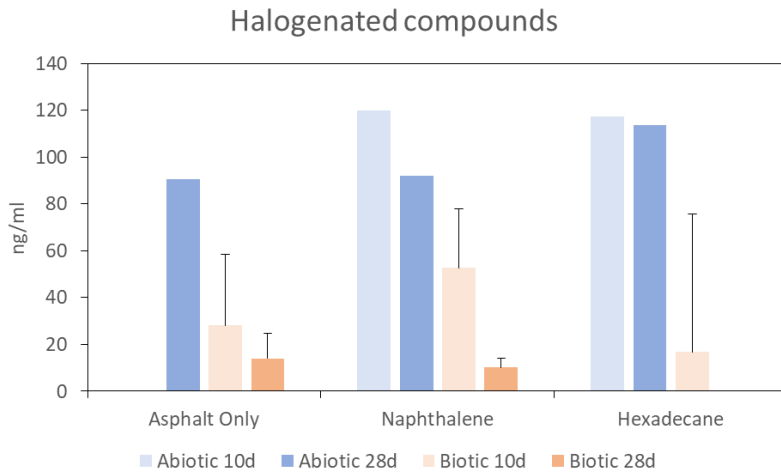


Figure 20. Bar chart showing concentration of halogenated compounds in the asphalt incubation experiment

3.1.9 Fatty acids

The fatty acids detected in the samples include predominantly saturated and even carbon numbered fatty acids, such as C_{14:0}, C_{16:0} and C_{18:0}, but also some unsaturated C_{16:1} and C_{18:1} were observed as well as odd carbon numbered C_{15:0} and C_{17:0} (Supplementary Figures 37 and 38). Additionally, short chain fatty acids C_{9:0}, C_{10:0}, C_{11:0} and C_{12:0} were observed. The abiotic controls contained fatty acids with concentrations around 15 to 37 ng/ml for ‘Hexadecane’ and a decrease from 32 to 26 ng/ml in the ‘Naphthalene’ between 10 and 28 days. Only ‘Hexadecane’ showed an increase after 28 days which is double its value after 10 days (Figure 21). The biotic incubations of the three experiments contain a higher amount of fatty acids compared to the dead controls and also exhibit a notable increase between 10 and 28 days. While values for the ‘Asphalt Only’ and ‘Naphthalene’ experiment increase from respective 34 and 48 to 93 and 61 ng/ml, fatty acid abundance in the ‘Hexadecane’ experiment are over an order of magnitude higher and increase from 648 to 1157 ng/ml between 10 and 28 days. Notably, the distribution of fatty acids in the dead controls are distinct from the live experiments (Supplementary Figure 38), while the dead controls are dominated by the short chain fatty acids, C_{9:0} to C_{11:0} and also contain C_{16:0} in similar amounts (with C_{12:0}, C_{14:0} and C_{18:0} only present in the Naphthalene abiotic control after 10 days), only the live experiments contain the odd carbon fatty acids as well as monounsaturated fatty acids (Supplementary Figure 38).

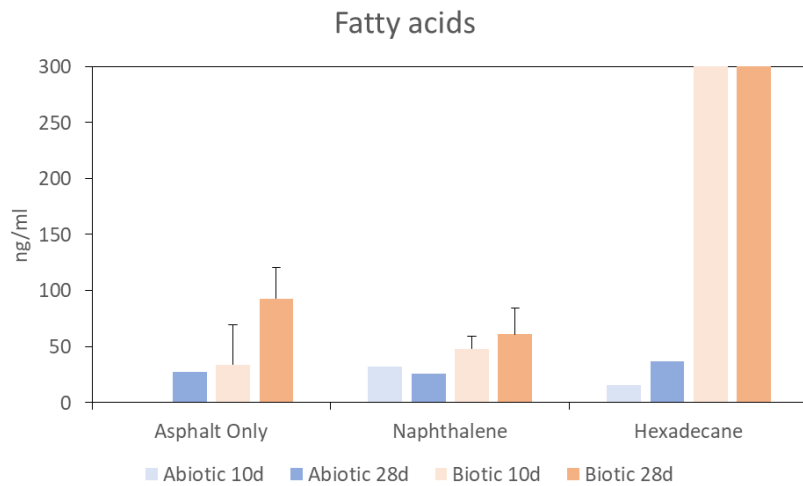


Figure 21. Bar chart showing concentration of fatty acids detected in the asphalt incubation experiment. The ‘y’ axis was reduced so as to make room for ‘Asphalt Only’ and ‘Naphthalene’

3.2 Environmental samples

The focus of this section will be centered on the oil components found in the organic extracts of various water samples collected at the Chapopote, Mictlan and Tsanyao Yang during the cruise M114. For most samples the entire organic extract were analyzed, but for some select and very oily samples (GeoB19336-5, GeoB19337-2, GeoB19351-14, and GeoB19337-9) were separated into different fractions and in this thesis only the saturate and aromatic fractions will be discussed.

3.2.1 Chapopote samples

Table 1 provides information on the site where the samples were taken as well as the instrumentation used while collecting the water samples at various water depths. All the water samples from Chapopote reported in this study were collected with Niskin racks attached to the side of the ROV except for sample GeoB19351-14, which was bottom water collected from a push corer device.

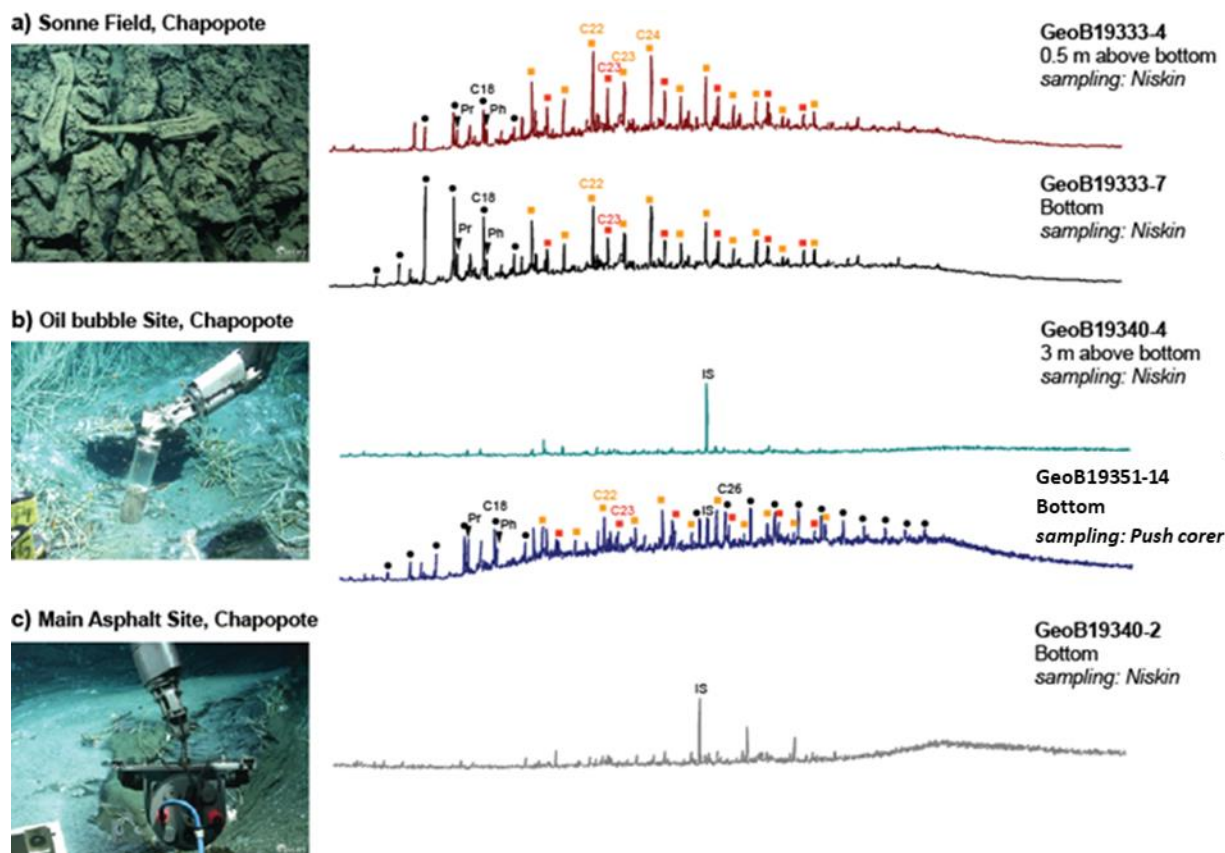


Figure 22. Images of locations and extracted ion chromatograms (EIC) m/z 85 of the water samples collected from Chapopote. (a) Sonne Field (b) oil bubble site (c) Main Asphalt Field. IS: internal standard, black circles: *n*-alkane homologous series, inverted black triangles: isoprenoids pristane (Pr) and phytane (Ph) red and orange squares: branched alkanes with quaternary carbon atoms (BAQCs) series. Images from the M114 cruise report (Sahling and Bohrmann, 2017).

Figure 22 depicts the extracted ion chromatogram (EIC) m/z 85 of the investigated Chapopote samples. With this mass trace n-alkane patterns can be compared among the different samples providing a first indication, whether oil compounds are dissolved in the water and to what level the oil in the water is biodegraded. While *n*-alkanes were found in some of the water samples collected at different water depths at the Chapopote, these samples also exhibit a kind of chaotic pattern of additional compounds detected with EIC m/z 85. In addition, the chromatograms of these samples exhibit a hump, which is caused by presence of an unresolved complex mixture (UCM), with the sample GeoB19351-14 having the most prominent UCM. The samples from the Sonne field (GeoB19333-4 & 7) and the bottom water sample (GeoB19351-14) from the oil bubble site show a low molecular weight *n*-alkane series, from C14 to C19 *n*-alkane, with a second higher molecular weight *n*-alkane series being present in sample GeoB19351-14 (from C25 to C25). Samples GeoB19340-2 and GeoB19340-4 shows no visible *n*-alkane peak. Next to the C17 and C18 *n*-alkanes are the isoprenoids pristane and phytane. Calculated pristane to C17 and phytane to C18 ratios, which are typically used to assess the level of biodegradation (Peter et al., 2004) are shown in Table 4. Pr/C17 and Ph/C18 values are lowest in sample GeoB19333-7 (bottom Sonne field), followed by GeoB19333-4 (0.5 m above Sonne field) and are comparably high in the bottom water sample of the oil bubble site (GeoB19351-14). The chaotic pattern was identified as two homologous series of branched alkanes with quaternary carbon atoms (BAQCs), which were first reported by Kenig et al. (2003) and later identified as contaminants coming from plastic bags used during sampling (Grosjean and Logan 2007; J.J. Brocks et al. 2008).

3.2.2 Mictlan samples

Water samples from the Mictlan area reported in this study were collected from two distinct locations namely the mussel bed area and the area where the asphalt tubes (also known as white coated chimneys) are located (Table 1; Figure 23). Samples GeoB19327-3 and 4 were collected with Niskin bottles attached to the side of the ROV at 0.5 m and 1 m above the mussel bed. Samples GeoB19336-6 oily and GeoB19336-6 were collected from the interior of the asphalt tubes and the surrounding water, respectively. Sample GeoB19336-5 was collected using a gas bubble sampler (GBS) from the asphalt tubes, while samples GeoB19346-4 and 15 were collected with a GBS from the mussel field. The oil slick sample was collected from the ship with the aid of a bucket which resulted in only minor mounts of oil being recovered. The *n*-alkane distribution as in Figure 23 shows distinct differences among the sample. All the samples collected from Mictlan have *n*-alkanes. Almost all samples exhibit a bimodal distribution, similar to the sample GeoB19351-14 from Chapopote, except for the two water samples collected 0.5 and 1 m above the mussel beds. In these two samples only the light end of the *n*-alkanes was present. In the oil slick the light end *n*-alkane series is missing, while the high molecular *n*-alkane series from C22 up to C36 were still present. Samples GeoB19327-3 and GeoB19327-4 are missing the high end *n*-alkanes (from C23 onwards) as opposed to other samples from this

area. In three of the water samples (GeoB19327-3, -4 and GeoB19336-6) the BAQCs contaminants were also observed. Isoprenoids pristane and phytane are seen to be present in all the samples except for the oil slick sample, resulting in varying Pr/C17 and Ph/C18 values (Table 4). Many of the samples had comparably low Pr/C17 and Ph/C18 ratios, two of which were collected with the GBS from the asphalt tubes and the mussel bed, but also one sample collected from the mussel bed had one of the highest Pr/C17 and Ph/C18 ratios.

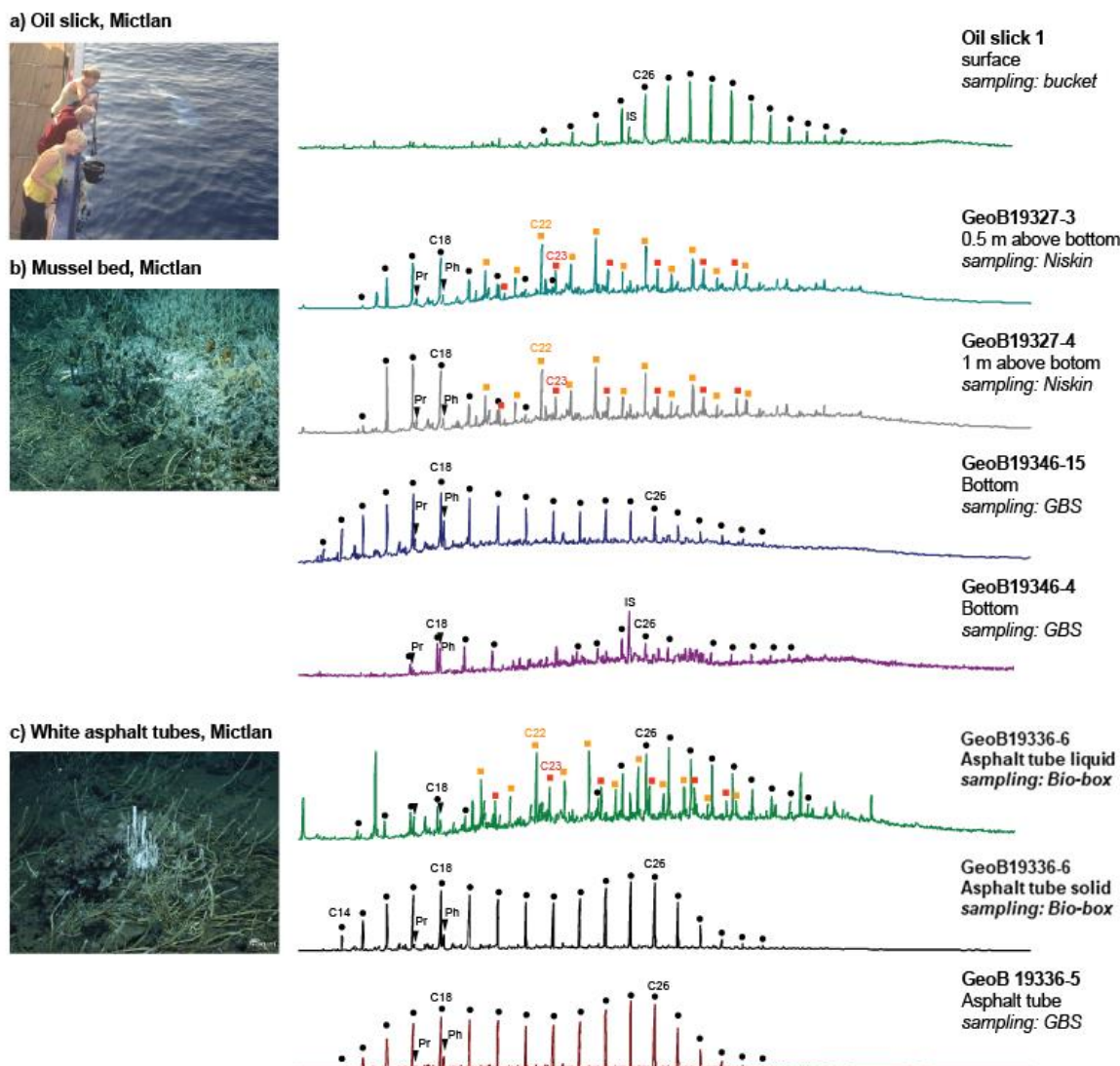


Figure 23. Images of locations and extracted ion chromatograms (EIC) m/z 85 of the water samples collected from Mictlan. (a) oil slick, (b) mussel bed, (c) white asphalt tubes. IS: internal standard, black circles: *n*-alkane homologous series, inverted black triangles: isoprenoids pristane (Pr) and phytane (Ph) red and orange squares: branched alkanes with quaternary carbon atoms (BAQCs) series. Images from the M114 cruise report (Sahling and Bohrmann, 2017).

3.2.3 Tsanyao Yang samples

Water samples from the Tsanyao Yang area were all collected from one particular location, defined as Site 1 by Sahling et al. (2016) and Römer et al. (2019) at varying water depths and using different instruments (Table 1 and Figure 24). Sample GeoB19337-2 was collected using a gas bubble sampler. Sample GeoB19337-3 was collected with a Niskin bottle attached to the side of the ROV at 1.5 masf while sample GeoB19337-9 were oil droplets recovered from a yellow net used to collect shells and tubeworms. While on a rubber boat, oil was collected using glass jars from oil bubbling to the ocean surface at Tsanyao Yang.

The full suite of *n*-alkanes, ranging from C16 to C34 were detected in three of the samples at Tsanyao Yang, one from the water column (collected by GBS) and the two oil slicks, where oil was recovered immediately after it bubbled to the surface (Florence Schubotz, personal communication). The oil sample collected in the net was devoid of *n*-alkanes, but instead shows the presence of a hump. Water sample GeoB19337-3, collected 1.5 masf only had the light *n*-alkane end present and also showed the presence of BAQCs compounds, which are known plastic contaminants.

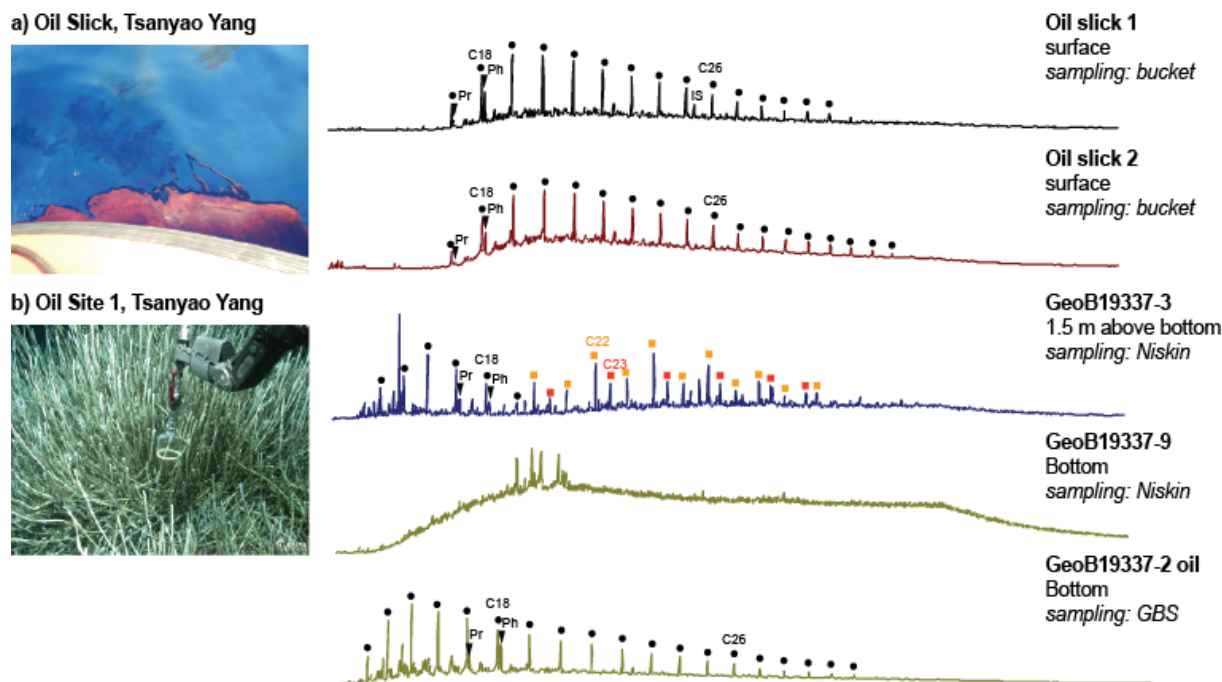


Figure 24. Images of locations and extracted ion chromatograms (EIC) m/z 85 of the water samples collected from Tsanyao Yang (a) oil slicks (b) oil bubble Site 1. IS: internal standard, black circles: *n*-alkane homologous series, inverted black triangles: isoprenoids pristane (Pr) and phytane (Ph), red and orange squares: branched alkanes with quaternary carbon atoms (BAQCs) series. Images gotten from. Römer et al. (2019).

3.3 Aromatic hydrocarbons and NSO compounds

All environmental samples were surveyed for the presence of the sample (mainly aromatic) compounds that were found in the asphalt incubation experiment (Table 6), however, most of them were not found. Instead, a lot of typical oil compounds were detected; including many PAHs, such as alkylated naphthalene, *n*-phenanthrene as well as alkylated phenantrenes, *n*-dibenzothiophenes and alkylated dibenzothiophenes. Some samples also contained alkylated aromatics (Supplementary Table 11). Also, some NSO-containing compounds were found, which includes benzenemethanethiol and benzyl methyl disulfide which are monoaromatic sulfur compounds and cycluron which is a nitrogen and oxygen containing compound. Other oxygenated compounds that were identified in this analysis includes benzyl alcohol which is an aromatic alcohols, 2,4-nonanedione, 2,6-di-tert-butylquinone and benzophenone which were classified as ketone compounds and some aromatic and fatty acids. Benzyl 2-chloroethyl sulfone which was classified as halogenated compound was also detected in some samples.

3.4 Biodegradation and water washing parameters

Ratios were computed that are commonly used to assess the level of biodegradation or water washing of oil samples (Table 4). These include the Pr/C17, Ph/C18 ratios which is based on the observation that biodegradation first consumes *n*-alkanes over isoprenoid compounds (Peter et al., 2004). Similarly alkylated PAH ratios C2-/C3-naphthalene, C1-/C2-phenantrane and C1-/C-DBT can be used to assess biodegradation based on the observation that the shorter chain alkylated compounds are consumed preferentially over longer chain alkylated aromatic compounds (Wang et al., 1998). These ratios can also be used to assess the level of water washing as lower molecular weight compounds also preferentially go into the water phase. PAH over PAHS ratios such as phenanthrene/DBT can also be used to assess either the level of biodegradation or water washing, as microorganisms preferentially consume non-S containing hydrocarbons (Tissot and Welte, 1978), but DBT is more soluble compared to phenanthrene (Price 1976; Palmer 1984). Table 4 shows the values (biodegradation and water washing parameters) for all environmental samples investigated during this thesis.

Using the Pr/C17 over Ph/C18 ratios (Table 4) together with *n*-alkane patterns observed in the EIC m/z 85 of the samples, the 18 samples could be roughly grouped into 4 categories from least biodegraded ('fresh') to most biodegraded. The 'Fresh' samples comprises of both unimodal and bimodal *n*-alkane distribution with the entire *n*-alkane series still intact and comparably low Pr/C17 over Ph/C18 ratios, samples defined as 'biodegraded' either had very high Pr/C17 over Ph/C18 ratios or were lacking *n*-alkanes. The samples that did not fit into either category were categorized as 'weathered' as they either had slightly enriched Pr/C17 over Ph/C18, a bimodal *n*-alkane distribution or exhibited the presence of a hump. Oil slicks were grouped separately.

‘Fresh’ samples were dominated by *n*-alkanes and typical oil compounds. Alkyl naphthalene (C1-C4) was observed to be predominant in the ‘fresh’ samples but was not detected in the biodegraded and oil slicks samples. The weathered samples show presence of alkyl benzene (once in ‘biodegraded’ GeoB19351-14). Phenanthrene was present in all samples class although in much lesser concentration in the biodegraded samples. Alkyl phenanthrene (C1, and C2) were present in the Fresh, weathered as well as the Tsanyao Yang oil slicks samples. Alkylated fluorene was only observed in the fresh samples with high concentration values for Tsanyao Yang sample GeoB19337-2. Presence of DBT and its alkylated homologues (C1- and C2-) were observed in the Fresh samples as well as the weathered samples although in much lower concentration compared to the Fresh samples. No account of DBT in the biodegraded and oil slick samples, however C1- and C2-DBT were seen in Tsanyao Yang oil slick samples, Chapopote GeoB19351-14 and Tsanyao Yang GeoB19337-9 biodegraded samples in very high concentrations. However, these compounds were absent in Mictlan oil slick sample. Benzyl alcohol is detected in all samples while ketones were also observed in the weathered samples in addition to some aromatic acids. No occurrence of fatty acids in the Fresh asphalt but were seen to be present in other sample classes although at varying degrees.

To better compare individual samples, cross plots of the individual ratios were made where the four different sample types were highlighted by different colors. Figure 25 depicts the cross plotting of Pr/C17 over Ph/C18, both the biodegraded sample as well as the oil slicks cluster together as they have higher values compared to the fresh and weathered samples. The fresh and weathered samples are more scattered although two data points from both sample class appear to be proximal with each other both having the lowest values.

Table 4. Biodegradation ratios of Pr/C17 and Ph/C18 and aromatic compounds

Sample type	Sample name	Pr/C17	Ph/C18	C2-Naph/C3-Naph	C1-Phen/C2-Phen	C1-DBT/C2-DBT	C1-Phen/C1-DBT	Phen/DBT
Fresh	Mictlan GeoB19336-6 oily	0.15	0.37	0.26	0.73	0.31	0.86	0.50
	Mictlan GeoB19336-5	0.16	0.37	0.13	0.66	0.44	0.28	0.52
	Mictlan GeoB19346-15	0.33	0.77	0.37	0.48	0.40	0.29	1.29
	Tsanyao Yang GeoB19337-2	0.56	0.89	0.39	0.69	0.46	0.73	0.69
Weathered	Mictlan GeoB19327-3	0.22	0.34		1.97	0.43	3.79	17.39
	Mictlan GeoB19327-4	0.21	0.38		2.55	0.55	3.77	17.42
	Chapopote GeoB19333-7	0.30	0.62		2.46	0.58	3.38	18.34
	Chapopote GeoB19333-4	0.37	0.81		1.92	0.41	2.80	16.51
	Mictlan GeoB19336-6	0.55	0.71		3.23	0.58	3.44	13.79
	Tsanyao Yang GeoB19337-3	0.49	0.73			1.64	1.75	12.57
Biodegraded	Chapopote GeoB19351-14	0.71	0.82		0.92	0.43	1.30	
	Mictlan GeoB19346-4	0.82	1.01					
	Chapopote GeoB19340-4							
	Chapopote GeoB19340-2							
	Tsanyao Yang GeoB19337-9				0.00	0.06	0.20	
Oil slicks	Tsang Yang Oil Slick 1	0.59	0.97		0.33	0.18	1.49	
	Tsang Yang Oil Slick 2	0.64	0.90		0.27	0.12	0.20	
	Mictlan Oil Slick							

A cross plot of C1-/ C2-phenanthrenes over C1-DBT/C2-DBT is shown in Figure 26 and C1-/C2-phenanthrenes against C1-phenanthrenes/C1-DBT in Figure 27. The first plot shows that the C1 alkylated compounds are less abundant than the C2 alkylated compounds in all samples compared to except for the weathered water samples. No distinct trend is observed for the other three sample category types. Although it is noticeably that the fresh water samples appear to cluster closely together as do the oil slicks. Notably, the oil slick values are only from Tsanyao Yang as these aromatic compounds were absent in the Mictlan oil slick.

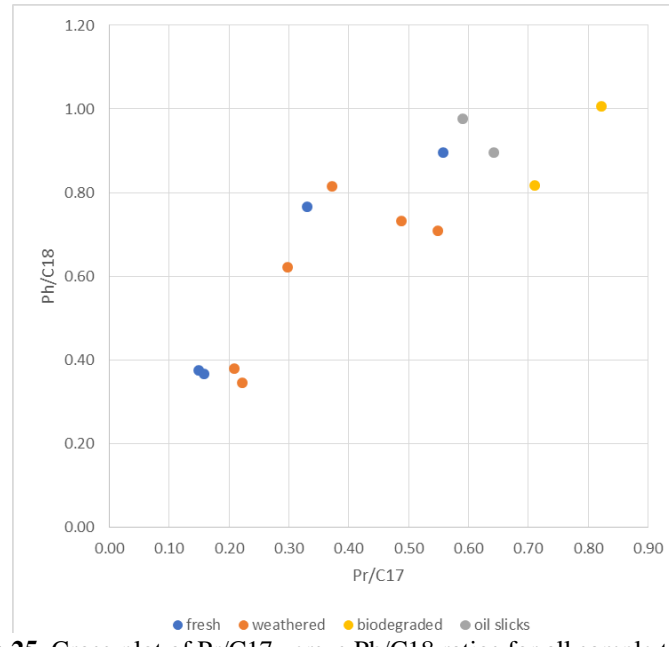


Figure 25. Cross-plot of Pr/C17 versus Ph/C18 ratios for all sample types

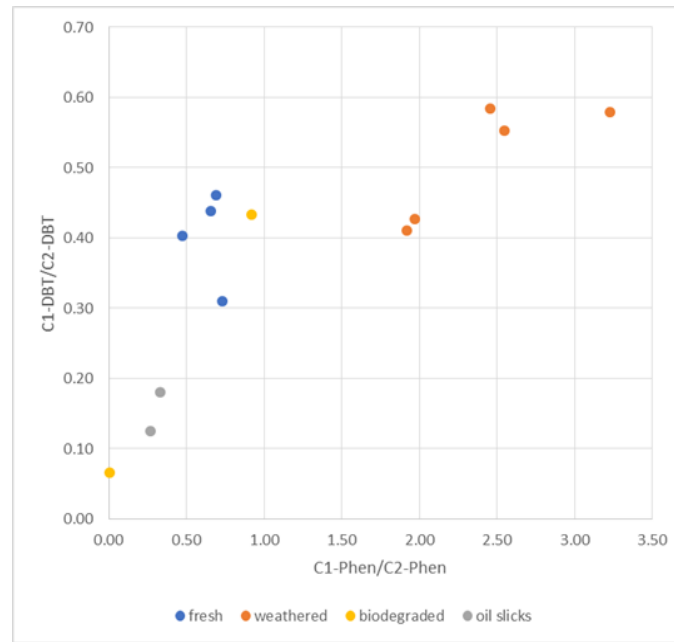


Figure 26. Cross-plot of C1-Phen/C2-Phen versus C1-DBT/C2-DBT ratios for all sample types

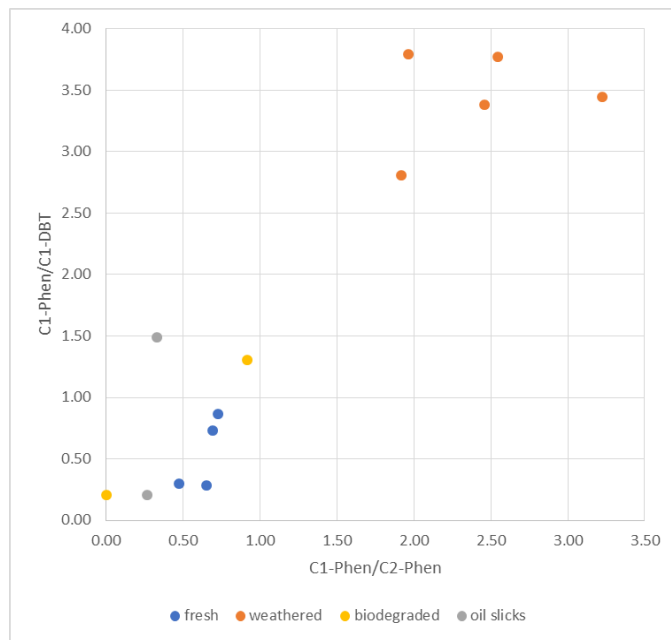


Figure 27. Cross-plot of C1-Phen/C2-Phen versus C1-Phen/C1-DBT for all sample types

The second plot (Figure 27) shows a comparable separation of the samples with the weathered samples exhibiting high values and clustering quite distal compared to the other sample types. The fresh sample type also clusters closely together having low values. The oil slicks in this case appear to be further apart exhibiting a similar trend observed for the biodegraded samples.

The last cross plot (Figure 28) depicts phenanthrene/C1-phentrene plotted against DBT/C1-DBT. Here, only the fresh and weathered samples could be plotted because the other samples were devoid of either DBT or phenanthrene. The fresh samples cluster closely together having much lower amounts of DBT and phenanthrene over their respective C1-alkylated derivatives compared to the weathered water samples which are more scattered and have higher values.

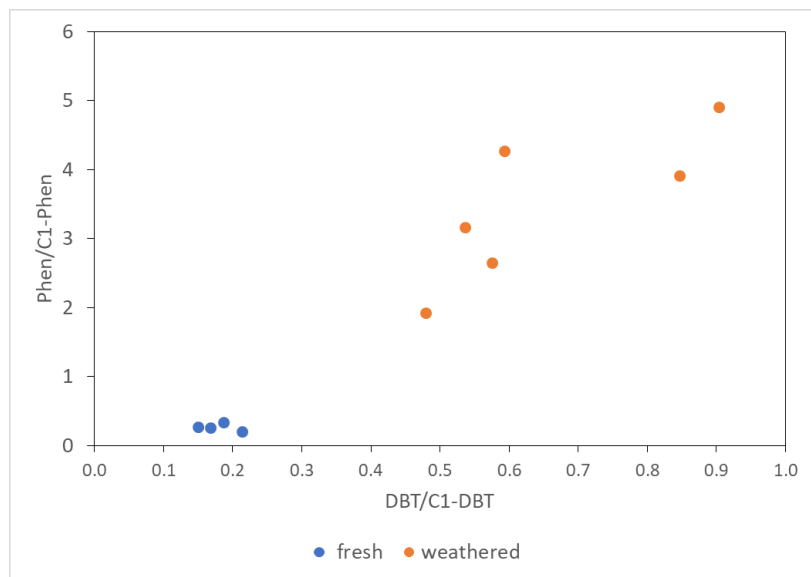


Figure 28. Cross-plot of Phen/C1-Phen versus DBT/C1-DBT ratios, for only fresh and weathered samples.

Table 5. Absolute concentrations of the 18 analyzed samples. The bold figures represent the sum total for each sample type.

Sample type	Samples	absolute concentration (ng/ml)
Fresh samples	Mictlan GeoB19336-6 oily	2824.19
	Mictlan GeoB19336-5	9630.03
	Mictlan GeoB19346-15	2219.41
	Tsanyao Yang GeoB19337-2	14347.97
		29021.61
Weathered samples	Mictlan GeoB19327-3	15.23
	Mictlan GeoB19327-4	15.30
	Chapopote GeoB19333-7	42.35
	Chapopote GeoB19333-4	7.79
	Mictlan GeoB19336-6	5.44
	Tsanyao Yang GeoB19337-3	3.26
		89.37
Biodegraded samples	Mictlan GeoB19346-4	8.61
	Chapopote GeoB19351-14	40.61
	Chapopote GeoB19340-4	5.96
	Chapopote GeoB19340-2	5.13
	Tsanyao Yang GeoB19337-9	7170.09
		7230.41
Oil slicks	Mictlan Oil Slick	1.00
	Tsang Yang Oil Slick 1	11.70
	Tsang Yang Oil Slick 2	85.74
		98.44

The sum total of the absolute concentration of every given sample is seen in Table 5. Figure 29 shows all the compounds identified and quantified for all environmental water samples. They are shown in the order of their biodegradation level as identified through the n-alkane patterns (see above, Table 4).

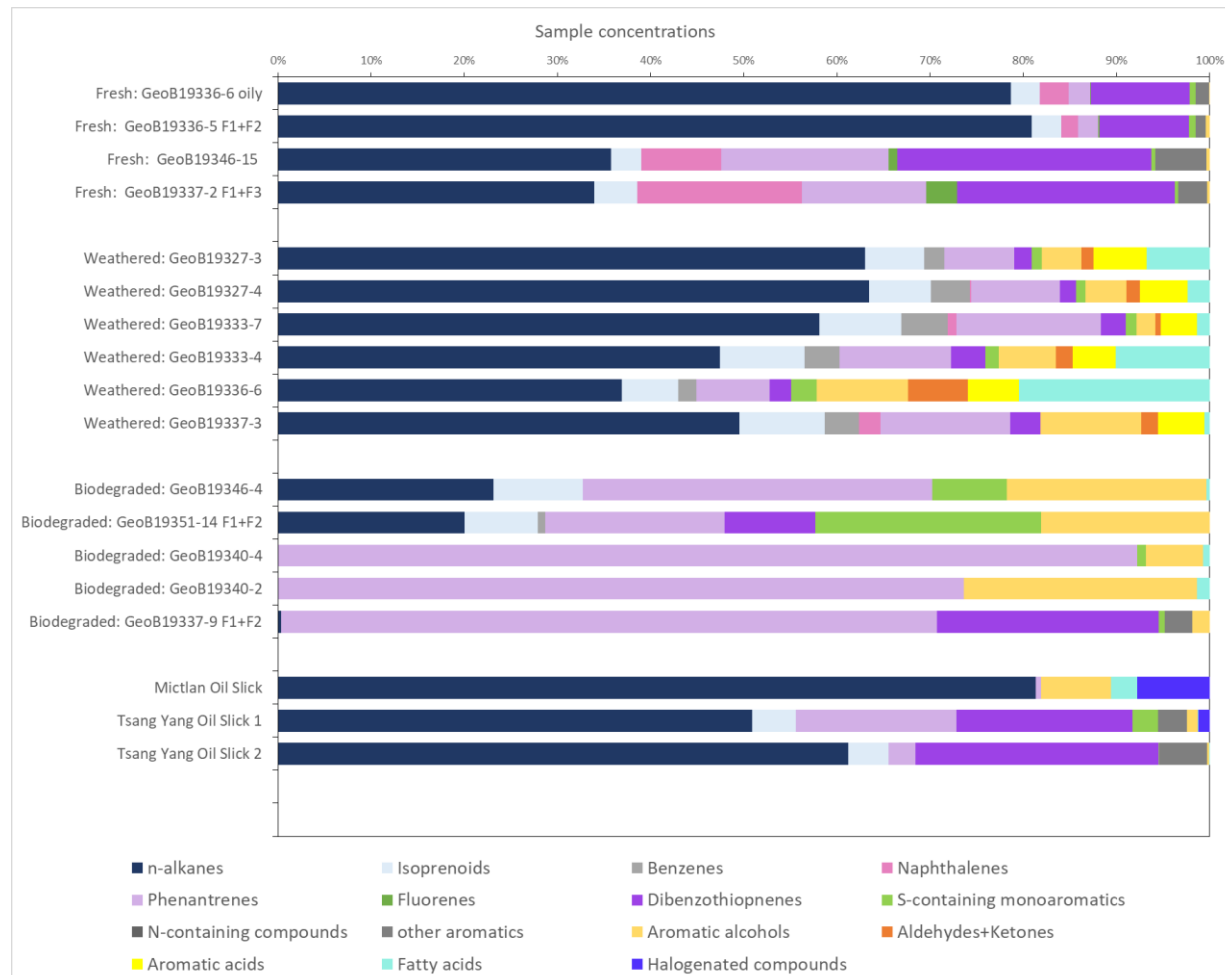


Figure 29. Relative abundance of all compounds identified and quantified in the environmental water samples. Samples classification is based on the level of biodegradation defined by *n*-alkane patterns and Pr/C17 and Ph/C18 ratios (see Table 4).

The first group of samples is the fresh sample type; these samples had the overall highest amounts of hydrocarbons (29021 ug/ml) and were dominated by *n*-alkanes. In addition, abundant PAHs and PASHs (alkylnaphthalenes, phenanthrenes and DBTs) were also present. The second group is the weathered sample type, which contained much lower absolute hydrocarbon concentrations (89 ng/ml). These samples still showed a predominance of *n*-alkanes, but already exhibit higher relative amounts of pristane and phytane and noticeably modifications in the distribution of PAHs and PASHs, whereby naphthalene and phenanthrene were relatively lower in abundance compared to the fresh water sample type. Also observed are other aromatic compounds that were not present in the fresh samples (or in much lower amounts). These include

mainly a number of aromatic alcohol and ketones as well as aromatic acids and fatty acids (see Supplementary Table 11). The third group are the biodegraded samples which have also very low hydrocarbon contents (7230 ng/ml on average) and are dominated by the PAH phenanthrene as well as varying amounts of long chain *n*-alkanes, alkylated benzenes, aromatic acids and fatty acids. In addition, some of these samples contained sulfur containing aromatics as well as aromatic alcohols and varying amounts of alkylated DBTs. The last group is represented by the oil slicks which contain abundant *n*-alkanes and in the case of Tsanyao Yang also similar PAHs and PASHs as the fresh samples, while the Mictlan sample is devoid of these aromatic compounds but instead halogenated compounds are detected.

4. Discussion

This chapter will first discuss the results of the asphalt incubation experiments and then put these into context to the observations that were made during the analysis of the water samples collected from the environment in the Campeche Bay area.

4.1 Asphalt incubation experiments

4.1.1 *n*-Alkanes and Cycloalkanes

Alkanes are saturated hydrocarbons with different sizes and structures which are chemically inert. They are known to be a major fraction of the complex mixture of compounds found in crude oil. Microorganisms like bacteria, filamentous fungi and yeasts are able to degrade alkanes thereby utilizing them as a carbon and energy source (van Beilen et al., 2003; Wentzel et al., 2007). Alkane compounds are very hydrophobic and known to be insoluble in water (Rojo 2009, 2010). A study by Eastcott et al., 1988 (Table 8) pointed out that solubility decreases with increase in molecular weight. Ferguson et al. 2009 conducted a study to determine the aqueous solubility of *n*-alkanes ranging from methane (C_1) to *n*-docosane (C_{22}) at 298 K (24.85°C) and 1 bar and the results showed an exponential decrease of solubility relative to carbon number. This observation was in excellent agreement with a previous experiment by Tolls et al. (2002) as well as a group contribution model by Plyasunov and Shock (2000).

As the whole suite of C16 to C24 *n*-alkanes were found in significant concentrations (up to 51 ng/ml), in the analytical blank (sample ‘Asphalt Only’ abiotic control, time point 10 days) we conclude that it is possible that *n*-alkanes might be either derived from laboratory contamination or from some sort of carry-over between the samples. However, since *n*-alkanes were not detected in the ‘Asphalt Only’ experiments after 28 days, this contamination does not seem to have affected all the samples, but seems to be derived from individual events that are currently hard to reconstruct as the samples were collected during another master thesis in 2017 (Brünjes, 2018). Alternatively, since minor microbial activity cannot be excluded from the dead controls as pasteurization may have resulted in the survival of spores, this activity could have resulted in the depletion of the remaining *n*-alkanes over time.

Notably, in both the ‘Naphthalene’ and ‘Hexadecane’ abiotic experiments a relative increase in the abundance of *n*-alkane was observed when comparing both time points. Considering the study by Ferguson et al. (2009), we assume the possibility that these compounds might have undergone some dissolution and water washing as incubation time progresses leading to higher portion of these compounds in the aqueous phase. It also needs to be considered that the addition of the ^{13}C -labeled substrates hexadecane and naphthalene may have enhanced the dissolution of compounds, resulting in higher *n*-alkane abundances compared to the ‘Asphalt Only’ experiment that was only amended with asphalt pieces.

The addition of ^{13}C -hexadecane also resulted in the very high concentrations of hexadecane in the ‘Hexadecane’ abiotic control after 28 days of up to 3360 ng/ml (Figure 12). It is conspicuous that such high concentrations were not yet observed after 10 days, this may be due to the slow dissolution of this compound in water. Furthermore, we explain the comparably elevated concentrations of hexadecane (117 ng/ml) compared to the other *n*-alkanes (7.3 ng/ml) in the ‘Naphthalene’ abiotic experiment after 28 days by minor carry-over from the ‘Hexadecane’ experiment as the ‘Naphthalene’ samples were collected directly after the ‘Hexadecane’ samples (Jonas Brünjes, personal communication).

In comparison to the abiotic controls that generally exhibited an increase in *n*-alkanes in the water phase over time, the biotic incubations show the opposite in that these compounds are removed over time. We assign this removal of *n*-alkanes as a clear indication of systematic consumption by alkane degrading bacteria. A number of research papers (van Beilen et al., 2003; van Beilen and Funhoff, 2007; Wentzel et al., 2007; Fritsche and Hofrichter 2000) have investigated the various aspects of the physiology, enzymes and pathways involved in aerobic alkane degradation. The primary activation of a hydrocarbons by microorganisms requires the presence of free oxygen and alkanes are transformed to alcohols via mono-oxygenase which is further oxidized to an aldehyde and then to a fatty acid (Fritsche and Hofrichter 2000). In this present study, compounds that were detected after 10 days appear to have been either partly (for the ‘Hexadecane’ experiment) or totally removed (for the ‘Asphalt Only’ and ‘Naphthalene’ after 28 days of incubation (Figure 13). Smaller alkane compounds below pentadecane (C_{15}) were not detected in this experiment, suggesting that these compounds might have already been taken up by the microbial community (Wegener et al., 2020) or due to their low boiling points might have more readily gone into the gas phase omitting their detection with the used instrumentation.

Similar to the abiotic controls, the added hexadecane substrate is also present in the biotic ‘Hexadecane’ samples, where it increased in concentration over time from 31 ng/ml after 10 days to 537 ng/ml after 28 days. Again, this increase in the substrate could be assigned to a gradual increase in dissolution of the hexadecane substrate. Notably, the value after 28 days is over six time lower than in the abiotic control and consequently can be assigned to microbes consuming this substrate in the live experiments.

The cycloalkanes (Figure 14) exhibit a similar trend as the *n*-alkanes in both the abiotic controls and the live experiments. Although, the ‘Naphthalene’ and ‘Hexadecane’ abiotic experiments experienced a two-fold increase in cycloalkanes in between the two time points, and even though no value was available for the ‘Asphalt Only’ abiotic control after 10 days, the values after 28 days were comparable to those of the other abiotic experiments. Similar to the *n*-alkanes, we conclude that dissolution of the asphalt resulted in the increase of these compounds in the water phase (Ferguson et al. 2009). Most of the biotic experiments show a decrease in cycloalkanes over time, albeit this decrease is not so clear in the ‘Hexadecane’ experiment. Similar to the decrease in the *n*-alkanes this can be assigned to microbial activation and consumption of these compounds over the course of the incubation. Cycloalkanes are biodegraded via co-oxidation

mechanism leading to the formation of a cyclic alcohol which is dehydrogenated to a ketone. The introduction of oxygen to the cyclic ketone by a monooxygenase enzyme facilitates the ring cleavage (Fritsche and Hofrichter 2000). Studies like (Morgan and Watkinson 1994) have indicated that alkylated cycloalkanes are more susceptible to biodegradation compared to the unsubstituted cycloalkanes as the alkyl side chains of the cycloalkanes enhance degradation. In this study we do observed the decrease in alkylated cycloalkanes, resulting in a more rapid decline of 77% of the detected compounds in the ‘Asphalt Only’ incubation while the ‘Naphthalene’ experiment shows a more mild 35% decrease while values stay the same in the ‘Hexadecane’ experiments. It is interesting to note that even with the addition of hexadecane as a substrate to trigger aliphatic degraders; minimal change is observed with respect to the living experiments. This might lead to the suggestion that the addition of substrate to the incubations might have partially hindered the activities of microorganisms. On the other hand, this could again be explained by facilitated dissolution of the asphalt by the addition of the respective ¹³C-labeled substrates which may act as a solvent for the asphalt-bound hydrocarbons.

4.1.2 Aromatic alcohols

Smith and Tatchell (1969) described aromatic alcohols to be compounds in which the hydroxyl group is attached to a side-chain carbon atom which is bonded to an aromatic ring and can be classified as primary, secondary, or tertiary depending on the degree of substitution of the carbon atom. In this study, we detected benzyl alcohol, C1-phenol / benzenedimethanol, phenol, 3-(1-methylethyl)-, phenol, p-tert-butyl-, C3-benzyl alcohol, and C2-benzenethanol (Supplementary Figure 32), which we assign to either being directly derived from the asphalt or which could be intermediates during petroleum hydrocarbon degradation. During the degradation of aromatic hydrocarbons, eukaryotic and prokaryotic microorganisms utilize these compounds via monooxygenases and dioxygenase pathways respectively (Atlas and Bartha 1998) and their respective products are furthered through a series of pathways to yield catechol (Okoh 2006; Fritsche and Hofrichter 2000), a central intermediate for aromatic hydrocarbons biodegradation. For example, the biological degradation of naphthalene involves the activation of the aromatic ring by the enzyme naphthalene dioxygenase to form cis-naphthalene dihydrodiol (Figure 8) (Bamforth and Singleton 2005; Goyal and Zylstra 1997; Simon et al., 1993). This is subsequently followed by dehydrogenation (Bamforth and Singleton 2005; Goyal and Zylstra 1997) and a series of metabolic pathways producing diverse metabolites (Goyal and Zylstra 1997; Baboshinet al., 2008; Kiyohara et al., 1994) e.g. decarboxylation of salicylate to yield catechol which is a distinctive intermediate attributed to degradation of naphthalene, and also the transformation of salicylate to gentisate (Bamforth and Singleton 2005; Fuenmayor et al., 1998). However, in this study we did not detect any of these intermediates.

In both the abiotic and biotic incubations an increase in the relative abundance of the detected aromatic alcohols were observed between the 10 and 28 day time points (Figure 15). Alcohols

are soluble in water due to the polar hydroxyl group which is able to form hydrogen bonds with water molecules. Therefore, these compounds can readily undergo dissolution which accounts for their steady increase overtime as observed in all abiotic incubation experiments. Benzyl alcohol, C3-phenol, p-tert-butyl-, methyl phenol and benzenedimethanol were present in the abiotic incubations and are therefore interpreted to come directly from the asphalt and are not necessarily activated by aromatic hydrocarbon degrading organisms. Methyl phenol exhibits different occurrence in the Asphalt only and Naphthalene incubations. Its appearance in the Asphalt only abiotic and biotic incubation after 28 days could be due to dissolution (abiotic) and microbial activation (biotic) over time but was more abundant in the Naphthalene abiotic incubations after 10 and 28 days having minimal occurrence in the biotic incubations after 10 days. The absence of this compound in the biotic experiment after 28 days implies subsequent removal of this compound by the microbial community. Also it could be that the addition of naphthalene as a substrate was not able to trigger microbial activity.

A similar, but more significant increase in aromatic alcohols in the aqueous phase is observed in the biotic incubations of all experiments. The relative increase in abundance over time strongly suggests the additional influence of microbial activity. The dissolution coupled with microbial activation of benzyl alcohol and phenol-p-tert butyl- in the biotic experiments results to a relative increase in concentration from 10 to 28 days. One might expect the reverse case in the biotic samples where compounds are depleted over the incubation period relating to microbial activity. However, before the compounds can be consumed, they need to be activated first by oxidative processes resulting in compounds such as the observed aromatic alcohols (Supplementary Figure 32). Moreover, the experiments might not have been conducted long enough to see the subsequent depletion. In the biotic two effects come into play: (1) These compounds are undergoing continuous dissolution as observed in the abiotic controls, which makes them readily available for microbial attack, (2) Microbial activity also results in the secretion of biosurfactant which additionally enhances asphalt dissolution thereby increasing its availability for easier assimilation into the cell (Das and Chandran, 2011). Another reason that could be responsible for the relative increase over time observed in these samples could be that the production rate of these compounds supersedes the microbial consumption rate. Perhaps there is a limited availability of the microbial community responsible for utilizing these sets of compounds with respect to the given incubation period. Mountfort et al., (1990) indicated that aromatic alcohols e.g. benzyl alcohol had been oxidized by cell suspensions of *Methylosinus trichosporium* yielding corresponding aldehydes, which was subsequently oxidized to the corresponding aromatic acids, revealing that methanol dehydrogenase is able to catalyze the oxidation of primary alcohols (Anthony 1986). Enzymes that catalyze the initial step in methane or methanol oxidation can also be involved in the oxidation of aliphatic and aromatic hydrocarbons for methane monooxygenase, while a selected range of unsaturated alcohols could be oxidized by methanol dehydrogenase. It has also been defined that benzyl alcohol is likely to be the primary product of methyl oxidation of aromatic hydrocarbons and a suspected source of benzaldehyde and benzoic acid (Grbic-Galic and Vogel 1987). Another important observation to note is that as

incubation progresses, the highest value was recorded in the ‘Asphalt Only’ experiment, followed by the ‘Naphthalene’ then the ‘Hexadecane’ incubations. This suggests that the addition of naphthalene and hexadecane as substrates might have slightly limited microbial activity and that their addition is not necessary when trying best to mimic natural conditions.

4.1.3 Aromatic Ketones

As already mentioned in the discussion of the aromatic alcohols, aromatic ketones, like benzaldehyde are common intermediates during microbial aromatic hydrocarbon degradation (Grbic-Galic and Vogel 1987). The absence of these compounds in the abiotic incubations (except for hydrocoumarin and naphthalenedione detected after 28 days in the ‘Naphthalene’ abiotic experiment) signifies that these compounds are indeed most likely a result of microbial activation. The detection of naphthalenedione and hydrocoumarin which is a derivative of coumarin after 28 days in the ‘Naphthalene’ abiotic samples could result from minor microbial activity in the abiotic control. As mentioned above pasteurization likely resulted in the death of many marine microbes, but some spores could still have been active in these samples (Jonas Brünjes and David Aromokeye, personal communication).

The aromatic ketones, and in particular naphthalenedione and hydrocoumarin, are predominantly present in the ‘Naphthalene’ live incubations whereas absent in the ‘Hexadecane’ and the ‘Asphalt Only’ incubations. C2-benzaldehyde was detected in the biotic samples at both time points for the three experimental set up. C3-benzaldehyde and C2-isobenzofuran-1-one were only present after 28 days in the ‘Asphalt Only’ and ‘Hexadecane’ experiments while they were detected at both time points in the ‘Naphthalene’ set-up. The predominance of these compounds in the biotic ‘Naphthalene’ incubations suggests that these compounds are mainly attributed to microbial degradation of naphthalene. Numerous environmental research papers have often used naphthalene as a model compound to investigate bacteria degradability of PAHs (Seo et al., 2009; Goyal and Zylstra 1997). Surprisingly, none of the intermediates identified in these studies were detect in this present study. In addition, investigations have been carried out to examine bacterial utilization of naphthalene as a source of carbon and energy. Results revealed organisms belonging to the genera *Burkholderia* sp. (Kang et al., 2003; Kim et al., 2003;), *Sphingomonas* sp. (Dutta et al., 1998; Jouanneau et al., 2007; Baboshin et al., 2008), *Pseudomonas* sp. (Denome et al., 1993; Fuenmayor et al., 1998) to be involved in its degradation. Annweiler et al., 2000 also investigated *Bacillus thermoleovorans* Hamburg 2 which is a thermophilic aerobic bacterium that grows at 60°C on naphthalene as the sole source of carbon and energy. Since 60°C was also the temperature used for pasteurization, this spore former could be a potential candidate to have been active in the abiotic control.

4.1.3.1 Coumarin

Coumarin which is an aromatic ketone was most abundantly detected in the biotic ‘Naphthalene’ incubations, with minor amounts present in the biotic and abiotic ‘Hexadecane’ incubations and biotic ‘Asphalt Only’ incubations (Figure 17). Coumarin has been identified to be a potential intermediate in the biodegradation of aromatic hydrocarbons especially naphthalene (Fernley & Evans 1958; Davies and Evans 1964; Seo et al., 2009). Fernley & Evans (1958) reported that acid ether extracts from naphthalene cultures would yield coumarin and was able to isolate coumarin from naphthalene cultures. Davies and Evans (1964) indicated that during the degradation of naphthalene by a soil pseudomonad, *cis*-*o*-hydroxybenzalpyruvate may undergo oxidative decarboxylation which results in the formation of coumarin. Figure 30 shows the proposed catabolic pathways of naphthalene degradation by bacteria (Seo et al., 2009).

In this present study, the drastic depletion of coumarin in the ‘Naphthalene’ incubation over the time period from 10 to 28 days (Figure 17) strongly suggests that coumarin is readily produced and subsequently consumed during the microbial breakdown of naphthalene. Coumarin was also seen in the ‘Asphalt only’ biotic incubation after 10 days but was quickly depleted after 28 days (Supplementary Table 6). Similarly, coumarin was completely consumed after 28 days in the ‘Hexadecane’ biotic incubation (where it was only detected in the 10 days’ time point). It’s presence in the ‘Naphthalene’ and ‘Hexadecane’ abiotic controls is again an indication that these dead controls were not completely dead, but were slightly stimulated by the addition of the substrates.

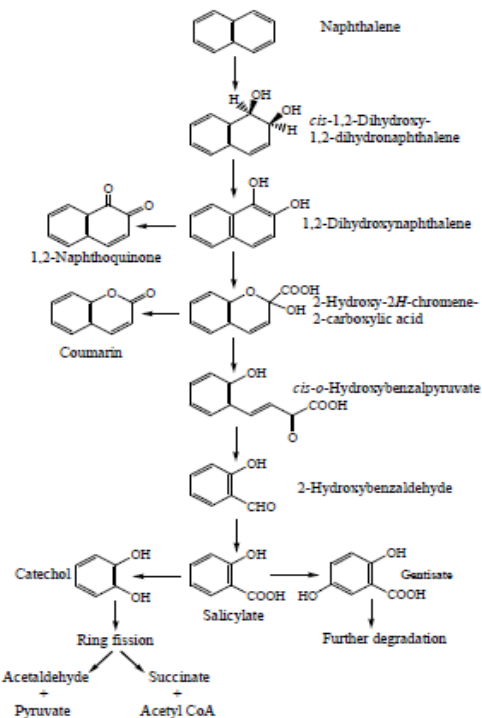


Figure 30. The figure shows the proposed catabolic pathways of naphthalene degradation by bacteria. Image gotten from Seo et al., (2009)

4.1.4 Aromatic acids

Distribution of aromatic acids, which include compounds such as alkylated (C2, C3 and C4) benzoic acids, C2-phenylacetic acid and mesitylactic acid exhibit a similar pattern as the aromatic alcohols. C2-phenylacetic acid and C2 benzoic acids are present in the abiotic controls (both time points of the ‘Naphthalene’ and ‘Hexadecane’ experiments), but there are no discernable increases or decreases in concentration, indicating that they are either derived from the dissolution of the asphalt or by background microbial activity of spores that got activated during pasteurization. In all live experiments, aromatic acids showed a drastic increase between the 10 and 28 day time points. Considering that aromatic acids such as salicylate *o*-hydroxy-trans-cinnamic acid (*o*-coumaric acid), *o*-hydroxyphenylpropionic acid (melilotic acid) (Fernley & Evans 1958) are formed during biodegradation of aromatic compound (e.g., naphthalene) although none of these compounds were identified in this present study, we assign this strong increase of the detected compounds to the increase in microbial activity during asphalt degradation.

Some of the compounds were distinct to individual experiments. For instance, C2-benzoic and C2-phenylacetic acid was the only aromatic acids detected in the dead controls of the ‘Hexadecane’ experiment, while only C2-phenylacetic acid was detected in the ‘Naphthalene’ abiotic experiment. The presence of these compounds in the dead controls may be due to the fact that some of the dead controls were still partly alive even though they were pasteurized, alternatively they could also be derived from the gradual dissolution of the asphalt. However, considering either scenario one would expect a larger suite of aromatic acids present, therefore it remains unclear which mechanism is responsible for their presence in the abiotic controls. C2-benzoic acid was also present in the ‘Asphalt Only’ biotic incubations after 10 days but was absent after 28 days indicating complete microbial transformation of this compound on a short timescale. This compound was also detected at both time points in most of the biotic replicates of ‘Hexadecane’ experiment samples with minor increase over time. Here, it is suspected that the ‘Hexadecane’ microbial community may not be as active in consuming C2-benzoic acid as the ‘Asphalt Only’ community. C2-phenylacetic acid was also observed after 28 days in the ‘Asphalt Only’ and ‘Hexadecane’ live experiments. For the biotic treatments it seems this compounds is released into the water as a result of biodegradation over time. Studies (Olivera et al., 1998; Luengo et al., 2001) reported phenylacetic acid (PAA) to be an important central intermediate during the microbial degradation of aromatic compounds (e.g. styrene, ethylbenzene, phenylacetaldehyde, phenylacetyl esters), and organisms such as *Rhodococcus* sp., *Escherichia coli*, and *Pseudomonas* sp. have been identified to be able to catabolize phenylacetic acid (PAA) (Navarro-Llorens et al., 2005; Ferrández et al., 1998 and 2000; Olivera et al., 1998). Also worth noting is the detection of isomers of (methylmethoxy)-benzoic acid after 28 days in the biotic ‘Hexadecane’ replicates. These compounds are suspected to be a result of biodegradation since they were only observed in the biotic experiments. The presence of mesitylactic acid in all biotic samples apart from the ‘Hexadecane’ incubation and tetramethyl benzoic acid after 28 days in all biotic samples imply that these compounds are also released into the water as a result

of biodegradation. Also, isomers of trimethyl benzoic acid and methylethyl benzoic acid were seen to elute at various retention time. In general, these compounds were mostly encountered after 28 days in the biotic incubations.

Overall, it is again notable that the identified aromatic acids had highest abundances in the ‘Asphalt Only’ experiments compared to the ‘Naphthalene’ and ‘Hexadecane’ incubations. This again suggests that instead of stimulating activity, the addition of substrates might have hindered microbial utilization and that natural conditions appear to be more suitable for microbes to degraded the asphalt hydrocarbons. It is quite surprising that the naphthalene experiment appeared to be the least favorable in this situation (Figure 18; Supplementary Table 6) because expectation was that naphthalene as a substrate would stimulate the microorganisms responsible for the activation and utilization of aromatic hydrocarbons and its subsequent intermediates.

4.1.5 Thiols and Thiophenic acids

3,4-Dimethylthiophene-2-thiol (Supplementary Figure 35) was the only thiol compound that was detected in all of the live samples and most dominant after 28 days. Notably, none of the compounds detected in the live incubations were observed in the dead control, which points to the fact that these compounds are released into the water due to the action of microorganism where they accumulate over the course of the incubation. 2(3H)-benzothiazolethione, 3-methyl- and 3,5-dimethylbenzo(b)thiophene-2-carboxylic acid also occurred in the 28 day time points of live samples of the ‘Asphalt only’ and most of the replicates of the ‘Naphthalene’ incubations.

Previous studies have reported pathways for metabolism of dibenzothiophene which includes the Kodama pathway also known as the ring-destructive pathway whereby one benzene ring of DBT is oxidized and cleaved to produce 3-hydroxy-2-formylbenzothiophene as the major product (Kodama et al., 1973), complete pathway involving the mineralization of dibenzothiophene to yield sulfite, carbon dioxide and water (van Afforded et al., 1990) and the 4S pathway also known as the sulfur-specific pathway which involves the desulfurization of DBT thereby releasing 2-hydroxybiphenyl as the end product without decreasing the number of carbon (Izumi et al., 1994; Oldfield et al., 1997; Rhee et al., 1998). The 4S pathway have been reported in previous studies while using microbial strains such as Gordona strain CYKS1 (Rhee et al., 1998), Rhodococcus sp. (Ma 2010; Oldfield et al., 1997), Mycobacterium sp. (Nekodzuka et al., 2009) to degrade DBT. A study by (Resnick and Gibson 1996) reported that the lateral ring dioxygenation observed in naphthalene dioxygenase from Pseudomonas sp. NCIB 9816-4 eventually yields dibenzothiophene dihydrodiol. Microbial strains e.g., *Pseudomonas* spp (Kropp et al. 1997) and *Sphingomonas paucimobilis* (Lu et al. 1999) have been isolated while investigating the degradation of dibenzothiophene (DBT) using naphthalene as a stimulating substrate and observed various metabolic intermediate involved for different strains. However, none of the observed intermediates were closely related to the ones that were detected during this study. Seo et al., 2006 reported intermediate compounds such as dibenzothiophene-diols,

benzo[b]thiophene-2,3-dicarboxylic acid and hydroxyl-benzo[b]thiophene carboxylic acid which attributed to the degradation of dibenzothiophene (DBT) by *Arthrobacter* sp. P1-1. This supports the observation made in this study which suggests that the thiol and thiophenic acids are intermediates produced during the biodegradation of DBT.

Dibenzothiophene is a common component of crude oils and like the PAHs are known to be recalcitrant in the environment. It was identified as one of the most abundant aromatic hydrocarbon in the Campeche Knoll oils Smit (2016) and Brünjes (2018) reported a relative increase of sulfur-containing formulae in the dissolved organic matter pool over the incubation period, with sulfur compounds comprising more than 50 % of total DOM formulae after 28 days. This is why we were curious to see if we can identify any sulfur containing compounds via GC-MS. Notably the detected thiols and thiophenic acids in this study are lower in concentrations than non-S containing aromatics (Figures. 15-18), however it is notable that the S-containing compounds increase notably after 28 days indicating their increasing formation by microbes and release into the water column. (Dyreborg et al., 1996c) pointed out that the biodegradation of benzothiophenes by the microbial community would be more effective with the presence of different growth substrates, however, in our case it looks like thiols and thiophenic acids are more abundantly produced without the addition of substrates.

4.1.6 Halogenated compounds

Halogenated compounds phenol, 2,6-dibromo-4-(1,1-dimethylethyl)-, phenol, 2-bromo-4-(1,1-dimethylethyl)-, 2-Naphthalenol, 1-bromo-, and 2,2-Dichloro-1,1-bis(4-methoxyphenyl)ethane were detected in most of the samples and notable concentrations were always highest after 10 days and decreased over time, more strongly in the biotic incubations than the abiotic controls. This indicates that halogenated compounds are either released out of the asphalt or alternatively, were intruded into the sample from another external source, but were then predominantly removed by microbial activity over the time of the experiment. The decrease in abundance of the halogenated compounds over time in the 'Hexadecane' abiotic incubations could also be within the range of quantification error. For the 'Naphthalene' incubations, the decrease in the abundance over time could be a result of precipitation and sorption to the asphalt or alternatively, assigned to minor microbial activity of spores that survived the pasteurization process.

Phenol, 2-bromo-4-(1,1-dimethylethyl) and 2,2-Dichloro-1,1-bis(4-methoxyphenyl)ethane are present in the abiotic control after 28 days with values 1.37 and 89.35 ng/ml respectively for the 'Asphalt Only' incubations, whereas only 2,2-dichloro-1,1-bis(4-methoxyphenyl)ethane was detected in the 'Naphthalene' and 'Hexadecane' abiotic experiments showing a minimal decrease in concentration overtime (from 10 -28 days). For the biotic experiments, the 'Asphalt Only' incubations showed all compounds except for 2-Naphthalenol, 1-bromo- to be present. A relative decrease in concentration was observed for phenol, 2,6-dibromo-4-(1,1-dimethylethyl)- 3.44ng/ml to 0.61 ng/ml and 2,2-dichloro-1,1-bis(4-methoxyphenyl)ethane 22.27ng/ml to 4.65

ng/ml from 10 to 28 days. Contrastingly, concentration of phenol, 2-bromo-4-(1,1-dimethylethyl)- was observed to increase from 2.37ng/ml to 8.63 ng/ml from 10 to 28 days. However, proper explanation for this observation could not be given because it is not clear what processes are involve in the mineralization of the bromo-halogen compounds found in this study. 2-Naphthalenol, 1-bromo- and 2,2-dichloro-1,1-bis(4-methoxyphenyl)ethane were detected in the 'Naphthalene' biotic experiment for both time points, with 2-naphthalenol, 1-bromo- having the highest value 17.82 ng/ml. The identified compounds also showed a decrease in concentration of both compounds from 10-28 days suggesting microbial uptake of these compounds. All compounds except for phenol, 2,6-dibromo-4-(1,1-dimethylethyl)- were detected in the 'Hexadecane' biotic samples after 10 days with 2,2-dichloro-1,1-bis(4-methoxyphenyl)ethane having the highest concentration of 16.04 ng/ml while phenol, 2-bromo-4-(1,1-dimethylethyl)- and 2-naphthalenol, 1-bromo- have very low concentrations of 0.43 and 0.27 ng/ml respectively. All compounds were absent after 28 day which could imply that they have been removed or altered by microorganisms. Microorganisms involved in breakdown of hydrocarbons also produce diverse halogenated natural intermediates. Gribble (2004) made an extensive study and discovered more than 4000 natural occurring organohalogens of which the compounds contain both chlorine and bromine and many of them are known to be produced by marine organism such as fungi, sponges, bacteria. Since the biotic incubations show a strong (and for the 'Hexadecane' incubation a complete) depletion, this is strong evidence that these compounds have been microbially consumed or systematically transformed as the incubation progresses. It was observed that marine organisms (e.g., sponges) oxidize preferentially bromide over chloride compounds which explains the abundance of bromoperoxidase (BPO) compared to chloroperoxidase (CPO) in the marine environment (Gribble, 1996a, 1998). Observations made in this study shows that bromide containing halogens were preferentially consumed over the chloride halogen which is noticeable from the low to no concentration observed for the bromide containing halogens compared to the higher concentrations of the chloride halogen which signifies microbial uptake. Generally, halogenated compounds are more resistant to bioremediation than non-halogenated compounds, and the degree of resistivity to biodegradation depends on the amount or number of halogens attached to the compound (FRTR). According to (Gribble, 1999), marine microorganisms have shown to be source of various bromo-organohalogenated compounds, whereas most chlorinated metabolites are known to have originated from terrestrial bacteria as well as fungi. This study indicates that the asphalts can be a source of natural halogenated compounds in the marine environment, although it seems they are recycled quickly by asphalt-degrading organisms as shown in all three experiments

4.1.7 Fatty acids

Under oxic conditions, heterotrophic bacteria and fungi are considered to be the dominant hydrocarbon degraders and since we also extracted this microbial biomass during the sample treatment, it is to be expected that we also find microbial biosignatures such as fatty acids derived from the asphalt-degrading biomass in our samples.

Indeed, fatty acids in the range of what is expected from bacteria, i.e. C14 to C18 fatty acids were found in the samples, predominantly in the biotic incubations. The abiotic controls also contained fatty acids, however, those were dominated by smaller fatty acids C9 to C12, which are most likely derived from lab contamination or perhaps from the activation and oxidation of *n*-alkanes. Fatty acid abundance in all abiotic controls ranges between 15ng/ml and 37 ng/ml. The biotic incubations for the three experimental set up shows an increase, reflecting the increase of hydrocarbon-degrading over time, which was also observed by Brünjes (2018) who reported increasingly turbid water and precipitation of white flocculates, which he assigned to presence of hydrocarbon-degrading microbes.

Notably, fatty acids such as monounsaturated fatty acids C16:1 and C18:1 and odd carbon numbered C15 and C17 fatty acids are only detected in the live experiments and these are also fatty acids that are typically assigned to bacterial sources in the marine environment (Wegener et al., 2016; Boschker et al., 1998). Even though C16:0 is the highest fatty acid in all live incubations and is also most likely derived from the asphalt-degrading microbes, it should be noted that C16:0 was also detected in the dead controls. As C16:0 and C18:0 are known common lab contaminants, using them solely as a microbial indicator is problematic. Based on the abundance of the monounsaturated and odd carbon numbered fatty acids, it can be concluded that the microbial activity of the ‘Asphalt Only’ and ‘Naphthalene’ incubations were on a similar order. However, the abundance of these fatty acids was an order of magnitude higher in the ‘Hexadecane’ incubations, indicating that this experiment resulted in the highest microbial activity. This confirms initial findings by Brünjes (2018) who also reported the ‘Hexadecane’ experiments to being most turbid and active during the course of the experiment. Even though the ‘Hexadecane’ experiment seems to have been most active, it is interesting that most of the oxygenated compounds were observed in highest abundances in the ‘Asphalt Only’ experiments, which led to the initial conclusion that this experiment was most active. Taking these observations together, although the addition of hexadecane strongly stimulated microbial activity, it seems like it predominantly stimulated the degradation of the substrate, but not of the asphalt. Similarly, the addition of naphthalene predominately stimulated the degradation of only naphthalene, as evidenced by the elevated presence of the intermediates coumarin and hydrocoumarin, while it seems that the most natural condition with no addition of substrates stimulated best the degradation of the asphalt.

4.2 Environmental samples

This chapter focuses on the interpretation of the results obtained for the environmental samples. It will start with a brief discussion of compounds assigned as contaminants, followed by a comparison with the asphalt incubation experiments and then a comparison of the different sites.

4.2.1 Branched alkanes with quaternary carbon (BAQCs) and other contaminants

In some of the hydrocarbon fractions of the water samples analyzed in this study two homologous series of branched alkanes with quaternary carbon atoms (BAQCs) were observed, one with an even over odd carbon predominance and the other with and odd over even carbon dominance (Figure 22, 23 and 24). These are compounds that have been reported previously in ancient rocks (Kenig et al., 2003), where they have been subsequently identified as contaminants coming from plastic materials (Brocks et al. 2008; Grosjean and Logan 2007). Grosjean and Logan 2007 conducted a detailed examination of solvent extracts stored in polyethylene plastic bags which revealed the presence of a wide range of hydrocarbons including methylalkanes and branched alkanes with quaternary carbon centers (BAQCs). Prior to these findings, a number of environmental research papers have emphasized BAQCs as biogenic products although their natural sources remained unknown (Kenig et al., 2003; Greenwood et al., 2004). For example, Kenig et al. 2003 suggest that BAQCs is derived from a group of related organisms and that the variations in relative abundance of BAQCs may be due to the biosynthetic response by source organism(s) to different environmental conditions. In addition, Kenig et al. 2003 reported BAQCs to be biomarkers for non-photosynthetic, sulfide oxidizing prokaryotes observed to inhabit benthic redox boundaries. However, other investigative studies (Brocks et al. 2008; Grosjean and Logan, 2007) have argued that presence of BAQCs in sample analysis indicates that the given sample (e.g. rock sample) has been extensively infiltrated by anthropogenic hydrocarbon contamination during sample storage. In this study, it is noticeable that these BAQCs were seen to occur only in samples retrieved using Niskin bottles and the GeoB19951-14 which was collected from the surface water of the push core. Notably, BAQCs were absent in water samples retrieved by Niskin sampling where other oil compounds such as *n*-alkanes were absent. Therefore, it is conceivable that these contaminants may be derived from the plastic material of the Niskin bottles and the push core. In this case, oil-rich waters may act as a solvent to release the BAQCs into the aqueous phase.

Other compounds that were identified as contaminants in the environmental samples includes nonanal and 2,4-di-tert-butylphenol and were found in almost all the environmental samples. Nonanal is an aldehyde that is derived from *n*-alkane transformation (*n*- nonane to nonanol to nonanal). Since no other aliphatic aldehyde was detected in this study, this compound is therefore regarded to be some kind of contaminant encountered during field or laboratory sampling. 2,4-di-tert-butylphenol is phenolic antioxidant (Grosjean et al., 2007) and has been reported to be a persistent organic pollutants (Aziz et al., 2018).

4.2.2 Comparison of environmental samples with asphalt incubation samples

Compounds identified in both experiments differ however, the presence of *n*-alkanes (C16 to C24) and biodegradation intermediate compounds such as benzyl alcohol and some fatty acids were observed in both cases. The presence of PAHs and PASHs in the environmental samples and their absence in the incubation samples could be because most of the environmental samples were collected in their pristine condition just immediately after seeping out from the sea floor using the GBS, while some were collected some meters above the sea floor within the water column. The incubation experiment was carried out over a 28 days period under controlled laboratory condition while the environmental samples are hydrocarbon water surrounding the asphalt exposure and oil seep sites which in some case have had longer exposure to microbial activation in the water column.

The resulting differences in the identified compounds in both experiments could be due to attributed to factors like but not limited to nutrients availability, oxygen content (Wang et al., 1998). Firstly, the incubation experiment was carried out in room temperature while that of the environmental samples is ca. 4°C. Lower temperature might have slowed down biodegradation processes in the environmental samples and vice versa.

4.2.3 Grouping of environmental samples into different sample types

Comparing the *n*-alkane and UCM patterns observed in the chromatograms of the 18 samples collected from the surrounding water and oil slicks, the samples could be categorized into four main types. Support for this classification comes from a quantitative assessment of hydrocarbon distribution in the samples (Figure 29) as well as biodegradation and water washing ratios identifying different levels of alteration (see also Figure 25 -28), as discussed below.

4.2.3.1 Type 1: Non-degraded ‘Fresh’ asphalt hydrocarbon -containing water samples.

As a first sample type, a ‘fresh’, non to slightly degraded asphalt-derived hydrocarbons dissolved in water is observed. These samples are characterized with intact *n*-alkanes patterns from C14 o C28 with both isoprenoids pristane and phytane still present. Also, the diverse suite of PAHs and PASHs and their alkyl homologues were still present in a similar order in abundance as observed for the ‘fresh’ asphalt type reported in the master thesis by Nadine Smit (Smit, 2016).

This sample type comprises of samples collected from the Mictlan and Tsanyao Yang Knoll and includes: GeoB19336-6 oily, GeoB19336-5, and GeoB19346-15 for Mictlan and GeoB19337-2 for Tsanyao Yang (Figure 23 and 24) (see also Supplementary Table 9). What these samples all have in common is that they were collected close to an active oil seepage site where fresh oil was visibly seeping out of the seafloor (Sahling and Bohrmann, 2017). Notably, samples

GeoB19336-6 oily, GeoB19336-5 and GeoB19346-15 show a slight bimodal *n*-alkane distribution indicating that the samples have already been slightly attacked by biodegradation, either by microorganisms living in the water column or before the oil seeped out of the seafloor. Microscopic analysis of the interior of the white asphalt tubes identified presence of ‘fleshy’ microbial mat and oil droplets as well as white precipitate (Wegener et al 2020) which proves that the oil seeping out of these asphalt tubes (‘fresh samples’) have been subjected to slight microbial transformation.

Naphthalene was not detected in any of the samples, which indicates that this compound is quickly consumed. However, homologues of alkyl-naphthalene (C1-C4 Naph) are detected in all samples in this category. Fluorene and phenanthrene and their alkyl-homologues (C1-C2) were present. Sulfur containing aromatics encountered include dibenzothiophene (DBT) and alkyl-dibenzothiophenes (C1 & C2 DBT). Compared to the other samples, particularly the abundance of naphthalene and DBTs in the ‘Fresh’ samples stands out, this indicates that these compounds are some of the first compound (e.g. naphthalene) that are preferentially consumed by microorganisms and readily undergo dissolution (e.g. DBT). Fluorene, phenanthrene, DBT and their respective C1 and C2 alkyl series as well as the alkyl- naphthalene show a relative increase in concentration with increasing alkylation. Considering that aromatic compounds exhibits increasing resistance to alteration processes with relative increase in ring number as well as the number of alkylation (Peters et al., 2005; Wang et al., 1998; Wardlaw et al., 2008), we suspect that the lower concentration of the C1 compared to the C2 compounds could simply be as a result of microbial consumption of the lighter aromatic compounds.

4.2.3.2 Type 2: Altered, biodegraded samples.

The second sample type is defined as water samples that contain oils that have been affected by biodegradation. Here, most of the *n*-alkanes and also the isoprenoids pristane and phytane and most of the PAHs and PASHs compounds have been removed in most of the samples. For many of them Pr/C17 and Ph/C18 ratios are either very high or could not be determined due to the lack of either compounds.

This category is comprised of samples from all three study areas Chapopote, Mictlan and Tsanyao Yang. For Chapopote the samples include GeoB19340-2, GeoB19340-4, and GeoB19351-14, for Mictlan GeoB19346-4, and for Tsanyao Yang GeoB19337-9 (Figure 22, 23 and 24) (see also Supplementary Table 10). *n*-Alkanes, pristane and phytane were only detected in the samples of Chapopote GeoB19351-14 and Mictlan GeoB19346-4, which also together with Tsanyao Yang sample GeoB19337-9 exhibited the most elevated UCMs. These oils are seeping out from sediments that are known to be affected by severe biodegradation such as the site at Chapopote (Schubotz et al., 2011a). In these samples naphthalene and its alkyl homologues were totally absent, further indicating a more advanced stage of biodegradation.

4.2.3.3 Type 3: Weathered hydrocarbon containing water samples

The third sample type includes samples that neither fit into the category of sample type 1 or 2. Most of the type 3 water samples still have an intact *n*-alkanes series (starting from C14), but with comparably higher Pr/C17 and Ph/C18 ratios than most of the fresh samples. Notably, the type 3 samples all have a relatively high UCM and many of them are affected by the BAQCs contaminant series. Also, more PAHs and PASHs were encountered for most of the samples compared to the type 2 biodegraded samples. It can be concluded that these types of samples have undergone some form of alteration compared to the ‘fresh’ sample type, while they are not yet as severely biodegraded as the type 2 samples. Very likely they have been also affected by biologic activity as can be seen as the increasing Pr/C17 and Ph/C18 ratios compared to the fresh samples. Nevertheless, it cannot be excluded that also abiotic processes such as simple dissolution of compounds has resulted in the loss (or enrichment) of compounds in this sample type.

These samples include GeoB19333-4, GeoB19333-7 from the Sonne Field and samples GeoB19327-3 and GeoB19327-4 from above the mussel bed and GeoB19336-6 from surrounding waters around the asphalt tubes at Mictlan and finally GeoB19337-3 from the oil site at Tsanyao Yang (Supplementary Table 11).

Surprisingly, alkylated benzene compound were also detected in this sample type, while these compounds were not as prominently detected in the other samples types. Since these compounds were not detected in the ‘fresh’ samples it can be concluded that they are not derived through simple dissolution of the asphalt and oil, but are possibly a by-product of asphalt hydrocarbon biodegradation. Also, the presence of aromatic alcohol (benzyl alcohol), ketones (e.g. benzophenone) and alkylated benzoic acid esters signifies biotic activation/ alteration of the monoaromatic compounds (Mountfort et al., 1990; Grbic-Galic and Vogel 1987).

4.2.3.4 Type 4: oil slicks

The oil slick samples are summarized in a distinct category as they are samples that are clearly affected by different processes as the deep-water samples. Photooxidation is one process that severely affects hydrocarbon compounds in oil slicks (Garret et al., 1998). Notably, the three samples look different, which is likely owed to the fact that the Tsanyao Yang samples were collected immediately after the oil bubbles reached the surface, while the Mictlan oil slick sample was already exposed to longer weathering before it was collected.

Interestingly all oil slick samples still have many of the *n*-alkanes still intact, this indicates that microbial degradation of *n*-alkanes has not progressed as far as for sample type 2 and some of sample type 3. Isoprenoid pristane and phytane only occurs in the Tsanyao Yang samples as the shorter chain saturate compounds have already been consumed at Mictlan indicating that the longer exposure for hours to days has already resulted in a significant decrease in n-alkane and

isoprenoid abundance. Neither naphthalene nor its alkyl homologues were detected. More so, most aromatic compounds for example phenanthrene and dibenzothiophene including their C1 & C2 homologs only appears in the Tsanyao Yang samples but are absent in the Mictlan. Again, this can be explained by the fact that the Tsanyao Yang samples were not yet exposed to longer biodegradation as was the Mictlan oil slick sample. Moreover, the presence of *n*-alkanes and absence of aromatic compounds in the Mictlan oil slick sample could be due to saturated compounds being more resistant to photooxidation compared to aromatic compounds which are particularly sensitive to photooxidation (Garret et al., 1998). Also, Increase in the alkylation of aromatic compounds makes it more sensitive and susceptible to photooxidation (Garret et al., 1998). Notably, the Tsanyao Yang oil slick samples show very similar trends to the Type 1 ‘fresh’ samples, whereby a relative increase in concentration with increasing alkylation is observed for the phenanthrene, including the C1-phanathrene and C2-phenanthrene and also for C1-DBT and C2-DBT. This implies a rapid transfer of oil bubbles from the seafloor to the surface which leaves little time for either microbial attack or dissolution as already observed by Römer et al. (2019). The absolute abundance [ng/ml] of compound classes (GC-MS) identified in the Oil slicks samples are shown in the Supplementary Table 12.

4.2.4 Biotic and abiotic processes affecting dissolved petroleum hydrocarbons

Aliphatic and aromatic hydrocarbons (such as PAHs and PASHs) show a higher resistance to alteration with relative increase in ring number as well as alkylation/ chain length (Peters et al., 2005; Wang et al., 1998).

4.2.4.1 Aliphatic hydrocarbons

Biodegradation of oil components results first in the removal of the *n*-alkanes and a visible accumulation of an UCM (Peters et al., 2005; Wardlaw et al., 2008; Head et al., 2003). Due to the low solubility of alkane compounds in water, it is congruent that the depletion of *n*-alkanes is attributed to microbial degradation hence the process of dissolution is negligible (Peters et al., 2005). The removal of low molecular weight *n*-alkanes observed in the type 1 fresh samples suggests that these samples might have already experienced mild biodegradation. The Pr/C17 and Ph/C18 ratios provide additional information on the level of biodegradation that occurred in each sample. Comparing the Pr/C17 and Ph/C18 ratios for all the samples (Table 4), the lowest values are found for the Mictlan ‘fresh’ and ‘weathered’ samples. The type 1 fresh samples of the Tsanyao Yang (GeoB19337-2) and of the Mictlan (GeoB19346-15) show a little bit of elevated Pr/C17 and Ph/C18 values, which implicates they are more degraded than indicated by the *n*-alkane pattern. This observed mismatch could possible result from mixing of biodegraded oil in the water column with fresh oil seeping out from the seafloor. This mixing could also explain the bimodal distribution observed in the chromatograms of Mictlan samples.

The ‘Weathered’ samples also feature Pr/C17 and Ph/C18 ratios which are comparable to the slightly degraded type 1 ‘fresh’ sample, implying that biodegradation in this sample group is also only mild to moderate. The appearance of a fairly large UCM in most ‘weathered’ samples

compared to a smaller UCM in the type 1 fresh samples indicates that both sample types have been biodegraded however to different degrees. The Type 2 ‘biodegraded’ samples show significantly higher (or absent) Pr/C17 and Ph/C18 ratios and feature minimal or no *n*-alkanes. The oil slicks show some slight biodegradation characteristics as a visible hump is seen for the Tsanyao Yang samples. The Pr/C17 and Ph/C18 ratios are also higher compared to the ‘fresh’ and ‘weathered’ samples. In addition, the disappearance of low molecular weight *n*-alkanes in the Mictlan sample also point to biodegradation.

4.2.4.2 Aromatic hydrocarbons

Microorganisms break down aromatic compounds to yield aromatic intermediates such as aromatic alcohols, ketones and aromatic acids (Mountfort et al., 1990). The most consistent trend for the aromatic compounds in all sample types is a relative increase in concentration with increase in alkylation. There are a few exceptions for example a reduced abundance of phenanthrene with increasing alkylation observed in the ‘weathered’ sample. The presence of low molecular weight aromatic compounds (e.g. alkyl benzenes in ‘weathered’ and alkynaphthalenes mostly in type 1 fresh samples (C1-C4) and minor amounts in the ‘weathered’ samples) suggest that the ‘fresh’ and ‘weathered’ samples seem to be experiencing biodegradation at varying degrees. A lot of factors can influence the mineralization of aromatic compounds by microorganisms such as dissolved oxygen, nutrients availability, temperature (Hazen et al. 2016; Wang et al., 1998). Since ambient water conditions are likely very similar among these samples, it is likely that a more important factor (such as duration of exposure of the samples) could influence biodegradation processes.

The absence of benzene, naphthalene and BT points to the fact that these compounds are already lost due to dissolution or early stages of biodegradation as studies (Peters et al., 2005; Volkman et al., 1984) have reported utilization of these compounds before *n*-alkane depletion. Organisms involved in the mineralization of alkylbenzene and alkynaphthalene under aerobic conditions could be Pseudomonas Spp. such as Flavobacterium (Aitken et al., 1998; Haritash and Kaushik, 2009; Kropp et al., 1994). The presence of benzyl alcohol (in all samples) and ketone components as well as aromatic acid (seen only in the weathered samples suggests these components could be biodegradation intermediate. Moreover, based on the observation of alkylbenzene in the type 3 ‘weathered’ samples, it is conceivable that the aromatic benzoic acid esters which was also detected in the type 3 ‘weathered’ samples could be possible biodegradation products of the alkylated benzene compounds.

A puzzling observation in this study was the enrichment of smaller compounds such as phenanthrene and DBT compared to their alkylated C1- and C2- derivatives in the weathered samples type 3 (i.e. Phen>C1>C2 and DBT<C1<C2) even though the opposite would be expected. In this case we argue that since the smaller compound more readily undergoes dissolution this results in higher ratios in the more abiotically weathered water samples. This explains the higher values for the weathered samples observed in the plot C1-Phen/C2-Phen

against C1-DBT/C2-DBT (Figure 26). In comparison, the Type 2 biodegraded and oil slick samples have comparably lower ratios as a result of microbial consumption of the short chain compounds. One of the Type 2 biodegraded samples (Chapopote GeoB19351-14) is seen to cluster together with the fresh samples. This sample is oily bubbles seeping from the oily sediment (Smit 2016) and also happens to be biodegraded but having values for C1- and C2-DBT and C1- and C2-phenanthrene. These elevated values suggest that these alkylated aromatic appear to be resistant to biodegradation in this particular sedimentary environment, perhaps owing to different preference of the prevailing anaerobic hydrocarbon degraders. Previous experimental data (Price 1976) have shown that sulfur-containing compounds (e.g. thiophene and 2-ethylthiophene) are more soluble in water compared to aromatic hydrocarbons and that hetero atomic compounds (e.g., dibenzothiophene) are highly resistant to biodegradation (Tissot and Welte, 1978).

Furthermore, alkylated fluorene compounds detected in the ‘fresh’ samples also shows similar trend as observed for most of the aromatic compound. A relative increase in concentration with increase in alkylation is observed which suggest microbial utilization and preference of smaller compounds over heavier ones. Organisms such as *Pseudomonas* sp. have been reported to degrade fluorene (Grifoll et al., 1994; Resnick S. M. and Gibson 1996; Medić et al., 2020). The pathway involves initial oxygenation of fluorene at C-9 to yield 9-fluorenol followed by a subsequent dehydrogenation to the corresponding ketone, 9-fluorenone. This goes through a series of degradation pathways to form phthalic acid (Grifoll et al., 1994).

Another unexpected observation were the high C1-Phen/C1-DBT values in type 3 weathered over type 1 fresh samples (Figure 27) as studies have shown that PASHs are more resistance to physical and biological alterations than PAHs (Connan et al., 1992; Hegazi and Andersson, 2007; Vairavamurthy et al., 1992; Wardlaw et al., 2011). The preferential consumption of DBTs over alkyl phenanthrene has been reported by Wang et al., (1998), suggesting that variables such as nutrient availability, oxygen levels, and composition of the oil does affect microbial hydrocarbon preferences. Also, Smit 2016 (Master thesis), reported a loss of DBTs homologues compared to phenanthrenes in oil impregnated biodegraded sediments and the exterior of asphalts, which are more affected by biodegradation. Smit 2016 explained this by a preferential utilization of sulfur containing compounds over the polycyclic aromatic compounds by the indigenous microorganisms in this environment.

5. Conclusion

The asphalt incubation experiment was conducted in the laboratory under room temperature using artificial sea water and nutrients to investigate the release of oil compounds into the water phase Brünjes (2018). Biotic and abiotic processes, such as microbial degradation and dissolution influenced the chemical composition of oil released into the water phase in the experiments. These results were then compared with water samples collected from three locations at the Campeche area in the southern Gulf of Mexico. Given the observations presented in this study when comparing the asphalt incubation to the environmental samples, it is conceivable that the oil in the water phase in both sample types was exposed to different alteration processes as a result of aerobic and to an extent anaerobic biodegradation as well as compound dissolution or other weathering processes such as photooxidation (in the oil slick samples).

PAHs such as naphthalene and phenanthrene and PASHs (e.g., dibenzothiophene) were not detected in the asphalt incubation experiments which falsifies the expectation in research question 1. However these compounds (PAHs and PASHs) were present in most of the environmental water samples ('fresh', 'weathered' and 'oil slicks' samples). The reason for their absence in the incubation samples and present in the environmental samples could be due to their quick consumption and transformation into other intermediates. In situ microbial activity in the marine environment is relatively slower due to colder temperatures and lower nutrient concentrations while the laboratory incubation exhibited a rather fast microbial transformation of these compounds. Intermediate compounds attributed to microbial hydrocarbon degradation were observed in all of the asphalt incubation samples and particularly prominent in the naphthalene-stimulated and asphalt only experiment, which prove the research question 2 to be true. Some degradation intermediates observed in the incubation experiments were also detected in the environmental samples; these include benzyl alcohol and a few selected fatty acids as expected in the research question 3. The environmental samples mainly show the presence of oil compounds with minor or major alterations. The oxygenated compounds observed in asphalt incubation experiments are related to microbial hydrocarbon degradation (Lemkau et al., 2014; Aeppli et al., 2012) and include phenol bound aromatic alcohols, aromatic aldehydes and ketone compounds, as well as fatty acids and aromatic acids. This is also congruent to the study by Brünjes (2018), which reported the increase in the proportion of polyphenols as well as oxygenated compounds. The depletion of bromide containing halogens over chloride halogen in the incubation experiments implies microbial consumption of bromo- over chloro-halogens. This also supports the findings in previous studies (Gribble, 1996a, 1998) which reported preferential oxidation of bromide over chloride compounds by marine organisms.

n-Alkanes were observed in the asphalt incubation experiment but was observed to be predominant in many of the environmental water samples. The relative presence of the isoprenoids pristane and phytane to their respective *n*-alkane compounds C17 and C18 provides insight on the level of degradation of these samples in the environmental samples, which identified the dissolved oil in many of the water samples to be slightly biodegraded. Together with the presence or absence of *n*-alkanes, this allowed the grouping of the environmental samples into four different samples types affected by different levels of biodegradation: type 1 'fresh', type 2 'biodegraded' type 3 'weathered' and type 4 'oil slicks' samples. The removal of *n*-alkanes observed in the Type 2 'biodegraded' samples mainly implies the action of microbial

degradation processes (Peters et al., 2005; Wang et al., 1998; Fritsche and Hofrichter, 2008), whereas biodegradation (Wang et al., 1998) or compound dissolution (Wardlaw et al., 2008) could account for the observed removal of aromatic compounds. For the aromatic compounds noticeable was a relative increase of compounds with more alkylations compared to lower alkylated aromatics, which implies preferential consumption of the shorter chain compounds by aromatic hydrocarbon degraders in the environmental water samples. *n*-Naphthalene was totally absent in all samples which suggest a quick removal and transformation of this compound by microorganism. The presence of alkynaphthalenes in all sample types except for the type 2 ‘biodegraded’ samples compared with the absence of *n*-naphthalene exemplifies the high resistance of alkylated aromatic hydrocarbons to alteration with the increasing number of alkyl substituents (Atlas and Bartha 1998).

Observed in the type 3 ‘weathered’ samples is a decrease of phenanthrene compounds that have a higher degree of alkylations compared to the ones with less alkylations (as opposed to what was observed for the biodegraded samples) while *n*-DBT and its alkyl-homologs show decreased abundance relative to phenanthrene and alkyl-phenantrenes. The increase in concentration of phenantrenes and its lesser alkyl substitutes could possibly denote an increased dissolution of the low molecular weight phenantrenes. However, dissolution would also result in an increased abundance of DBT compounds relative to phenanthrene, which is not observed, therefore, preferential degradation of DBT over phenantrenes by the microbial community could be the case. Similar observations were also reported by Smit (2016) and Wang et al., (1998) where the alkyl-DBT’s were more easily degraded than the phenanthrenes. Notably, the type 3 ‘weathered’ samples is seen to have a lot of oxygenated compounds. Some of the samples appear to be degraded while some only exhibits slight biodegradation characteristics. The presence of aromatic alcohols, ketones and acids shows these samples are already undergoing alterations. Also the presence of BAQC’s in the weathered samples was not expected but is suspected to be coming from the plastic material (Niskin bottles) used for collecting the samples.

The Mictlan oil slick was seen to have a high *n*-alkane series, however, was devoid of aromatic compounds. Generally, the presence of *n*-alkanes and absence of aromatic hydrocarbon compounds in the Mictlan oil slick sample suggests alterations due to photooxidation since aromatic hydrocarbon compounds are more susceptible to photooxidation (Garret et al., 1998). The oil slick samples from Tsanyao Yang appears to still be in pristine form as oil bubbles make their way to the ocean surface with minimal microbial attack, where they were immediately collected, while the Mictlan oil slick was exposed for a longer period of time before the sample was collected.

6. Outlook

Considering that the difference in temperature, oxygen and nutrient concentration in the asphalt incubation experiments compared to the *in situ* conditions could have influenced hydrocarbon microbial degradation, future experiments should be carried out resembling better *in situ* conditions so as to better mimic natural settings. Also to investigate the reproducibility of the abiotic processes, it would be best to prepare replicates for the dead control similar to the live incubations. This could provide a better understanding of abiotic related processes.

Following the observed presence of BAQCs compounds which are known plastic contaminants and other compounds identified as contaminants in both the asphalt incubation experiments and environmental samples, extreme care should be taken while carrying out sampling and constructing the experiments. The use of plastic materials for sampling and storage has been observed to introduce the particular class of contaminants for the BAQCs and di-tert-butylbenzoquinone (Brocks et al. 2008; Grosjean and Logan 2007). Different experiments need to be carried out to get a better idea of the processes relating to the BAQCs by using water, solvent, and a mixture of water and solvent (best to be oil related) in plastic retainers (e.g., niskin bottles) and glass retainers which would be subjected to extractions and subsequent analysis. The idea behind this is to investigate first where the contamination is coming from and secondly, how best to minimize infiltration of contaminants during sampling.

In order to achieve a more comprehensive analysis whereby all the compounds can be detected also those of which are currently hidden behind the UCM, comprehensive two dimensional gas chromatography mass spectrometry (GCxGC-MS) would be an excellent analytical method for the separation of complex petroleum mixtures and to better resolve the UCM observed in altered oil samples. The GCxGC-MS separation is done based on volatility and polarity while the conventional GC used in this study separates compounds according to their volatility.

Acknowledgement

I am very grateful to the almighty God for His infinite mercies in helping me come to the end of the Msc. program.

I would like to express my deepest appreciation to my academic supervisor and course adviser Dr. Florence Schubotz for giving me the opportunity to pursue this comprehensive research in petroleum and microbial related activities and for sharing her knowledge in this field. I sincerely appreciate the time and effort you invested during this period; our discussions during our zoom meetings, your guidance and encouragement as well as prompt email responses. I am privileged to have shared with you such a wonderful experience.

I would also like to thank Dr. Christian Hallmann for accepting to co-supervise my Master Thesis and allowing me carry out an initial analysis of the samples in his laboratory.

I am thankful to my course lecturers who have committed their time in impacting their valuable knowledge to me which has propelled me to achieving my aim of study.

A Special thanks to Xavier Prieto-Mollar for assisting me with analytical devices that was used in running my samples. Also, thanks to Kai-Uwe Hinrichs for giving me the opportunity to make use of the laboratory facilities. To the members of the working group Organic Geochemistry in MARUM, a big thank you for being very cheerful and accommodating.

I would also like to express my gratitude to my parents Mr. Samuel C. Nwabor and Ms. Evelyn N. Okeke, my grandfather Sir Ernest Okeke and my siblings: Blessing I. Nwabor-Ojile, Maryann, Emmanuel and Christian Nwabor and Brian Mbonu for their encouragement and support through prayers. Also, I would like to thank my colleagues and friends with whom I have spent my time at the University of Bremen.

Most especially I would like to thank my soul mate Jenna Völlers for her understanding and patience while bearing the parenting burdens through the period of this Thesis. To her parents Peter and Petra Völlers, I would like to thank you for being very supportive.

Finally, a heartfelt thank you to my daughter, Livia Chidera Nwabor who encouraged me with her smiles in the final months of this thesis. You are more than a source of inspiration and motivation to me and I am so honored to be your dad.

References

- Aeppli, C., Carmichael, C.A., Nelson, R.K., Lemkau, K.L., Graham, W.M., Redmond, M.C., Valentine, D.L. and Reddy, C.M. (2012) Oil Weathering after the Deepwater Horizon Disaster Led to the Formation of Oxygenated Residues. *Environmental Science & Technology* 46, 8799- 8807.
- Aitken, M. D., W. T. Stringfellow, R. D. Nagel, C. Kazunga, and S.-H. Chen, 1998. Characteristics of phenanthrene-degrading bacteria isolated from soils contaminated with polycyclic aromatic hydrocarbons: Canadian journal of microbiology, v. 44, p. 743-752.
- Annweiler, E., Richnow, H. H., Antranikian, G., Hebenbrock, S., Garms, C., Franke, S., Francke, W., & Michaelis, W. (2000). Naphthalene degradation and incorporation of naphthalene-derived carbon into biomass by the thermophile *Bacillus thermoleovorans*. *Applied and environmental microbiology*, 66(2), 518–523. <https://doi.org/10.1128/aem.66.2.518-523.2000>
- Anthony C. 1986. Bacterial Oxidation of Methane and Methanol. Advances in Microbial Physiology. Volume 27. Pages 113-210. ISSN 0065-2911. ISBN 9780120277278. [https://doi.org/10.1016/S0065-2911\(08\)60305-7](https://doi.org/10.1016/S0065-2911(08)60305-7).
- Atlas R. and Bragg J. Bioremediation of marine oil spills: when and when not--the Exxon Valdez experience. *Microb Biotechnol*. 2009;2(2):213-221. doi:10.1111/j.1751-7915.2008.00079.x
- Atlas R.M., Bartha R. Fundamentals and Applications. In *Microbial Ecology*. Benjamin/Cummings Publishing Company, Inc. California, USA. 4th Ed. (1998) pp. 523-530.
- Aziz, A., Agamuthu, P. and Fauziah, S. (2018). Removal of bisphenol A and 2,4-Di-tert-butylphenol from landfill leachate using plant- based coagulant. *Waste Management & Research*, 36(10), 975–984. <https://doi.org/10.1177/0734242X18790360>
- Baboshin M., Akimov V., Baskunov B., Born T., Khan S. and Golovleva L. (2008). Conversion of polycyclic aromatic hydrocarbons by *Sphingomonas* sp.VKM B-2434. *Biodegradation*. 19. 567-76. 10.1007/s10532-007-9162 2.
- Bamforth, S.M. and Singleton, I. (2005) Bioremediation of polycyclic aromatic hydrocarbons: Current knowledge and future directions. *Journal of Chemical Technology & Biotechnology* 80, 723-736.
- Boetius, A., K. Ravenschlag, C. J. Schubert, D. Rickert, F. Widdel, A. Gieseke, R. Amann, B. B. Jørgensen, U. Witte, and O. Pfannkuche, 2000, A marine microbial consortium apparently mediating anaerobic oxidation of methane: *Nature*, v. 407, p. 623-626.
- Boschker H., Nold S., Wellsbury P., Bos D., de Graaf W., Pel R., Parkes R. and Cappenberg T. Direct linking of microbial populations to specific biogeochemical processes by ¹³C- labelling of biomarkers. *Nature* 392, 801–805 (1998). <https://doi.org/10.1038/33900>

Bowden, S. A., P. Farrimond, C. E. Snape, and G. D. Love, 2006, Compositional differences in biomarker constituents of the hydrocarbon, resin, asphaltene and kerogen fractions: An example from the Jet Rock (Yorkshire, UK): *Organic Geochemistry*, v. 37, p. 369-383.

Brocks J. J., Grosjean E., Logan G. A. (2008). Assessing biomarker syngeneity using branched alkanes with quaternary carbon (BAQCs) and other plastic contaminants. *Geochimica et Cosmochimica Acta* 72 (2008) 871–888

Brüning, M., H. Sahling, I. R. MacDonald, F. Ding, and G. Bohrmann, 2010, Origin, distribution, and alteration of asphalts at Chapopote Knoll, Southern Gulf of Mexico: *Marine and Petroleum Geology*, v. 27, p. 1093-1106.

Brünjes J. (2018) Experimental studies on the fate of dissolved petroleum compounds of a natural asphalt seep in the Gulf of Mexico. Master Thesis, Department of Geoscience. University of Bremen, Bremen.

Bryant WR, Lugo J, Cordova C, Salvador A (1991) Physiography and bathymetry v. J. Boulder, Geological Society of America, Decade of North American Geology, The Gulf of Mexico Basin, pp 13–30

Ceramicola S., Dupré S., Somoza L. and Woodside J. (2018). Cold Seep Systems. 10.1007/978-3-319-57852-1_19.

Connan, J., A. Nissenbaum, and D. Dessert, 1992, Molecular archaeology: Export of Dead Sea asphalt to Canaan and Egypt in the Chalcolithic-Early Bronze Age (4th-3rd millennium BC): *Geochimica et Cosmochimica Acta*, v. 56, p. 2743-2759.

Cordes, E.E., Cunha, M.R., Galéron, J., Mora, C., Olu-Le Roy, K., Sibuet, M., Van Gaever, S., Vanreusel, A. and Levin, L.A. (2010), The influence of geological, geochemical, and biogenic habitat heterogeneity on seep biodiversity. *Marine Ecology*, 31: 51-65. doi:10.1111/j.1439-0485.2009.00334.x

Cozzarelli I. M. and Baehr A. L. (2003). Volatile Fuel Hydrocarbons and MTBE in the Environment. *Treatise on Geochemistry*. TrGeo...9..433C, p 612. doi:10.1016/B0-08-043751-6/09054-X

Das, N. and Chandran, P. (2011) Microbial Degradation of Petroleum Hydrocarbon Contaminants: An Overview. *Biotechnology Research International* 2011.

Davies J. I., Evans W. C. (1964). Oxidative metabolism of naphthalene by soil pseudomonads. *Biochem. J.* 91 251 261

Ding, F., V. Spiess, M. Brüning, N. Fekete, H. Keil, and G. Bohrmann, 2008, A conceptual model for hydrocarbon accumulation and seepage processes around Chapopote asphalt site, southern Gulf of Mexico: from high resolution seismic point of view: *Journal of Geophysical Research: Solid Earth* (1978–2012), v. 113.

- Dutta T. K., Selifonov S.A., Gunsalus I.C. (1998). Oxidation of methyl-substituted naphthalenes: Pathways in a versatile *Sphingomonas paucimobilis* strain. *Appl. Environ. Microbiol.* 64, 1884-1889.
- Dyreborg, S., Arvin, E., Broholm, K. and Christensen, J., 1996c. Biodegradation of thiophene, benzothiophene and benzofuran with eight different primary substrates *Environ. Toxic. Chem.*, 5: 2290-2292.
- Eastcott L., Shiu W.Y., Mackay D. (1988). Environmentally relevant physical-chemical properties of hydrocarbons: a review of data and development of simple correlations *Oil & Chem. Pollut.*, 4 pp. 191-216
- Edwards, J.D.. (2001). Twenty-first-century energy: Decline of fossil fuel, increase of renewable nonpolluting energy sources. *AAPG Memoir.* 74. 21-34.
- Ferguson A. L., Debenedetti P. G., and Panagiotopoulos A. Z. (2009). Solubility and Molecular Conformations of *n*-Alkane Chains in Water. *The Journal of Physical Chemistry B* 113 (18), 6405-6414 DOI: 10.1021/jp811229q
- Fernley H., Evans W. (1958) Oxidative Metabolism of Polycyclic Hydrocarbons by Soil Pseudomonads. *Nature* 182, 373–375 . <https://doi.org/10.1038/182373a0>
- Ferrández, A., García, J.L. & Díaz, E. (2000) Transcriptional regulation of the divergent paa catabolic operons for phenylacetic acid degradation in *Escherichia coli*. *J Biol Chem* 275: 12214– 12222.
- Ferrandez, A., Minambres, B., Garcia, B., Olivera, E. R., Luengo, J. M., Garcia, J. L., and Diaz, E. (1998) Catabolism of phenylacetic acid in *Escherichia coli*. Characterization of a new aerobic hybrid pathway. *J. Biol. Chem.*, 273, 25974–25986.
- Foght J. (2008). Anaerobic biodegradation of aromatic hydrocarbons: pathways and prospects. *J. Mol. Microbiol. Biotechnol.*, 15 (2–3) pp. 93-120
- Fritzsche W. and Hofrichter M. (2000) Aerobic Degradation by Microorganisms. In: Klein, J., Ed, Environmental Processes-Soil Decontamination, Wiley-VCH, Weinheim, 146-155.
- FRTR Federal Remediation Technologies Roundtable (Remediation Technologies Screening Matrix and Reference Guide, Version 4.0)
- Fuenmayor, S.L.; Wild, M.; Boyes, A.L.; Williams, P.A. (1998). A gene cluster encoding steps in conversion of naphthalene to gentisate in *Pseudomonas* sp. Strain U2. *J. Bacteriol.* 180, 2522-2530.
- Garrett R.M., Pickering I.J., Haith C.E. and Prince R.C. (1998). Photooxidation of Crude Oils *Environmental Science & Technology* 32 (23), 3719-3723 DOI: 10.1021/es980201r

- Goyal, A.K. and Zylstra, G.J. (1997). Genetics of naphthalene and phenanthrene degradation by Comamonas testosteroni. *J. Ind. Microbiol. Biotechnol.* 19, 401-407.
- Grbic-Galic, D., and Vogel, T. 1987. Transformation of Toluene and Benzene by Mixed Methanogenic Cultures . *APPL. ENVIRON. MICROBIOL.* p. 254-260.
- Greenwood, P.F., Arouri, K.R., Logan, G.A., Summons, R.E., 2004. Abundance and geochemical significance of C_{2n} dialkylalkanes and highly branched C_{3n} alkanes in diverse Mesoand Neoproterozoic sediments. *Organic Geochemistry* 35, 331–346
- Gribble G. W. Natural Organohalogens: A New Frontier for Medicinal Agents? *Journal of Chemical Education* 2004 81 (10), 1441 DOI: 10.1021/ed081p1441
- Gribble, G.W., 1996a. Naturally occurring organohalogencompounds—A comprehensive survey. *Prog. Chem. Org.Nat. Prod.* 68, 1–423.
- Gribble, G.W., 1998. The diversity of natural organochlorinesin living organisms. *Acc. Chem. Res.* 31, 141–152.
- Gribble, G.W., 1999. The diversity of naturally occurringorganobromine compounds. *Chem. Soc. Rev.* 28, 335–346.
- Grifoll M., Selifonov S A. and Chapman P. J. (1994). Evidence for a novel pathway in the degradation of fluorene by *Pseudomonas* sp. strain F274. *Applied and Environmental Microbiology*. 60 (7) 2438-2449; CODEN: AEMIDF; ISSN: 0099-2240
- Grosjean E. and Logan G. A. (2007). Incorporation of organic contaminants into geochemical samples and an assessment of potential sources: Examples from Geoscience Australia marine survey S282. *Organic Geochemistry* 38 (6) 853–869
- Grosjean, E., Logan, G.A., Rollet, N., Ryan, G.J., Glenn, K., 2007. Geochemistry of shallow tropical marine sediments from the Arafura Sea, Australia. *Organic Geochemistry*, in press.
- Haddock J. (2010). Aerobic Degradation of Aromatic Hydrocarbons: Enzyme Structures and Catalytic Mechanisms. 10.1007/978-3-540-77587-4_74.
- Hahn CJ, Laso-Pérez R, Vulcano F, Vaziourakis K-M, Stokke R, Steen IH, Teske A, Boetius A, Liebeke M, Amann R, Knittel K, Wegener G. 2020. “Candidatus Ethanoperedens,” a thermophilic genus of Archaea mediating the anaerobic oxidation of ethane. *mBio* 11:e00600-20. <https://doi.org/10.1128/mBio.00600-20>.
- Haritash, A. K., and Kaushik, C. P. (2009). Biodegradation aspects of polycyclic aromatic hydrocarbons (PAHs): a review. *J. Hazard. Mater.* 169, 1–15. doi: 10.1016/j.jhazmat.2009.03.137

Hazen T. C., Prince R. C., and Mahmoudi N. (2016) Marine Oil Biodegradation. Environmental Science & Technology 50 (5), 2121-2129 DOI: 10.1021/acs.est.5b03333

Head I. M., Jones D. M. and Larter S. R. 2003, Biological activity in the deep subsurface and the origin of heavy oil: Nature, v. 426, p. 344-352.

Head, I. M., Gray, N. D. and Larter, S. R. (2014). Life in the slow lane; biogeochemistry of biodegraded petroleum containing reservoirs and implications for energy recovery and carbon management. *Front. Microbiol.* 5.10.3389/fmicb.2014.00566

Hegazi, A. H., and J. T. Andersson, 2007, Characterization of polycyclic aromatic sulfur heterocycles for source identification: Oil spill environmental forensics. Fingerprinting and source identification. Elsevier, Boston, MA, p. 147-168.

Izumi Y, Ohshiro T, Ogino H, Hine Y, Shimao M (1994) Selective desulphurization of dibenzothiophene by *Rhodococcus erythropolis* D-1. *Appl Environ Microbiol* 60: 223–226.

Jouanneau, Y.; Micoud, J.; Meyer, C. (2007). Purification and characterization of a three-component salicylate 1-hydroxylase from *Sphingomonas* sp. Strain CHY-1. *Appl. Environ. Microbiol.* 73, 7515-7521.

Kang, H.; Hwang, S.Y.; Kim, Y.M.; Kim, E.; Kim, Y.S.; Kim, S.K. (2003). Degradation of phenanthrene and naphthalene by a Burkholderia species strain. *Can. J. Microbiol.* 49, 139-144.

Kenig F., Simons D-J. H., Crich D., Cowen J. P., Ventura G. T., Rehbein-Khalily T., Brown T. C., and Anderson K. B. (2003) Branched aliphatic alkanes with quaternary substituted carbon atoms in modern and ancient geologic samples. *PNAS* vol. 100 no. 22 12554–12558. www.pnas.org/cgi/doi/10.1073/pnas.1735581100

Kim, T.J.; Lee, E.Y.; Kim, Y.J.; Cho, K.S. (2003). Ryu, H.W. Degradation of polyaromatic hydrocarbons by Burkholderia cepacia 2A-12. *World J. Microbiol. Biotechnol.* 19, 411- 417.

Kiyohara, H.; Torigoe, S.; Kaida, N.; Asaki, T.; Iida, T.; Hayashi, H.; Takizawa, N. (1994). Cloning and characterization of a chromosomal gene cluster, pah, that encodes the upper pathway for phenanthrene and naphthalene utilization by *Pseudomonas putida* OUS82. *J. Bacteriol.* 176, 2439-2443.

Klapp, S. A., M. M. Murshed, T. Pape, H. Klein, G. Bohrmann, P. G. Brewer, and W. F. Kuhs, 2010, Mixed gas hydrate structures at the Chapopote Knoll, southern Gulf of Mexico: Earth and Planetary Science Letters, v. 299, p. 207-217.

Kodama K, Umehara K, Shimizu K, Nakatani S, Minoda Y, Yamada K (1973) Identification of microbial products from dibenzothiophene and its proposed oxidation pathway. *Agr Biol Chem* 37, 45–50.

Kropp, K. G., J. A. Gonçalves, J. T. Andersson, and P. M. Fedorak, 1994, Microbially mediated formation of benzonaphthothiophenes from benzo [b] thiophenes: Applied and environmental microbiology, v. 60, p. 3624-3631.

Kropp, K.G., Andersson, J.T. and Fedorak, P.M. (1997) Biotransformations of Three Dimethyldibenzothiophenes by Pure and Mixed Bacterial Cultures. Environmental Science & Technology 31, 1547-1554.

Kvenvolden, K., and C. Cooper, 2003, Natural seepage of crude oil into the marine environment: Geo-Marine Letters, v. 23, p. 140-146.

Le Borgne S. and Ayala M. (2010). Microorganisms Utilizing Sulfur-Containing Hydrocarbons. 10.1007/978-3-540-77587-4_154.

Leahy, J. G., and R. R. Colwell, 1990, Microbial degradation of hydrocarbons in the environment: Microbiological reviews, v. 54, p. 305-315.

Lemkau, K.L., McKenna, A.M., Podgorski, D.C., Rodgers, R.P. and Reddy, C.M. (2014) Molecular Evidence of Heavy-Oil Weathering Following the M/V Cosco Busan Spill: Insights from Fourier Transform Ion Cyclotron Resonance Mass Spectrometry. Environmental Science & Technology 48, 3760-3767.

Lu J., Nakajima-Kambe T., Shigeno T., Ohbo A., Nomura N. and Nakahara T. (1999). Biodegradation of dibenzothiophene and 4,6-dimethyldibenzothiophene by *Sphingomonas paucimobilis* strain TZS-7. Journal of Bioscience and Bioengineering. V. 88, Issue 3. Pages 293-299. ISSN 1389-1723. [https://doi.org/10.1016/S1389-1723\(00\)80012-2](https://doi.org/10.1016/S1389-1723(00)80012-2).

Luengo, J.M., García, J.L. and Olivera, E.R. (2001), The phenylacetyl-CoA catabolon: a complex catabolic unit with broad biotechnological applications. Molecular Microbiology, 39: 1434-1442. doi:10.1046/j.1365-2958.2001.02344.x

Ma, Ting. (2010). The Desulfurization Pathway in *Rhodococcus*. 10.1007/978-3-642-12937-7_8.

MacDonald, I., G. Bohrmann, E. Escobar, F. Abegg, P. Blanchon, V. Blinova, W. Brückmann, M. Drews, A. Eisenhauer, and X. Han, 2004, Asphalt volcanism and chemosynthetic life in the Campeche Knolls, Gulf of Mexico: Science, v. 304, p. 999-1002.

Macgregor D. S. (1993). Relationships between seepage, tectonics and subsurface petroleum reserves. Marine and Petroleum Geology. Volume 10, Issue 6. Pages 606-619. ISSN 0264-8172. [https://doi.org/10.1016/0264-8172\(93\)90063-X](https://doi.org/10.1016/0264-8172(93)90063-X).

Marcon Y, Sahling H, MacDonald IR, Wintersteller P, dos Santos Ferreira C, Bohrmann G (2018) Slow volcanoes: the intriguing similarities between marine asphalt and basalt lavas. Oceanography 31(2):194–205

McDonald, I. R., Miguez, C. B., Rogge, G., Bourque, D., Wendlandt, K. D., Groleau, D., et al. (2006). Diversity of soluble methane monooxygenase-containing methanotrophs isolated from polluted environments. FEMS Microbiol. Lett. 255, 225–232.

Meckenstock R. U., Safinowski M. and Griebler C. (2004). Anaerobic degradation of polycyclic aromatic hydrocarbons, FEMS Microbiology Ecology, Volume 49, Issue 1, Pages 27–36, <https://doi.org/10.1016/j.femsec.2004.02.019>

Medić A., Lješević M., Inui H., Beškoski V., Kojić I., Stojanović K. and Karadžić I. (2020). Efficient biodegradation of petroleum n -alkanes and polycyclic aromatic hydrocarbons by polyextremophilic *Pseudomonas aeruginosa* san ai with multidegradative capacity. RSC Advances. 10. 14060-14070. 10.1039/C9RA10371F.

Morgan P., and Watkinson R.J. Biodegradation of components of petroleum. In Biochemistry of Microbial Degradation (Ratledge C. ed.) Kluwer Academic Publishers, Dordrecht, Netherlands (1994) pp. 1-31.

Mountfort, D.O., White, D., & Asher, R.A. (1990). Oxidation of Lignin-Related Aromatic Alcohols by Cell Suspensions of *Methylosinus trichosporium*. Applied and environmental microbiology, 56 1, 245-9 .

Naehr, T. H., D. Birgel, G. Bohrmann, I. R. MacDonald, and S. Kasten, 2009, Biogeochemical controls on authigenic carbonate formation at the Chapopote “asphalt volcano”, Bay of Campeche: Chemical Geology, v. 266, p. 390-402.

Navarro Llorens J., Patrauchan M., Stewart G., Davies J., Eltis L. and Mohn W. (2005). Phenylacetate Catabolism in *Rhodococcus* sp. Strain RHA1: a Central Pathway for Degradation of Aromatic Compounds. Journal of bacteriology. 187. 4497-504. 10.1128/JB.187.13.4497-4504.2005.

Nekodzuka S., Nakajima-Kambe T., Nomura N., Lu J. and Nakahara T. (2009). Specific Desulfurization of Dibenzothiophene by *Mycobacterium* sp. Strain G3. Biocatalysis and Biotransformation. 15. 17-27. 10.3109/10242429709003607.

Okoh A.I., Biodegradation alternative in the cleanup of petroleum hydrocarbon pollutants. Biotechnology and Molecular Biology Review (2006) 1: 38-50.

Olajire A, Essien J (2014) Aerobic degradation of petroleum components by microbial consortia. J Petrol Environ Biotechnol 5:195

Oldfield C, Pogrebinsky O, Simmonds J, Olson ES, Kulpa CF (1997) Elucidation of the metabolic pathway for dibenzothiophene desulfurization by *Rhodococcus* sp. IGTS8 (ATCC 53968). Microbiology 143:2961–2973

Olivera, E. R., Minambres, B., Garcia, B., Muniz, C., Moreno, M. A., Ferrandez, A., Diaz, E., Garcia, J. L., and Luengo, J. M., Molecular characterization of the phenylacetic acid

catabolic pathway in *Pseudomonas putida* U: the phenylacetyl-CoA catabolon. Proc. Natl. Acad. Sci. U. S. A., 95, 6419–6424 (1998).

Palmer S. E. (1984) Effect of Water Washing on C15+ Hydrocarbon Fraction of Crude Oils from Northwest Palawan, Philippines. American Association of Petroleum Geologists Bulletin V. 68, No. 2, P. 137-149.

Pape, T., Bahr, A., Rethemeyer, J., Kessler, J. D., Sahling, H., Hinrichs, K.-U., et al. (2010). Molecular and isotopic partitioning of low-molecular-weight hydrocarbons during migration and gas hydrate precipitation in deposits of a high-flux seepage site. Chem. Geol. 269, 350–363. doi: 10.1016/j.chemgeo.2009.10.009

Peters K., Walters C. and Moldowan J. (2004). Biodegradation parameters. In The Biomarker Guide (pp. 645-708). Cambridge: Cambridge University Press. doi:10.1017/CBO9781107326040.007

Peters, K., C. Walters, and J. Moldowan, 2005, The Biomarker guide, biomarkers and isotopes in petroleum exploration and earth history, vol 1–2, Cambridge University Press, New York.

Philip, J. C., Bamforth, S. M., Singleton, I., and Atlas, R. M. (2005). “Environmental pollution and restoration: a role for bioremediation,” in Bioremediation: Applied Microbial Solutions for Real-World Environmental Cleanup eds R. M. Atlas and J. Philip (Washington, DC: ASM Press), 1–48.

Plyasunov A.V., Shock E.L. (2000). Thermodynamic functions of hydration of hydrocarbons at 298.15 K and 0.1 MPa. Geochim. Cosmochim. Acta 64, 439–468

Price, L. C, 1976, Aqueous solubility of petroleum as applied lo its origin and primary migration: AAPG Bulletin, v. 60, p. 213-244.

Prince, R. C.; Walters, C. C.; Wang, Z.; Stout, S. (2007). Biodegradation of Oil Hydrocarbons and Its Implications for Source Identification; Elsevier Academic Press Inc: San Diego, p 349–379.

Resnick, S.M. and Gibson, D.T. (1996) Regio- and stereospecific oxidation of fluorene, dibenzofuran, and dibenzothiophene by naphthalene dioxygenase from *Pseudomonas* sp. strain NCIB 9816-4. Appl. Environ. Microbiol. 62, 4073-4080.

Rhee S.K., J.H. Chang, Y.K. Chang and H.N. Chang. 1998. Desulfurization of dibenzothiophene and diesel oils by a newly isolated Gordona strain, CYKS1. Appl. Environ. Microbiol. 64:2327-2331.

Rojo F. (2010) Enzymes for Aerobic Degradation of Alkanes Handbook of Hydrocarbon and Lipid Microbiology, ISBN : 978-3-540-77584-3

Rojo, F. (2009), Degradation of alkanes by bacteria. *Environmental Microbiology*, 11: 2477-2490. doi:10.1111/j.1462-2920.2009.01948.x

Römer M., Hsu C., Loher M., MacDonald I., Ferreira C., Pape T., Mau S., Bohrmann G. and Sahling H. (2019). Amount and Fate of Gas and Oil Discharged at 3400 m Water Depth From a Natural Seep Site in the Southern Gulf of Mexico. *Frontiers in Marine Science*. 6. 10.3389/fmars.2019.00700.

Römer M., Weinrebe R. W., Wintersteller P. and Bohrmann G. (2020): Sediment echosounder raw data (Atlas Parasound P70 echosounder) of RV METEOR during cruise M134/1. PANGAEA, <https://doi.pangaea.de/10.1594/PANGAEA.921193>

Rubin-Blum M., Antony C.P., Borowski C., Sayavedra L., Pape T., Sahling H., Bohrmann G., Kleiner M., Redmond M. C., Valentine D. L. and Dubilier N. (2017). Short-chain alkanes fuel mussel and sponge Cycloclasticus symbionts from deep-sea gas and oil seeps. *Nat Microbiol*. 2:17093. Published 2017 Jun 19. doi:10.1038/nmicrobiol.2017.93

Ruddy, B.M., Huettel, M., Kostka, J.E., Lobodin, V.V., Bythell, B.J., McKenna, A.M., Aeppli, C., Reddy, C.M., Nelson, R.K., Marshall, A.G. and Rodgers, R.P. (2014) Targeted Petroleomics: Analytical Investigation of Macondo Well Oil Oxidation Products from Pensacola Beach. *Energy & Fuels* 28, 4043-4050.

Sadek M. E., Seheimy A. E., El-Tokhy T. T. and Allah M. A. (2017) Management Process of Oil Spill in Water Plants. *J Pollut Eff Cont* 5: 205. doi: 10.4176/2375- 4397.1000205

Sahling H., Rickert D., Lee R. W., Linke P. and Suess E. (2002). Macrofaunal community structure and sulfide flux at gas hydrate deposits from the Cascadia convergent margin, NE Pacific. *Mar Ecol Prog Ser* 231: 121-138

Sahling, H., Ahrlich, F., Bohrmann, G., Borowski, C. and Breitzke, M., Buchheister, S., Büttner, H., Ferreira, C., Gaytán-Caballero, A., Geprägs, P., Groeneveld, J.-D., Hsu, C.-W., Jiménez-Guadarrama, E., Klar, S., Klaucke, I., Klüber, S., Leymann, T., Loher, M., Mai, H.-A., Mau, S., MacDonald, I., Marcon, Y., Meinecke, G., Melcher, A.-C., Morales-Dominguez, E., Raeke, A., Rehage, R., Renken, J., Reuter, M., Rohleder, C., Römer, M., Rubin-Blum, M., Schade, T., Schubotz, F., Seiter, C., Smrzka, D., Spiesecke, U., Torres, M., Vittori, V., Von Neuhoff, S., von Wahl, T., Wegener, G., Wiebe, M., Wintersteller, P., Zarrouk, M., Zwicker, J. (2017) R/V METEOR Cruise Report M114, Natural hydrocarbon seepage in the southern Gulf of Mexico, Kingston – Kingston, 12 February – 28 March 2015. University of Bremen, Bremen.

Sahling, H., M. Rubin Blum, C. Borowksi, E. Escobar-Briones, A. Gaytan-Caballero, C. W. Hsu, I. MacDonald, Y. Marcon, T. Pape, M. Römer, F. Schubotz, D. Smrzka, G. Wegener, and G. Bohrman, 2016, Seafloor observations at Campeche Knolls, southern Gulf of Mexico: coexistence of asphalt deposits, oil seepage, and gas venting: *Biogeosciences Discuss*. Doi: 10.5194/bg-2016-101.

Salvador, A., 1991 b, Triassic-Jurassic: The Gulf of Mexico Basin: Boulder, Colorado, Geological Society of America, Geology of North America, v. J, p. 131-180.

Schubotz, F., 2009, Microbial community characterization and carbon turnover in methane-rich marine environments - case studies in the Gulf of Mexico and the Black Sea: PhD thesis, University of Bremen, Bremen, Germany, 222 p.

Schubotz, F., J. S. Lipp, M. Elvert, and K.-U. Hinrichs, 2011,a, Stable carbon isotopic compositions of intact polar lipids reveal complex carbon flow patterns among hydrocarbon degrading microbial communities at the Chapopote asphalt volcano: *Geochimica et Cosmochimica Acta*, v. 75, p. 4399-4415.

Schubotz, F., J. S. Lipp, M. Elvert, S. Kasten, X. P. Mollar, M. Zabel, G. Bohrmann, and K.-U. Hinrichs, 2011,b, Petroleum degradation and associated microbial signatures at the Chapopote asphalt volcano, Southern Gulf of Mexico: *Geochimica et Cosmochimica Acta*, v. 75, p. 4377-4398.

Seo, J.-S., Keum, Y.-S. and Li, Q. X. Bacterial degradation of aromatic compounds. *Int. J. Environ. Res. Public Health* 6, 278–309 (2009).

Seo, J.S.; Keum, Y.S.; Cho, I.K.; Li, Q.X. (2006). Degradation of dibenzothiophene and carbazole by Arthrobacter sp. P1-1. *Int. Biodeter. Biodeg.* 58, 36-43.

Simon, M.J. Osslund, T.D. (1993). Saunders, R.; Ensley, B.D.; Suggs, S.; Harcourt, A.; Suen, W.C.; Cruder, D.L.; Gibson, D.T.; Zylstra, G.J. Sequences of genes encoding naphthalene dioxygenase in *Pseudomonas putida* strains G7 and NCIB 9816-4. *Gene* 127, 31-37.

Smit N. (2016) Geochemical characterization of asphalt deposits in the Campeche Bay (southern Gulf of Mexico), Master Thesis, Department of Geoscience. University of Bremen, Bremen.

Smith P.W.G. and TATCHELL A.R. (1969). Aromatic Alcohols and Carbonyl Compounds. Aromatic Chemistry, Pergamon, Pages 144-175, ISBN 9780080129488, <https://doi.org/10.1016/B978-0-08-012948-8.50010-3>.

Tissot B. P. and Welte D. H. 1984, Petroleum formation and occurrence.

Tolls, J.; van Dijk, J.; Verbruggen, E. J. M.; Hermens, J. L. M.; Loeprecht, B.; Schuurmann, G. (2002). Aqueous solubility-molecular size relationships. A mechanistic case study using C10-to C19-alkanes. *J. Phys. Chem. A*, 106 (11): 2760–2765.

Tsai J.-C., Kumar M., and Lin J.-G. 2009, Anaerobic biotransformation of fluorene and phenanthrene by sulfate reducing bacteria and identification of biotransformation pathway: *Journal of hazardous materials*, v. 164, p. 847 855.

U.S. Energy Information Administration (EIA). eia.gov

Vairavamurthy, A., B. Manowitz, W. Zhou, and Y. Jeon, 1992, Environmental Geochemistry of Sulfide Oxidation: ACS Symposium Series, p. 413.

van Afforded M, Schacht S, Klein J, Truer HG (1990) " Degradation of dibenzothiophene by Brevibacterium sp. DO. Arch Microbiol 153, 324–8.

van Beilen J.B. and Funhoff E.G. Alkane hydroxylases involved in microbial alkane degradation. Appl Microbiol Biotechnol. 2007;74(1):13-21. doi:10.1007/s00253-006-0748-0

van Beilen J.B., Li Z., Duetz W., Smits THM. and Witholt B. (2003). Diversity of Alkane Hydroxylase Systems in the Environment. Oil & Gas Science and Technology – Rev. IFP Éditions Technip Oil & Gas Science and Technology – Rev. IFP. 58. 427-440. 10.2516/ogst:2003026.

Vernon J. W. and Slater R. A. (1963). "Submarine Tar Mounts, Santa Barbara County, California" AAPG Bulletin 47(8):1624–1627, <https://doi.org/10.1306/bc743aff-16be-11d7-8645000102c1865d>.

Volkman, J. K., R. Alexander, R. I. Kagi, S. J. Rowland, and P. N. Sheppard, 1984, Biodegradation of aromatic hydrocarbons in crude oils from the Barrow Sub-basin of Western Australia: Organic Geochemistry, v. 6, p. 619-632.

Wang, Z., M. Fingas, and K. Li, 1994, Fractionation of a light crude oil and identification and quantitation of aliphatic, aromatic, and biomarker compounds by GC-FID and GC-MS, part II: Journal of chromatographic science, v. 32, p. 367-382.

Wang, Z., M. Fingas, S. Blenkinsopp, G. Sergy, M. Landriault, L. Sigouin, J. Foght, K. Semple, and D. Westlake, 1998, Comparison of oil composition changes due to biodegradation and physical weathering in different oils: Journal of Chromatography A, v. 809, p. 89-107.

Wardlaw, G. D., J. S. Arey, C. M. Reddy, R. K. Nelson, G. T. Ventura, and D. L. Valentine, 2008, Disentangling oil weathering at a marine seep using GC \times GC: Broad metabolic specificity accompanies subsurface petroleum biodegradation: Environmental science & technology, v. 42, p. 7166-7173.

Wardlaw, G. D., R. K. Nelson, C. M. Reddy, and D. L. Valentine, 2011, Biodegradation preference for isomers of alkylated naphthalenes and benzothiophenes in marine sediment contaminated with crude oil: Organic Geochemistry, v. 42, p. 630-639.

Wegener G., Knittel K., Bohrmann G., Schubotz F. (2020) Benthic Deep-Sea Life Associated with Asphaltic Hydrocarbon Emissions in the Southern Gulf of Mexico. In: Teske A., Carvalho V. (eds) Marine Hydrocarbon Seeps. Springer Oceanography. Springer, Cham. https://doi.org/10.1007/978-3-030-34827-4_5

Wegener G., Shovitri M., Knittel K., Niemann H., Martin H. and Boetius A. (2016): Microbial community, biomarker concentrations and their isotopic signature in sediment of Gullfaks

and Tommeliten methane seeps in the Northern North Sea. PANGAEA, <https://doi.org/10.1594/PANGAEA.860780>

Weiland, R.J., Adams, G.P., McDonald, R.D., Rooney, T.C., Wills, L.M., 2008. Geological and Biological Relationships in the Puma Appraisal Area: from Salt Diapirism to Chemosynthetic Communities. Offshore Technology Conference, 5–8 May 2008, Houston, Texas, USA.

Wenger, L. M., and G. H. Isaksen, 2002, Control of hydrocarbon seepage intensity on level of biodegradation in sea bottom sediments: Organic Geochemistry, v. 33, p. 1277-1292.

Wentzel A., Ellingsen T.E., Kotlar H-K., Zotchev S.B. and Throne-Holst M. Bacterial metabolism of long-chain n-alkanes. *Appl Microbiol Biotechnol* 76, 1209–1221 (2007). <https://doi.org/10.1007/s00253-007-1119-1>

Whyte L. G., Hawari J., Zhou E., Bourbonnière L., Inniss W. E. and Greer C. W. Biodegradation of variable-chain length alkanes at low temperatures by a psychrotrophic *Rhodococcus* sp. *Appl Environ Microbiol.* 1998;64(7):2578 2584. doi:10.1128/AEM.64.7.2578-2584.1998

Widdel F. and Musat F. (2010). Diversity and Common Principles in Enzymatic Activation of Hydrocarbons. [10.1007/978-3-540-77587-4_70](https://doi.org/10.1007/978-3-540-77587-4_70).

Widdel, F. and Bak, F. (1992) Gram-Negative Mesophilic Sulfate-Reducing Bacteria, in: A., B., H.G., T., M., D., W., H., KH, S. (Eds.), *The Prokaryotes*. Springer, New York.

Williamson, S.C., Zois, N., Hewitt, A.T., 2008. Integrated site investigation of seafloor features and associated fauna, Shenzi Field, Deepwater Gulf of Mexico. 2008 Offshore Technology Conference, 5–8 May 2008, Houston, Texas.

Yemashova N., Murygina V., Zhukov D., Zakharyantz A., Gladchenko M., Appanna V. and Kalyuzhnyi S. (2007). Biodeterioration of Crude Oil and Oil Derived Products: A Review. *Reviews in Environmental Science and Biotechnology.* 6. 315-337. [10.1007/s11157-006-9118-8](https://doi.org/10.1007/s11157-006-9118-8).

Appendix

Supplementary Figures

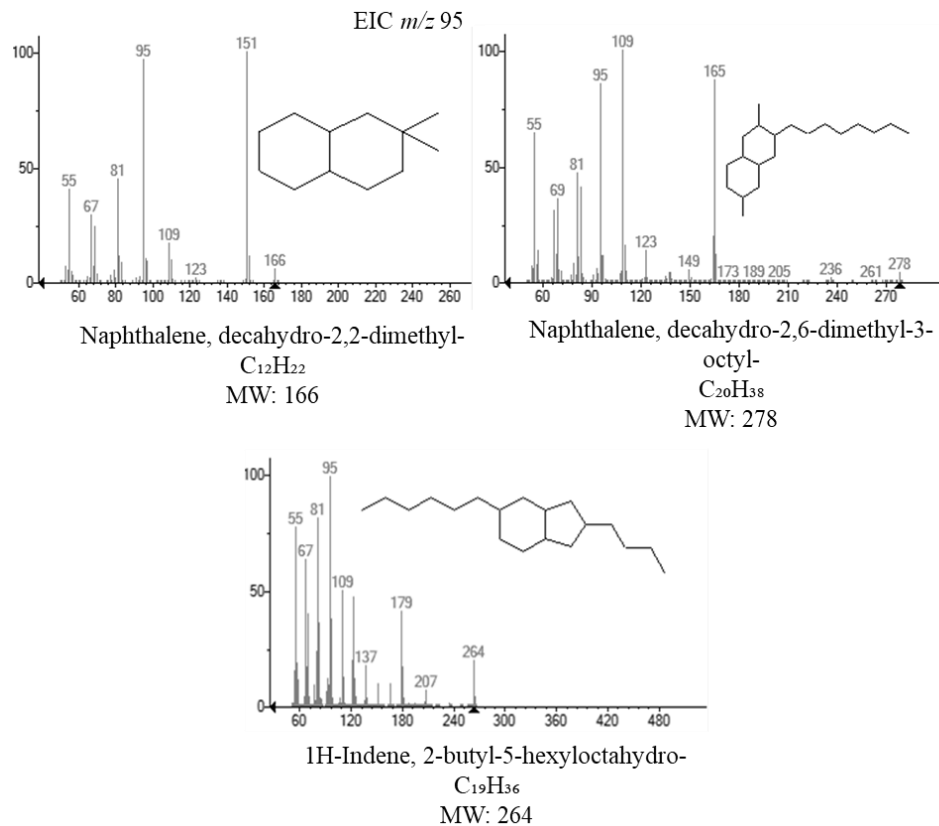


Figure 31. Tentative Structures and mass spectral data of cycloalkanes detected in the asphalt incubation experiments

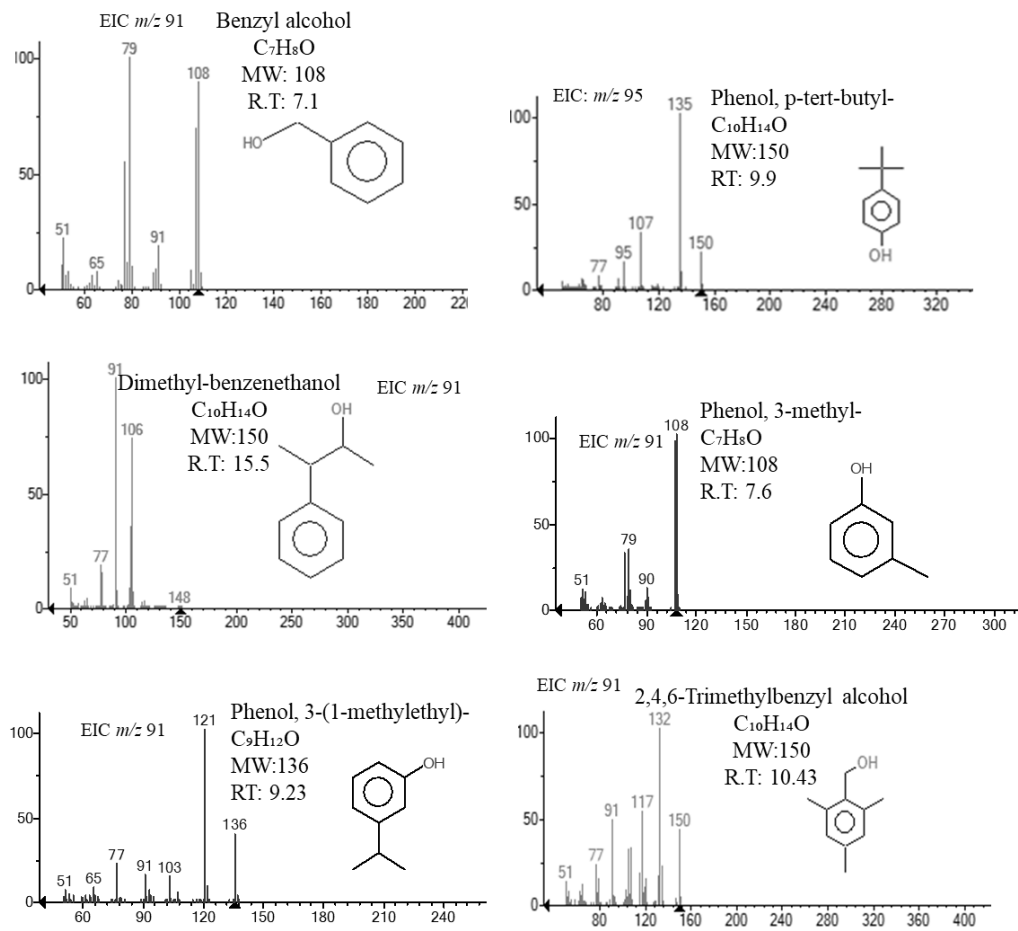


Figure 32. Mass spectral data with tentative structures and sum formulae for the detected aromatic alcohols in the asphalt incubation experiments. MW: Molecular weight, R.T: Retention time (in minutes)

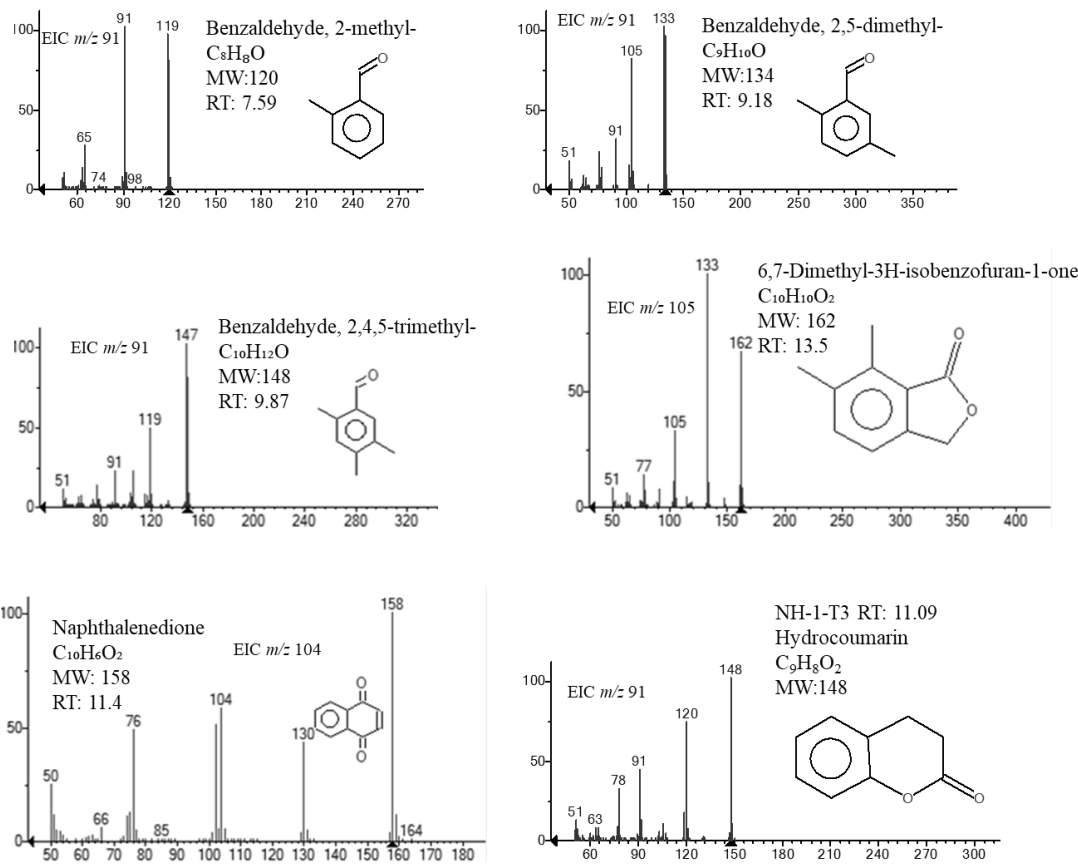


Figure 33. Mass spectral data with tentative structures and sum formulae for the detected aromatic ketones in the asphalt incubation experiments. MW: Molecular weight, R.T: Retention time (in minutes)

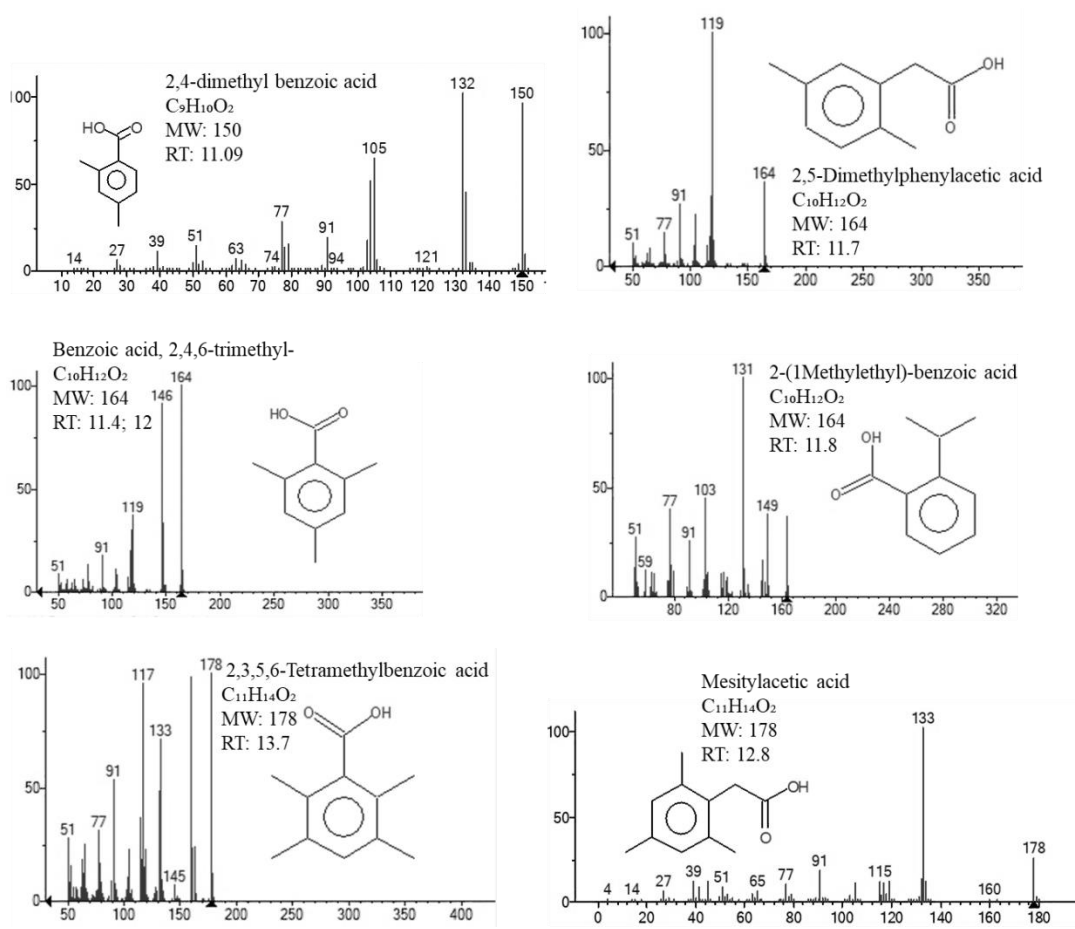


Figure 34. Mass spectral data with tentative structures and sum formulae for the detected aromatic acids in the asphalt incubation experiments. MW: Molecular weight, R.T: Retention time (in minutes)

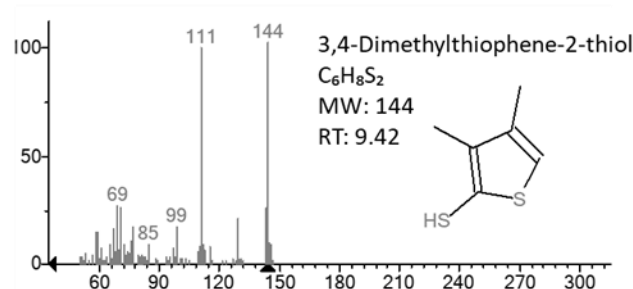
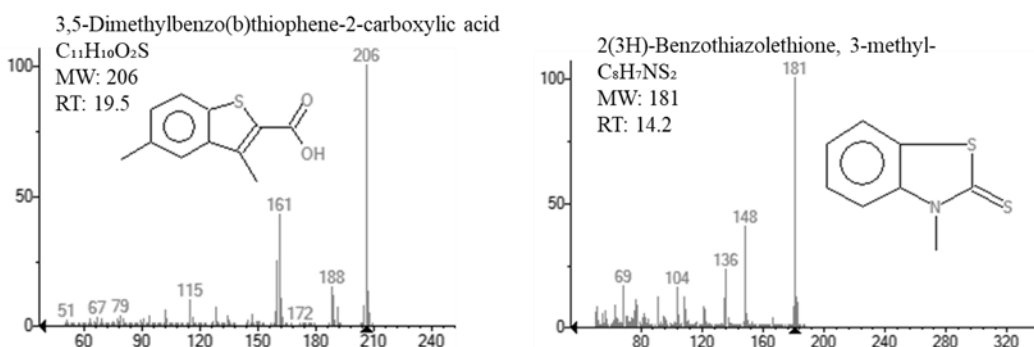


Figure 35. Mass spectral data with tentative structures and sum formulae for the detected thiol and thiophenic acid in the asphalt incubation experiments. MW: Molecular weight, R.T: Retention time (in minutes)

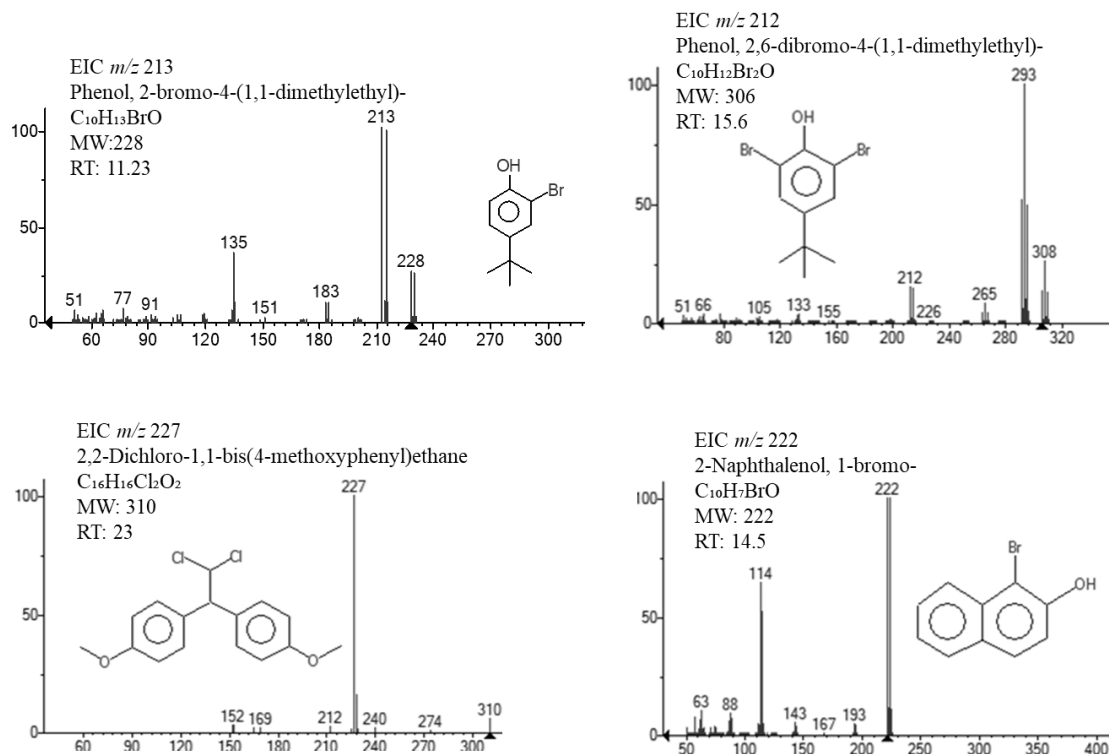


Figure 36. Mass spectral data with tentative structures and sum formulae for the 4 detected halogenated compounds in the asphalt incubation experiments. MW: Molecular weight, R.T: Retention time (in minutes)

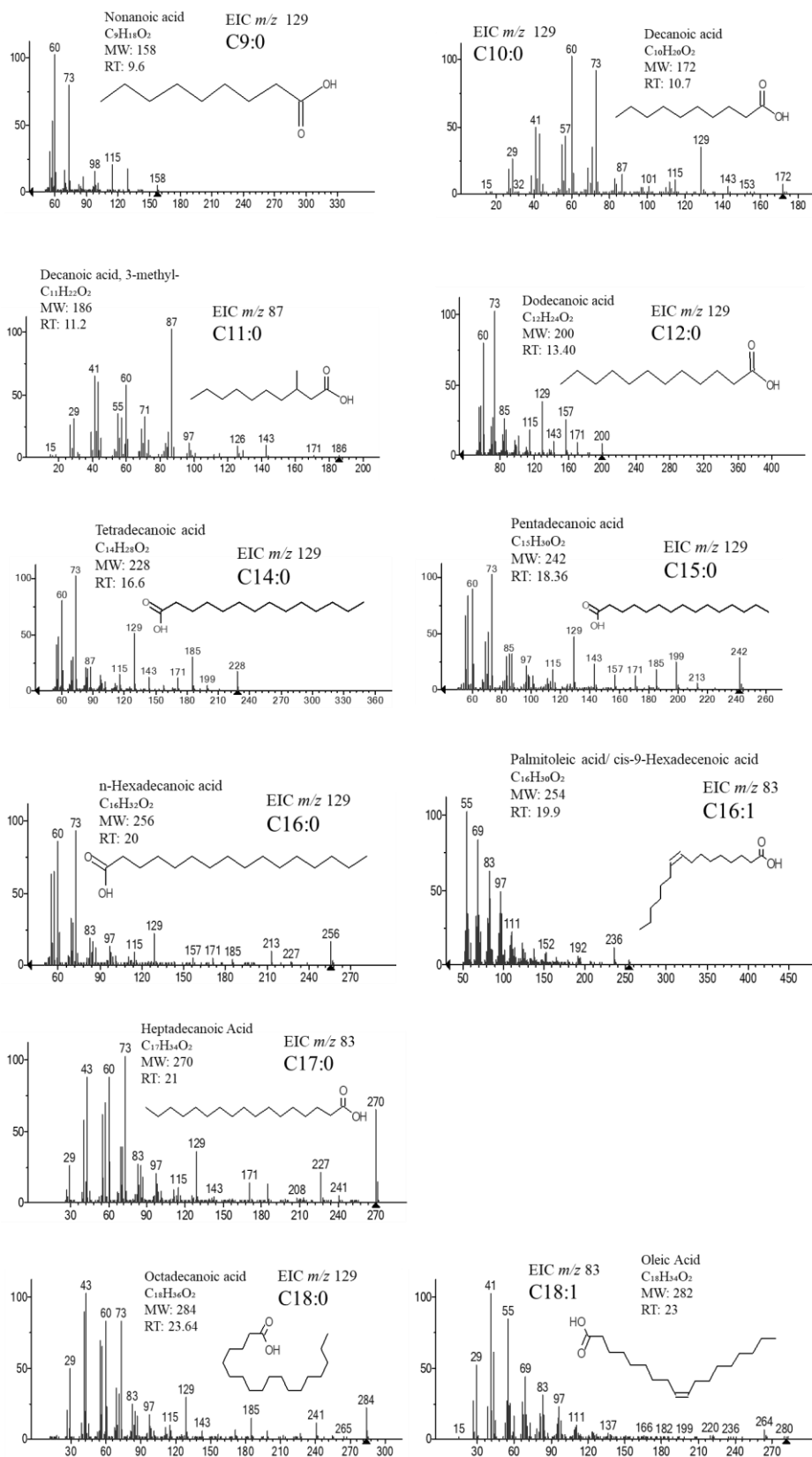


Figure 37. Mass spectral data with tentative structures and sum formulae for the fatty acid compounds in the asphalt incubation experiments. MW: Molecular weight, R.T: Retention time (in minutes)

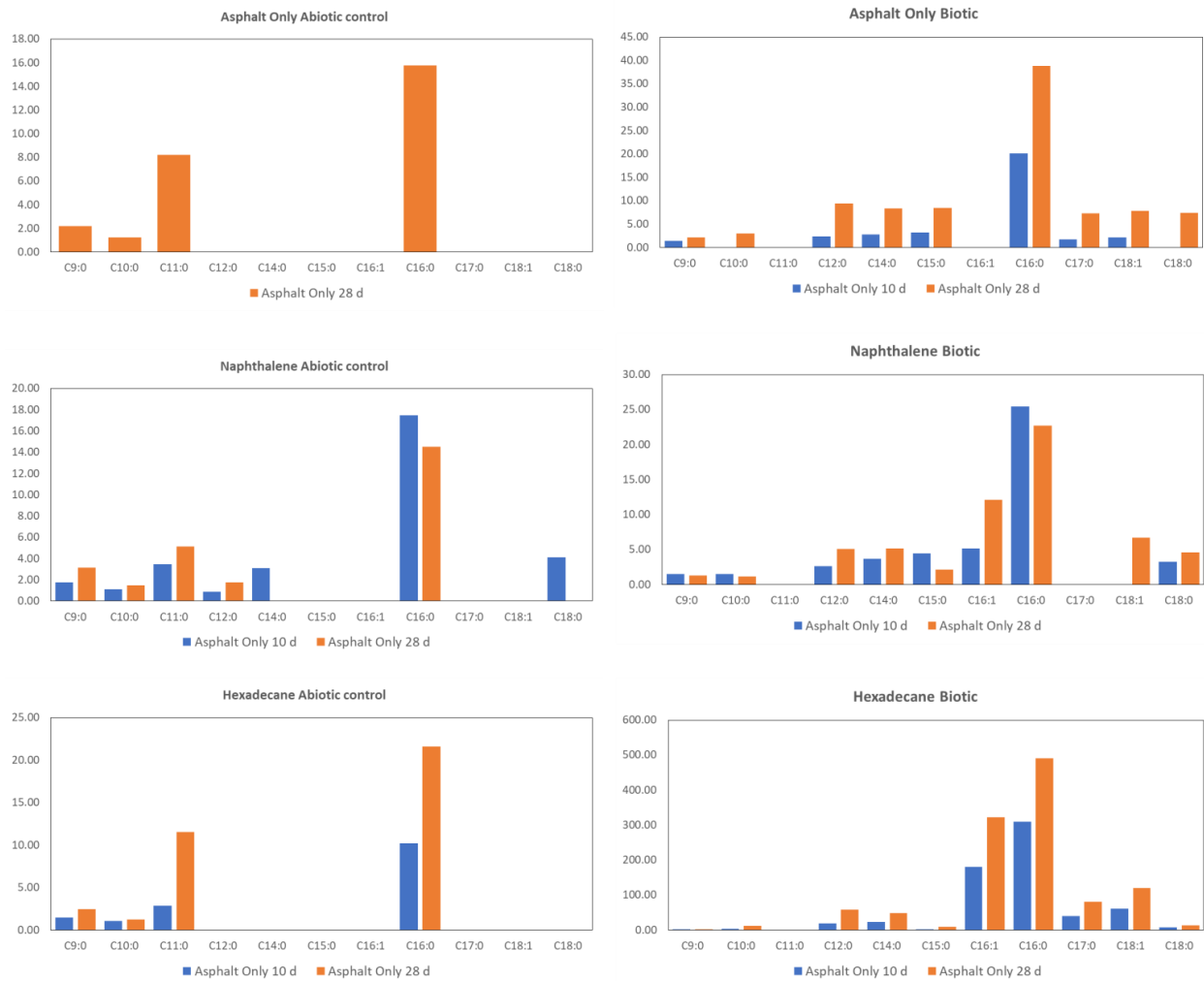


Figure 38. Plots showing the distribution of the concentration of fatty acids detected in the ‘Asphalt Only’, ‘Naphthalene’ and ‘Hexadecane’ incubation experiment

Supplementary Tables

Table 6. Compounds identified in the asphalt incubation experiment and their respective concentration values. Also, the calculated standard deviation for the triplicate is shown.

Compound class	Incubation	Abiotic 10d	Abiotic 28d	Biotic 10d	Biotic 28d	Biotic 10d	Biotic 28d
				MEAN	MEAN	STDEV	STDEV
Hexadecane	Asphalt Only	0.00	0.00	4.96	0.00	4.72	0.00
	Naphthalene	2.89	117.12	0.00	0.00	0.00	0.00
	Hexadecane	0.00	3366.12	30.69	537.95	27.67	414.41
<i>n</i> -Alkanes	Asphalt Only	0.00	0.00	5.34	0.00	1.23	0.00
	Naphthalene	6.63	7.33	1.06	0.00	0.75	0.00
	Hexadecane	1.79	17.50	7.75	3.79	1.11	1.81
Cycloalkanes	Asphalt Only	0.00	200.31	75.28	16.82	4.34	2.09
	Naphthalene	82.00	205.26	47.03	30.41	2.74	5.72
	Hexadecane	74.93	157.66	24.73	24.76	29.22	19.96
Aromatic alcohols	Asphalt Only	0.00	58.19	37.02	107.50	7.54	13.01
	Naphthalene	31.91	59.53	27.80	83.38	1.81	2.77
	Hexadecane	27.77	33.32	25.56	62.99	5.63	44.06
Aromatic ketones	Asphalt Only	0.00	0.00	1.99	26.43	2.11	19.18
	Naphthalene	0.00	9.87	119.20	214.27	56.34	35.00
	Hexadecane	0.00	0.00	5.17	46.09	4.75	34.44
Coumarin	Asphalt Only	0.00	0.00	2.96	0.00	2.59	0.00
	Naphthalene	1.42	8.42	832.10	79.75	348.81	100.01
	Hexadecane	1.72	1.12	1.67	0.00	0.23	0.00
Aromatic acids	Asphalt Only	0.00	0.00	19.93	211.68	24.17	68.98
	Naphthalene	40.73	30.37	2.35	73.18	2.17	52.35
	Hexadecane	21.70	21.84	7.92	118.49	11.83	54.91
Thiols/thiophenic acids	Asphalt Only	0.00	0.00	0.65	52.06	1.13	24.90
	Naphthalene	0.00	0.00	0.63	23.88	0.55	12.16
	Hexadecane	0.00	0.00	0.00	5.13	0.00	2.52
Halogenated compounds	Asphalt Only	0.00	90.72	28.07	13.90	30.53	10.85
	Naphthalene	120.01	92.00	52.75	10.03	25.13	3.84
	Hexadecane	117.45	113.58	16.73	0.00	59.12	0.00
Fatty acids	Asphalt Only	0.00	27.39	33.82	92.92	35.55	27.64
	Naphthalene	31.77	25.89	47.78	61.02	11.23	22.92
	Hexadecane	15.61	36.85	648.78	1157.36	376.92	636.66

Table 7. List of some suspected contaminants encountered in the asphalt incubation samples.

Incubation samples	
Name	Sum Formula
Heptyl-benzene	C13H20
Isopropyl palmitate	C ₁₉ H ₃₈ O ₂
Benzyl 2-chloroethyl sulfone	C ₉ H ₁₁ ClO ₂ S
Ethanol, 2-(2-butoxyethoxy)-, acetate	C ₁₀ H ₂₀ O ₄
Bibenzyl	C ₁₄ H ₁₄
Cyclodecane	C ₁₀ H ₂₀
Ethanol, 2-(2-butoxyethoxy)-	C ₈ H ₁₈ O ₃
1,2-Benzenedicarboxylic acid, bis(2-methylpropyl) ester	C ₁₆ H ₂₂ O ₄
2-Butoxyethyl oleate	C ₂₄ H ₄₆ O ₃
Octadecanoic acid, 1,2-ethanediyl ester	C ₃₈ H ₇₄ O ₄
Nonanal	C ₉ H ₁₈ O
Dodecanal	C ₁₂ H ₂₄ O
Hexadecanoic acid, methyl ester	C ₁₇ H ₃₄ O ₂
Heptadecane	C ₁₇ H ₃₆
Octadecane	C ₁₈ H ₃₈
2,4-Di-tert-butylphenol	C ₁₄ H ₂₂ O

Table 8. The table shows the solubility of representative *n*-alkanes in an aqueous medium at 25°C. The table is gotten from F. Rojo 2010. Original data obtained from Eastcott et al., 1988.

<i>n</i>-Alkanes	Carbon atoms	Molecular weight	Solubility (mol L⁻¹)
Propane	3	44.1	5x10 ⁻³
Hexane	6	86.2	1.4x10 ⁻⁴
Nonane	9	128.3	10 ⁻⁶
Dodecane	12	170.3	2x10 ⁻⁸
Hexadecane	16	226.4	2x10 ⁻¹⁰
Eicosane	20	282.6	10 ⁻¹²
Hexacosane	26	366.7	4x10 ⁻¹⁶

Table 9. Absolute abundance [ng/ml] of compounds (GC-MS) in type 1 ‘fresh’ samples; the emboldened figures represent the sum total of all the compounds in each compound class.

Name	Short ID	sum formula	Mictlan			Tsanyao Yang
			GeoB193 36-6 oily	GeoB1933 6-5 F1+F2	GeoB19 346-15	GeoB1933 7-2 F1+F2
			ng/ml	ng/ml	ng/ml	ng/ml
n-alkanes			2221.58	7787.88	787.90	4869.71
Tetradecane	C14	C ₁₄ H ₃₀	26.34	19.70	19.88	316.74
Pentadecane	C15	C ₁₅ H ₃₂	66.07	121.13	36.04	516.18
Hexadecane	C16	C ₁₆ H ₃₄	116.63	272.56	47.93	543.19
Heptadecane	C17	C ₁₇ H ₃₆	176.69	472.92	74.19	529.68
Octadecane	C18	C ₁₈ H ₃₈	164.28	645.32	53.99	410.11
Nonadecane	C19	C ₁₉ H ₄₀	152.54	560.46	56.36	338.55
Eicosane	C20	C ₂₀ H ₄₂	157.42	606.24	54.45	368.79
Heneicosane	C21	C ₂₁ H ₄₄	148.94	529.79	59.09	322.88
Docosane	C22	C ₂₂ H ₄₆	148.93	555.59	55.58	303.59
Tricosane	C23	C ₂₃ H ₄₈	150.29	574.52	51.90	243.68
Tetracosane	C24	C ₂₄ H ₅₀	201.64	753.89	59.93	244.68
Pentacosane	C25	C ₂₅ H ₅₂	222.74	874.50	65.55	234.64
Hexacosane	C26	C ₂₆ H ₅₄	237.48	890.79	57.89	198.84
Heptacosane	C27	C ₂₇ H ₅₆	166.87	603.78	50.72	164.76
Octacosane	C28	C ₂₈ H ₅₈	84.71	306.70	44.42	133.42
Isoprenoids			87.97	311.44	76.16	662.53
Pristane	Pr	C ₁₇	26.63	75.52	24.60	295.64
Phytane	Ph	C ₁₈	61.34	235.92	51.56	366.89
Naphthalenes			86.83	172.49	191.28	2540.19
Monomethylnaphthalene	C1-Naph	C ₁₁ H ₁₀	0.58	29.15	7.65	49.98
Dimethylnaphthalene	C2-Naph	C ₁₂ H ₁₂	12.54	9.19	29.43	509.75
Trimethylnaphthalene	C3-Naph	C ₁₃ H ₁₄	47.70	68.82	79.08	1301.01
Tetramethylnaphthalene	C4-Naph	C ₁₄ H ₁₆	26.01	65.33	75.12	679.44
Phenantrenes			65.30	208.83	397.92	1910.79
Phenanthrene	Phen	C ₁₄ H ₁₀	8.10	19.97	30.00	146.72
Monomethylphenanthrene	C1-Phen	C ₁₅ H ₁₂	24.13	74.87	118.87	722.71

Dimethylphenanthrene	C2- Phen	C ₁₆ H ₁₄	33.08	114.00	249.05	1041.36
Fluorenes			3.40	9.30	21.11	473.84
Methyl Fluorene	C1- Fluor	C ₁₄ H ₁₂	3.40	3.63	9.07	137.39
Dimethyl Fluorene	C2- Fluor	C ₁₅ H ₁₄	0.00	5.67	12.03	336.45
Dibenzothiopnenes			297.78	925.72	605.09	3358.97
Dibenzothiopnene	DBT	C ₁₂ H ₈ S	16.06	38.36	23.18	212.27
Monomethyldibenzothiophene	C1- DBT	C ₁₃ H ₁₀ S	85.73	254.77	137.48	992.28
Dimethyldibenzothiophene	C2- DBT	C ₁₄ H ₁₂ S	195.99	632.59	444.42	2154.41
S-containing monoaromatics			18.73	67.84	10.01	47.99
Bzenemethanethiol	BMT	C ₇ H ₈ S	18.73	46.12	10.01	41.71
Benzyl methyl disulfide	BMDS	C ₈ H ₁₀ S ₂	0.00	21.72	0.00	6.28
other aromatics			41.97	107.82	120.15	449.51
Naphtho[2,3-b]thiophene, 4,9-dimethyl-	DMNT	C ₁₄ H ₁₂ S	39.14	100.95	76.33	386.69
Phenanthrone, 9,10-dihydro-1-methyl-	C1-2H- Phen	C ₁₅ H ₁₄	2.83	6.86	43.82	62.83
Aromatic alcohols			0.63	38.72	8.40	34.44
Benzyl alcohol		C ₇ H ₈ O	0.63	38.72	8.40	34.44

Table 10. Absolute abundance [ng/ml] of compounds (GC-MS) in type 2 ‘biodegraded’ samples; the emboldened figures represent the sum total of all the compounds in each compound class.

Name	Short ID	Sum formul ar	Mictla n GeoB1 9346-4	Chapopote			Tsanyao Yang GeoB193 37-9 F1+F2
				GeoB19 351-14 F1+F2	GeoB19 340-4	GeoB19 340-2	
		ng/ml	ng/ml	ng/ml	ng/ml	ng/ml	ng/ml
n-alkanes			1.9900 039	8.13598 1	0	0	25.10892
Tetradecane	C14	C ₁₄ H ₃₀	0.00	0.35	0.00	0.00	25.11
Pentadecane	C15	C ₁₅ H ₃₂	0.00	0.86	0.00	0.00	0.00
Hexadecane	C16	C ₁₆ H ₃₄	0.00	0.95	0.00	0.00	0.00
Heptadecane	C17	C ₁₇ H ₃₆	0.25	1.73	0.00	0.00	0.00
Octadecane	C18	C ₁₈ H ₃₈	0.61	2.40	0.00	0.00	0.00
Nonadecane	C19	C ₁₉ H ₄₀	0.59	1.85	0.00	0.00	0.00
Eicosane	C20	C ₂₀ H ₄₂	0.53	0.00	0.00	0.00	0.00
Heneicosane	C21	C ₂₁ H ₄₄	0.00	0.00	0.00	0.00	0.00
Isoprenoids			0.83	3.19	0.00	0.00	0.00
Pristane	Pr	C17	0.21	1.23	0.00	0.00	0.00
Phytane	Ph	C18	0.62	1.96	0.00	0.00	0.00
Benzenes			0.00	0.34	0.00	0.00	0.00
Benzene, (1-methyldodecyl)-		C ₁₉ H ₃₂	0.00	0.34	0.00	0.00	0.00
Phenantrenes			3.23	7.81	5.50	3.77	5044.38
Phenantrene	Phen	C ₁₄ H ₁₀	0.00	4.57	0.00	0.03	0.00
Monomethylphenantrene	C1- Phen	C ₁₅ H ₁₂	0.00	1.55	0.00	0.00	20.69
Dimethylphenantrene	C2- Phen	C ₁₆ H ₁₄	3.23	1.68	5.50	3.74	5023.69
Dibenzothiophenes			0.00	3.95	0.00	0.00	1711.20
Dibenzothiophene	DBT	C ₁₂ H ₈ S	0.00	0.00	0.00	0.00	0.00
Monomethyldibenzothiophene	C1- DBT	C ₁₃ H ₁₀ S	0.00	1.19	0.00	0.00	103.88
Dimethyldibenzothiophene	C2- DBT	C ₁₄ H ₁₂ S	0.00	2.76	0.00	0.00	1607.31
S-containing monoaromatics			0.69	9.85	0.06	0.00	44.62
Benzenemethanethiol	BMT	C ₇ H ₈ S	0.69	9.51	0.06	0.00	44.62
other aromatics			0.00	0.00	0.00	0.00	213.19
Naphtho[2,3-	DMN	C ₁₄ H ₁₂ S	0.00	0.00	0.00	0.00	213.19

b]thiophene, 4,9-dimethyl-	T						
Aromatic alcohols			1.85	7.34	0.37	1.28	131.59
Benzyl alcohol		C ₇ H ₈ O	1.85	7.34	0.37	1.28	131.59
Fatty acids			0.03	0.00	0.04	0.07	0.00
Nonanoic acid		C ₉ H ₁₈ O ₂	0.03	0.00	0.00	0.07	0.00
n-Hexadecanoic acid		C ₁₆ H ₃₂ O ₂	0.00	0.00	0.04	0.00	0.00

Table 11. Absolute abundance [ng/ml] of compounds (GC-MS) in type 3 weathered samples; the emboldened figures represent the sum total of all the compounds in each compound class.

Name	Short ID		Mictlan GeoB1 9327-3	Mictlan GeoB1 9327-4	Chapop ote GeoB1 9333-4	Chapop ote GeoB1 9333-7	Mictlan GeoB1 9336-6	Tsanya o Yang GeoB1 9337-3
			ng/ml	ng/ml	ng/ml	ng/ml	ng/ml	ng/ml
n-alkanes			9.60	9.71	3.70	24.61	2.01	1.61
Tetradecane	C14	C ₁₄ H ₃₀	0.00	0.00	0.00	0.47	0.00	0.08
Pentadecane	C15	C ₁₅ H ₃₂	0.13	0.26	0.06	1.58	0.00	0.19
Hexadecane	C16	C ₁₆ H ₃₄	0.99	1.56	0.28	4.81	0.13	0.30
Heptadecane	C17	C ₁₇ H ₃₆	1.59	1.83	0.55	4.94	0.22	0.30
Octadecane	C18	C ₁₈ H ₃₈	1.78	1.66	0.62	3.60	0.30	0.21
Nonadecane	C19	C ₁₉ H ₄₀	1.20	0.99	0.39	1.92	0.23	0.12
Eicosane	C20	C ₂₀ H ₄ ₂	1.06	0.99	0.62	1.99	0.29	0.12
Heneicosane	C21	C ₂₁ H ₄ ₄	0.63	0.68	0.38	1.45	0.20	0.00
Docosane	C22	C ₂₂ H ₄ ₆	1.32	1.05	0.80	2.37	0.35	0.17
Tricosane	C23	C ₂₃ H ₄₈	0.89	0.68	0.00	1.48	0.30	0.13
Isoprenoids			0.97	1.01	0.71	3.71	0.33	0.30
Pristane	Pr	C17	0.36	0.38	0.20	1.48	0.12	0.15
Phytane	Ph	C18	0.61	0.63	0.50	2.24	0.21	0.15
Benzenes			0.32	0.64	0.29	2.11	0.10	0.12
Benzene, (1-methyldecyl)-		C ₁₇ H ₂₈	0.09	0.15	0.09	0.54	0.00	0.04
Benzene, (1,3,3-trimethylnonyl)-		C ₁₈ H ₃₀	0.00	0.26	0.00	0.87	0.08	0.05
Benzene, (1-methyldodecyl)-		C ₁₉ H ₃₂	0.08	0.08	0.07	0.29	0.03	0.02
Benzene, (1-methylhexadecyl)-		C ₂₃ H ₄₀	0.15	0.15	0.14	0.41	0.00	0.00
Naphthalenes			0.00	0.02	0.00	0.39	0.00	0.08
Dimethylnaphthalene	C2-Naph	C ₁₂ H ₁₂	0.00	0.00	0.00	0.10	0.00	0.02
Trimethylnaphthalene	C3-Naph	C ₁₃ H ₁₄	0.00	0.02	0.00	0.29	0.00	0.06
Phenantrenes			1.14	1.45	0.94	6.59	0.43	0.45
Phenanthrene	Phen	C ₁₄ H ₁₀	0.73	1.07	0.63	5.12	0.26	0.36
Monomethylphenanthrene	C1-Phen	C ₁₅ H ₁₂	0.28	0.27	0.20	1.04	0.13	0.08
Dimethylphenanthrene	C2-Phen	C ₁₆ H ₁₄	0.14	0.11	0.10	0.42	0.04	0.01

Dibenzothiopnenes			0.29	0.27	0.28	1.12	0.12	0.11
Dibenzothiopnene	DBT	C ₁₂ H ₈ S	0.04	0.06	0.04	0.28	0.02	0.03
Monomethyldibenzo thiophene	C1-DBT	C ₁₃ H ₁₀ S	0.07	0.07	0.07	0.31	0.04	0.05
Dimethyldibenzothiophene	C2-DBT	C ₁₄ H ₁₂ S	0.17	0.13	0.17	0.53	0.07	0.03
S-containing monoaromatics			0.17	0.15	0.11	0.49	0.15	0.00
Benzenemethanethiol	BMT	C ₇ H ₈ S	0.17	0.15	0.11	0.30	0.15	0.00
Benzyl methyl disulfide	BMD	C ₈ H ₁₀ S ₂	0.00	0.00	0.00	0.19	0.00	0.00
N-containing compounds			0.70	0.60	0.34	0.30	0.38	0.20
Cycluron		C ₁₁ H ₂₂ N ₂ O	0.70	0.60	0.34	0.30	0.38	0.20
Aromatic alcohols			0.65	0.68	0.48	0.86	0.53	0.35
Benzyl alcohol		C ₇ H ₈ O	0.65	0.68	0.48	0.86	0.53	0.35
Aldehydes+Ketones			0.20	0.22	0.14	0.24	0.35	0.06
2,4-Nonanedione		C ₉ H ₁₆ O ₂	0.10	0.12	0.07	0.00	0.26	0.00
2,6-Di-tert-butylquinone		C ₁₄ H ₂₀ O ₂	0.04	0.04	0.02	0.14	0.03	0.02
Benzophenone		C ₁₃ H ₁₀ O	0.15	0.13	0.08	0.43	0.04	0.05
Aromatic acids			0.86	0.78	0.36	1.65	0.30	0.16
Benzoic acid, 2-ethylhexyl ester		C ₁₅ H ₂₂ O ₂	0.26	0.31	0.05	0.65	0.05	0.05
Benzoic acid, pentadecyl ester		C ₂₂ H ₃₆ O ₂	0.30	0.22	0.15	0.51	0.12	0.05
Benzoic acid, hexadecyl ester		C ₂₃ H ₃₈ O ₂	0.31	0.25	0.15	0.49	0.13	0.07
Fatty acids			1.03	0.36	0.79	0.57	1.11	0.02
Nonanoic acid			0.04	0.06	0.05	0.08	0.04	0.01
n-Decanoic acid			0.05	0.05	0.04	0.11	0.04	0.00
Dodecanoic acid			0.73	0.11	0.53	0.09	0.86	0.01
Tetradecanoic acid			0.04	0.03	0.04	0.07	0.09	0.00
n-Hexadecanoic acid		C ₁₆ H ₃₂ O ₂	0.17	0.12	0.13	0.22	0.09	0.00
Halogenated compounds			1.32	1.06	0.94	1.41	0.92	0.45
Benzyl 2-chloroethyl sulfone		C ₉ H ₁₁ ClO ₂ S	1.32	1.06	0.94	1.41	0.92	0.45

Table 12. Absolute abundance [ng/ml] of compounds (GC-MS) in the Oil slicks samples; the emboldened figures represent the sum total of all the compounds in each compound class.

Name	Short ID		Mictlan Oil Slick	Tsang Yang Oil Slick 1	Tsang Yang Oil Slick 2
<i>n</i>-alkanes			0.81	5.96	52.49
Hexadecane	C16	C ₁₆ H ₃₄	0.00	0.04	0.12
Heptadecane	C17	C ₁₇ H ₃₆	0.01	0.18	0.99
Octadecane	C18	C ₁₈ H ₃₈	0.00	0.45	3.45
Nonadecane	C19	C ₁₉ H ₄₀	0.00	0.61	4.96
Eicosane	C20	C ₂₀ H ₄₂	0.02	0.68	5.76
Heneicosane	C21	C ₂₁ H ₄₄	0.02	0.70	6.43
Docosane	C22	C ₂₂ H ₄₆	0.03	0.60	5.13
Tricosane	C23	C ₂₃ H ₄₈	0.04	0.54	4.87
Tetracosane	C24	C ₂₄ H ₅₀	0.07	0.55	5.31
Pentacosane	C25	C ₂₅ H ₅₂	0.11	0.48	4.77
Hexacosane	C26	C ₂₆ H ₅₄	0.16	0.45	4.28
Heptacosane	C27	C ₂₇ H ₅₆	0.16	0.37	3.51
Octacosane	C28	C ₂₈ H ₅₈	0.18	0.32	2.93
Nonacosane	C29	C ₂₉ H ₆₀	0.17	0.30	3.00
Triacontane	C30	C ₃₀ H ₆₂	0.15	0.23	2.39
Isoprenoids			0.00	0.54	3.72
Pristane	Pr	C17	0.00	0.11	0.64
Phytane	Ph	C18	0.00	0.44	3.08
Phenanthrenes			0.01	2.02	2.45
Phenanthrene	Phen	C ₁₄ H ₁₀	0.01	0.03	0.11
Monomethylphenanthrene	C1-Phen	C ₁₅ H ₁₂	0.00	0.50	0.50
Dimethylphenanthrene	C2-Phen	C ₁₆ H ₁₄	0.00	1.49	1.85
Dibenzothiophenes			0.00	2.21	22.39
Monomethyl dibenzothiophene	C1-DBT	C ₁₃ H ₁₀ S	0.00	0.34	2.47
Dimethyl dibenzothiophene	C2-DBT	C ₁₄ H ₁₂ S	0.00	1.87	19.92
S-containing monoaromatics			0.00	0.32	0.09
Benzene methanethiol	BMT	C ₇ H ₈ S	0.00	0.21	0.00
Benzyl methyl disulfide	BMDS	C ₈ H ₁₀ S ₂	0.00	0.11	0.09
other aromatics			0.00	0.36	4.38
Naphtho[2,3-b]thiophene, 4,9-dimethyl-	DMNT	C ₁₄ H ₁₂ S	0.00	0.36	4.38
Aromatic alcohols			0.07	0.14	0.17
Benzyl alcohol		C ₇ H ₈ O	0.07	0.14	0.17
Fatty acids			0.03	0.00	0.04
Nonanoic acid			0.00	0.00	0.02
n-Decanoic acid			0.00	0.00	0.02
Dodecanoic acid			0.02	0.00	0.00
Tetradecanoic acid			0.01	0.00	0.00
Halogenated compounds			0.08	0.14	0.00
Benzyl 2-chloroethyl sulfone		C ₉ H ₁₁ ClO ₂ S	0.08	0.14	0.00

Table 13. Shows the list of identified contaminants encountered in the environmental water sample. The absolute concentrations of these branched alkanes with quaternary carbon atoms (BAQCs) were calculated by integration of the m/z 85 signal during GC-mass spectrometry (GC-MS).

Name	Sum Formula	Mictlan GeoB19 327-3	Mictlan GeoB19 327-4	Chapop ote GeoB19 333-4	Chapop ote GeoB19 333-7	Mictlan GeoB19 336-6	Tsanyao Yang GeoB193 37-3
3-Ethyl-3-methylheptadecane	C ₂₀ H ₄₂	1.61	1.29	1.14	4.22	0.49	0.22
5,5-Diethylheptadecane	C ₂₁ H ₄₄	1.09	0.82	0.79	2.45	0.35	0.15
3,3-Diethylheptadecane	C ₂₁ H ₄₄	1.24	1.06	0.88	2.78	0.43	0.19
3-Ethyl-3-methylnonadecane	C ₂₂ H ₄₆	2.55	2.00	1.63	5.26	0.77	0.38
Heneicosane, 3-methyl-	C ₂₂ H ₄₆	1.32	0.99	0.73	2.38	0.38	0.15
Tricosane, 2-methyl-	C ₂₄ H ₅₀	1.89	1.36	1.27	3.56	0.60	0.26
3,3,13,13-Tetraethylpentadecane	C ₂₃ H ₄₈	2.28	1.74	1.43	4.21	0.62	0.31
Butyl-docosane	C ₂₆ H ₅₄	2.96	2.26	1.64	5.33	0.91	0.43
Tricosane, 2-methyl-	C ₂₄ H ₅₀	1.84	1.52	1.15	3.60	0.55	0.28
2-Methylpentacosane	C ₂₆ H ₅₄	1.93	1.52	1.12	3.48	0.55	0.25
Tetracosane, 3-ethyl-	C ₂₆ H ₅₄	3.52	2.32	1.60	5.91	0.85	0.41
Tetracosane, 5-ethyl-5-methyl-	C ₂₇ H ₅₆	2.07	1.49	1.27	4.30	0.69	0.32
Hexacosane, 9-octyl-	C ₃₄ H ₇₀	2.34	1.83	1.08	3.89	0.56	0.31
2-Methylheptacosane	C ₂₈ H ₅₈	2.30	1.69	1.18	3.77	0.62	0.27